Republic of Iraq
Ministry of Higher Education
and Scientific Research
University of Babylon
College of Engineering
Civil Engineering Department

Experimental Study on the Flexural Performance of Reinforced Concrete Beams Strengthened by Ultra-High-Performance Concrete Laminate

A Thesis
Submitted to the College of Engineering at University of Babylon
inPartial Fulfillment of the Requirements for the Degree of Master Science in Engineering/ Civil Engineering /Structures

By

Dhafer Mirdan Soud Meshad

Supervised by

Asst. Prof. Dr. Abdul Riduh Saleh Alfatlawi

2023A.D **1444 A.H**

بِسْمِ اللَّهِ الرَّحْمَنِ الرَّحِيمِ

فَأَمَّا الزَّبَدُ فَيَذْهَبُ جُفَاءً وَأَمَّا مَا يَنفَعُ النَّاسَ فَيَمْكُثُ فِي الْأَرْضِ

صَدَقَ اللَّهُ العلي العَظِيمُ

سورة الرعد (اية 17)

Dedication

To everyone who has devoted their life to the service of science and humanity.

To those who did not have access to education and strived to educate their children.

In memory of my father, brother and friend.

Acknowledgments

To my honorable supervisor, Mr. Abdul-Ridha Saleh, who spared no effort in ensuring the dissertation was properly completed.

To my good friend Wissam Nadir, who was a great help and guide, having been a constant companion since secondary school.

To Dr. Ali Abdel-Hussein, who provided many constructive comments and notes.

To my beloved family who have given me great support.

To my beloved family who have given me great support.

To all the friends and loved ones who supported me with words and deeds.

Abstract

The durability of reinforced concrete buildings is vulnerable to several threats, severe environmental damage, and other external stresses. To increase the service life of buildings, strengthening and repair methods are often utilized to improve their strength and durability. This research looked at the effect of adding a UHPC overlay to exiting reinforced concrete beam, both with and without construction joints in the UHPC overlay. In the present experimental program, nineteen reinforced concrete beams were tested. The factors included the continuity of the UHPC overlay, the kind of reinforcement in the UHPC overlay, the location of the construction joint in the UHPC overlay, and the shape of the construction joint. According to the findings, adding UHPC layers to the RC beams' tensile side greatly enhanced their stiffness (20–132%) and postponed the crack's onset. At the same time, the UHPC overlay's construction joint reduced the effectiveness of the strengthening technique. The performance of the strengthened beams is greatly affected by the reinforcement ratio in the UHPC overlay. The results showed that compared to the control specimen, the UHPC that had been reinforced with 2Ø 10 mm steel bar had a higher ultimate load (17.5-23.1%) and stiffness (78%). Moreover, utilizing GFRP as reinforcement for UHPC overlay improves the load-bearing capacity, stiffness, and delays the emergence of flexural cracks in reinforced specimens. Results showed that the UHPC overlay had a strong enough connection to the concrete that the load-bearing capacity increased by 40% and the stiffness increased by 30%. The effect of the construction joint is mitigated by the use of steel or GFRP bar to reinforce the UHPC overlay. As a result, neither the form nor the position of the construction joint had any effect on the behavior of the strengthened specimens created by the reinforced UHPC overlay. Thus, it is advised to employ vertical joints in the UHPC overlay if necessary. Before

the enhanced beams can perform to their full potential, concrete cover separation at the ends of the UHPC overlay causes the steel bar/GFRP bar reinforced beams that were strengthened by UHPC to fail. This is a significant problem, thus caution should be used while using this procedure to reinforce the beams.

List of Content

List of Tables

List of Figures

List of Plate

List of Notations

Notations	
a_s	Depth of concrete strut
D	Distance from the beam's top face to the centre of its tensile reinforcement
Au	Cross-sectional area of overlay
σ_t	Tensile strength of UHPC
d_u	Distance from the beam's top face to the center of the overlay
A_{ru}	Area of overlay reinforcement
σ_{ru}	Stress in overlay reinforcement
d_{ru}	Distance from the beam's top face to the center of the overlay
A'_s	Area of longitudinal compressive reinforcement in the RC beam
σ'_s	The stress of longitudinal compressive reinforcement in the RC beam
d'	Distance from the beam's top face to the center of its compressive Reinforcement.
μ	Ductility index

List of Abbreviations

Abbreviations	
3D	Three Dimension
ACI	American Concrete Institute
ACI-ASCE	Joint of American Concrete Institute with American Society of Civil Engineers
ASTM	American Society for Testing and Materials
BS	British Standard
DIC	Digital Image Correlation
ECC	Engineering Cementitious Composite
FRC	Fiber-Reinforced Concrete
GFRP	Glass Fiber Reinforced Polymer
HPFRCC	High-Performance Fiber Reinforced Cementitious Composite
HSC	High-Strength Concrete
IQS	Iraqi Specifications
LVDT	Linear Variable Differential Transducer
NSC	Normal Strength Concrete
RC	Reinforced concrete
SD	Standard Deviation
SF	Silica Fume
SFRC	Steel Fiber Reinforced Concrete
SP	Superplasticizer
UHPC	Ultra-High Performance Concrete

Chapter One

Introduction

1.1Introduction

Due to its strength, durability, and cost-effectiveness, concrete is a popular construction material. Nevertheless, concrete structures are prone to damage and deterioration, despite their benefits. The reasons for concrete deterioration can be diverse and numerous, leading to damage ranging from minor cracks to severe structural collapse.

One of the primary reasons for concrete deterioration is aging. Over time, concrete can become weaker due to environmental factors such as exposure to moisture, freeze-thaw cycles, and chemical attacks. Another factor that can lead to concrete deterioration is exposure to severe environments. For example, the steel reinforcement within a concrete structure can corrode when exposed to saltwater, acidic chemicals, or high humidity levels.

Natural and human-made extreme events, such as earthquakes or vehicular impacts, can also cause significant damage to concrete structures.

Finally, changes in design codes or usage can also lead to concrete deterioration. For example, a building that was designed for one purpose may be repurposed for another use, placing different demands on the structure. Similarly, changes in design codes may require modifications to the building to ensure compliance with new standards.

In summary, concrete structures are vulnerable to deterioration due to various factors, and rehabilitation may be necessary to ensure the continued safety and stability of the building.

Overall, it is essential to address any issues with RC buildings promptly and effectively to avoid potential safety risks and economic costs associated with reconstruction. By using the appropriate methods to strengthen or rehabilitate the structure, it is possible to extend its lifespan and maintain its functionality in a cost-effective and sustainable manner [1][2][3].

There are various situations that may require the strengthening of RC buildings. For instance, if a mistake was made during the initial design, the structure may need to be reinforced to ensure its safety and longevity. Additionally, if the building's purpose or usage changes, it may need to be modified to support different loads or functions. Similarly, if a specific component is needed to bear a greater weight, the structure may require reinforcement [4].

In recent decades, various techniques have been developed to strengthen existing RC structures, including epoxy-bonded steel plates, external post-tensioning, and externally bonded carbon fiber-reinforced polymer [5]. While these methods have the potential to achieve strengthening goals and enhance the strength and durability of RC structures, they also have certain drawbacks.

For example, concrete jacketing, which involves adding a new layer of concrete to an existing structure, can increase the mass of the building and produce a larger structural member [6][7]. This can be problematic for buildings with limited space or capacity. Additionally, steel bonding strengthening can be vulnerable to corrosion, fire resistance issues, length

limits, and debonding of the steel plate as the adhesion component deteriorates over time [8].

Similarly, fiber-reinforced polymer (FRP) bar and laminate strengthening methods lack fire resistance and may lose their adherence over time, potentially leading to reduced effectiveness [9][10]. It is essential to consider these drawbacks and challenges when selecting the appropriate strengthening technique for a specific RC structure. By understanding the benefits and limitations of each method, engineers can determine the most effective and sustainable solution to strengthen the RC structure and ensure its long-term safety and durability.

Ultra high-performance concrete (UHPC) is a type of cement-based material that has gained popularity in recent years for its use in the repair and strengthening of existing reinforced concrete structures. UHPC is characterized by its exceptionally high compressive and tensile strength, remarkable ductility, and low permeability, making it an ideal material for repairing and retrofitting deteriorating RC structures [11].

UHPC is defined as a cementitious composite material with a low water/binder ratio, reinforced with a high volume fraction of fiber, and an optimal gradation of granular materials [12]. Its compressive strength ranges from 120 to 250 MPa, and its tensile strength exceeds 5 Mpa [13][14]. These exceptional mechanical and durability properties make UHPC a promising solution for strengthening and repairing RC structures.

By using UHPC, engineers can increase the strength and durability of RC structures while minimizing the need for bulky reinforcements. This can lead to cost savings and a more sustainable solution for maintaining the structural integrity of buildings.

1.2 Ultra High-Performance Concrete (UHPC)

UHPC is a relatively new construction material that has exceptional durability, significant compressive and tensile strength and thus it perfect for strengthening/rehabilitation [15]. One of UHPC's exceptional mechanical properties is its compressive strength, which is at least 120 MPa [16][17], tensile strength exceeding 5 MPa [18][17][19], a high capacity for absorbing energy as well as little permeability, shrinkage, and creep [20], [21][19]. UHPC has gained popularity in the construction industry because of its distinct features, such as exceptional durability, high compressive and tensile strength, and resistance to environmental factors like a chemical attack. Additionally, its high strength-to-weight ratio and affordable cost make it a desirable choice for retrofitting RC structures. Rehabilitation and retrofitting of concrete structures using UHPC have proven to enhance their load-carrying capacity, ductility, and durability [22]–[25]

Using UHPC for strengthening flexural RC structures offers several benefits, including a significant increase in load-carrying capacity and durability. Additionally, this method allows for rapid construction through prefabrication and assembly, with minimal change in section size and minimal disruption to traffic service. This material is increasingly being used for bridge decks, beams, columns, and other structural elements in the construction industry due to its unique properties. Furthermore, the use of UHPC has been shown to reduce the need for maintenance and repair, making it a cost-effective solution in the long term [26][27].

Although UHPC is a pricier material than NSC, using it to strengthen the existing buildings is a more cost-effective solution than using traditional retrofitting techniques. In many countries, the cost of materials is much lower than the cost of labor. Furthermore, UHPC technology enables a significant reduction in the duration of the construction process, which

subsequently leads to a reduction in indirect expenses and maintenance fees due to the material's excellent durability [28].

The Swiss Society of Engineers and Architects released a technical document in 2016 which includes concepts for applying a reinforced layer of UHPC to existing RC structures. The information presented in the document is the outcome of 20 years of research and has been validated through controlled experiments as well as real-life applications [28].

1.3 Properties of UHPC make it a good solution for strengthening or repairing RC structures.

In 2018 Al-Osta [29] investigated in detail the properties of UHPC that make it a promising material for strengthening and repairing RC buildings. The conclusion that may be derived from the above is as follows:

1. First, as seen in Figure 1.1, the UHPC has a strain-hardening response and high tensile strength that are comparable to steel.

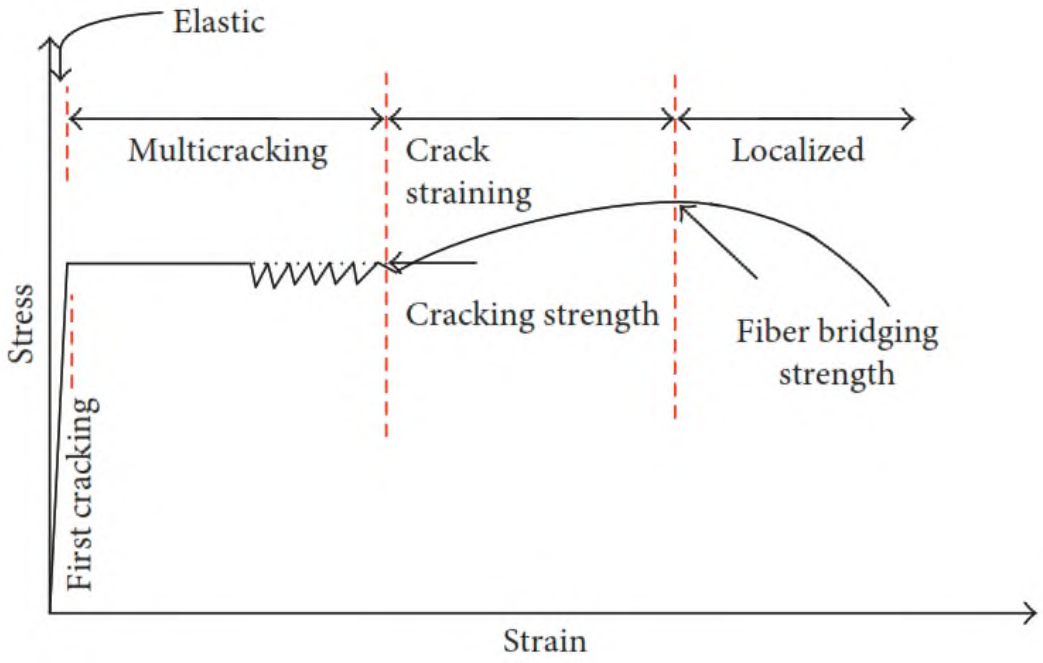

Figure 1.1 Idealized tensile mechanical response of UHPC [30].

2. UHPC is highly dense, making it difficult for foreign substances to penetrate it. As a result, UHPC is impervious to carbonation, sulfate attack, and chloride penetration. Experimental testing showed that UHPC is highly resistant to scaling, abrasion, freeze-thaw, and alkali-aggregate reactions, as shown in Figure 1.2.
3. The coefficient of thermal expansion of UHPC was found to be slightly higher than that of NSC. As the coefficients of thermal expansion of UHPC and NSC are extremely similar, UHPC may be utilized as a repair material without causing differential thermal expansion between the UHPC and the host concrete [31].
4. Fire testing indicated that UHPC spalls explosively at 790 degrees Celsius, which is 100 degrees Celsius and 190 degrees Celsius higher than the corresponding temperatures for HPC and NSC, respectively [32].

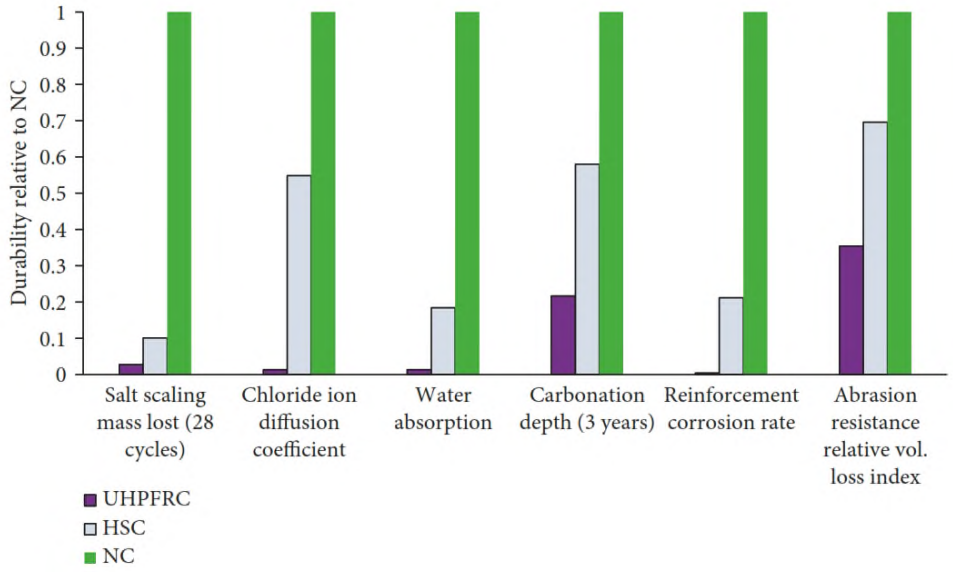

Figure 1.2 Experimental tests revealed that UHPC has a significant resistance [33].

In comparison to alternative methods, using UHPC as a repair and strengthening material might provide a number of advantages [34]:

1. Extremely low permeability, which improves the durability and service life of the repaired or strengthened part and will have a stronger resistance to additional damage or vandalism of the element.

2. Compared to FRP wrapping, it is less sensitive to concrete surface preparation.

3. May serve as a replacement for patching materials in the process of repairing the loss in a concrete section.

4. Strong resistance to shear stress, which may reduce the need for extra transverse reinforcement.

5. Very flowable and self-consolidating, making it suitable for crowded areas.

6. Comparatively less of an increase in section dimensions as compared to concrete jacketing.

1.4 Application of UHPC

There are two main uses for UHPC: repairing and strengthening existing buildings, and constructing new one, frequently precast buildings [35]. UHPC is most often used in the construction or rehabilitation of bridge parts like decks and piers[36], [37], and joining prefabricated RC elements [38]. Figure 1.3 presents selected applications of UHPC in the country.

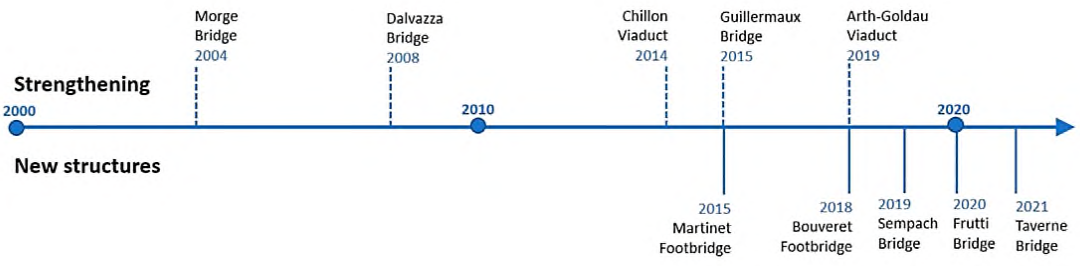

Figure 1.3 Timeline for selected application of UHPC in strengthening and new structures [39].

Switzerland has been using the UHPC overlay since 2004 as a practical solution to strengthen its buildings. The first attempt was made in 2004 by repairing and enlarging the existing short-span bridge across the river la Morge at Chateauneuf, as shown in Plate 1.1 [40]. Since then, several other bridges of historical significance have undergone restoration work, including the 1925-built Dalvazza Bridge and the 1920-built Guillermaux Bridge, both of which were identified as National Historic Landmarks. These restoration efforts have allowed the bridges to retain their historic appearance while being upgraded to accommodate modern traffic [41].

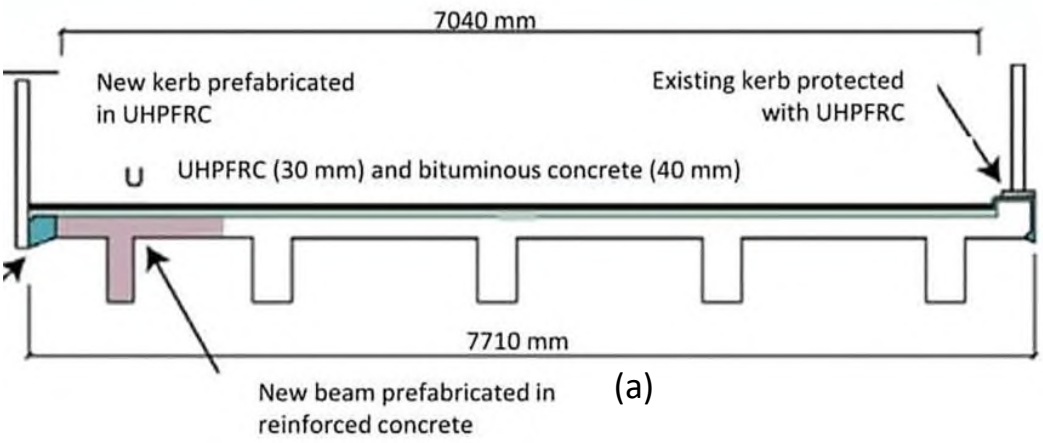

(b)

Plate 1.1 La Morge Bridge, a) scheme of the strengthening using UHPC, b) the bridge after 18 years of strengthening [41].

As shown in Plate 1.2a, in 2015, a UHPC overlay was used to repair the Chillon Viaduct, which connects the Swiss towns of Chillon and Montreux. Although being constructed in 1969, the viaduct structures had begun to deteriorate due to the increased weight of trucks. As can be seen in Plate 1.2b, the UHPC was used to increase capacity utilizing a UHPC overlay [42].

Recently (In 2020), three long-span bridges in the US were repaired utilizing UHPC overlay. UHPC overlays were applied to extensive parts of the bridge deck in these test projects [41]. These bridges included;

- Commander Barry Bridge: UHPC application has the potential to save over $200 million in construction costs and add another 30 years to the service life of the bridge deck (Plate 1.3).
- Delaware Memorial Bridge: the application of UHPC overlay save $60 million compared with the removal and replacement (Plate 1.4).
- Claiborne Pell Bridge (Plate 1.5).

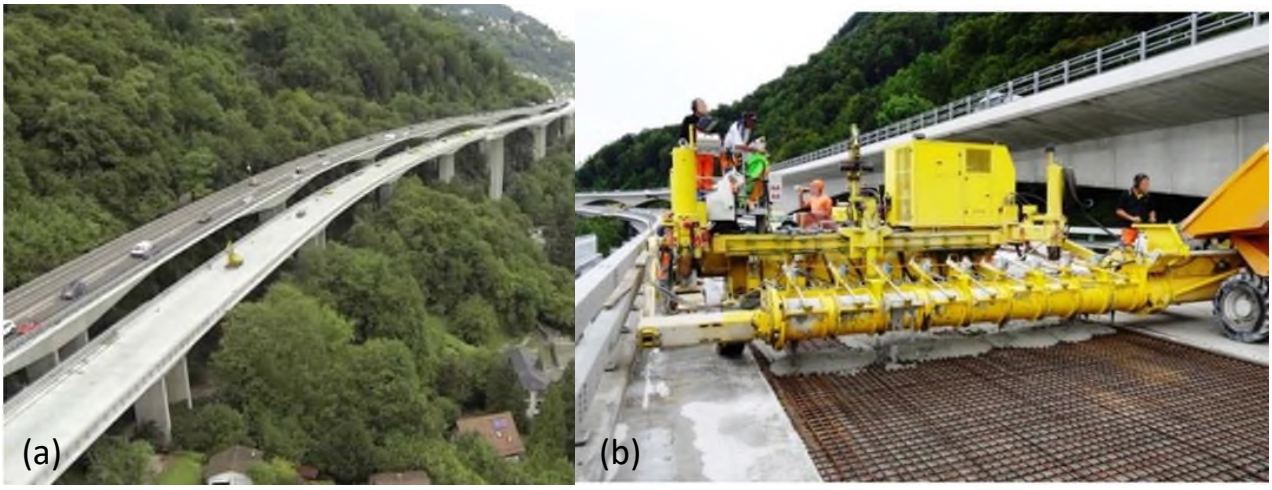

Plate 1.2 Strengthening of Chillon Viaduct, a) Chillon Viaduct during UHPC deck overlay construction, b) pouring UHPC overlay [41].

Plate 1.3 UHPC overlay installation over Barry Bridge [41].

Plate 1.4 Application of UHPC over the duck of Delaware Memorial Bridge [41].

Plate 1.5 Pell Bridge with Strengthening Claiborne UHPC overlay [41].

1.5 Problem statement

One significant challenge in using UHPC is that it is a new strengthening technique compared to other methods. There have been no recorded instances of using UHPC for strengthening concrete beams, and only bridge deck slabs have been commonly strengthened using UHPC. Limited studies have focused on the behavior of beams strengthened with UHPC overlay, and several factors must be considered, such as UHPC properties, reinforcement of the UHPC strengthening layer, thickness of the UHPC layer, surface condition of the strengthened element, and bonding between UHPC and NSC. Further studies are required to support this strengthening technique.

In construction projects, it is sometimes necessary to create construction joints due to the nature of working conditions, supply shortages, project timelines, or unexpected malfunctions. In these situations, it is crucial to design and detail phased construction joints that are waterproof while also allowing for stress transmission. Surface preparation of the hardened UHPC is crucial for enhancing bonding between the hardened UHPC and fresh UHPC, and the use of reinforcing bar dowels may also be necessary between phases [34].

1.6 Amis and objectives

The current study aims to enhance the flexural strength of RC beams by applying a UHPC overlay at the tension side. The objectives of this study are as follows:

1 An experimental investigation is being conducted to strengthen the RC beams utilizing a UHPC overlay.
2 Experimentally investigate the effect of different types of reinforcement used in UHPC overlay.

3 Experimentally investigate the effect of the presence of construction joint in the UHPC overlay on the efficiency of this strengthening technique.
4 Also, studying the effect of the construction joint's location and shape on this strengthening technique's efficiency.
5 Try to improve the bonding between NSC and UHPC by roughing the NSC surface with water jetting and using epoxy adhesion.

1.7 Thesis outline

This thesis is structured into five chapters that aim to provide a comprehensive study on the behavior of RC beams strengthened with an UHPC overlay. The following is an overview of each chapter:

Chapter One presents an introduction to the research and provides a brief background on the strengthening techniques, problem statement, and amis of study.

Chapter Two reviews the existing literature on the use of UHPC in strengthening RC structures, focusing on its properties, advantages, and limitations. It also discusses other strengthening techniques and their drawbacks.

Chapter Three describes the experimental program carried out at the University of Babylon. It includes details of the tested specimens, materials properties, construction method and the testing procedure.

Chapter Four presents the results of the experimental program and analyzes the behavior of the RC beams strengthened with UHPC overlay. It includes graphs, tables, and figures to illustrate the data obtained and draws conclusions on the effectiveness of the UHPC overlay technique.

Chapter Five summarizes the research findings and draws conclusions on the use of UHPC overlay in strengthening RC beams. It also makes recommendations for future research in this area, based on the limitations and gaps identified in the current study.

Chapter Two

Literature Review

2.1 Introduction

In this chapter, an overview is provided of the different methods that can be employed to improve the strength and restore reinforced concrete structures. The chapter summarizes the results of strengthening beams, and then goes on to detail the effectiveness, advantages, and disadvantages of each repair or strengthening technique, taking into account the specific application, the amount of effort required, and the extent to which it can be applied.

2.2 Repair and strengthening techniques

RC constructions are a popular choice for a wide range of buildings and infrastructure projects around the world, due to their durability and strength. However, these structures require ongoing maintenance and repair to ensure their continued safety and functionality [43]. As reinforced concrete buildings age, they are prone to developing issues with serviceability, sustainability, and durability, which can result from environmental changes and heavy mechanical loading [2][3]. To extend the useful life of these buildings and minimize costly maintenance, it is crucial to strengthen them. In recent years, several methods and materials have been used to rehabilitate existing RC buildings, including epoxy repair, removal and replacement, fiber-reinforced polymer, external wrapping, and near-surface mounted [46][47][48]. While these methods can effectively enhance strength and durability, they may also have drawbacks such as an increase in building

weight due to concrete jacketing, corrosion, and fire resistance issues when using the steel plate approach, and aging of adhesion materials at the interface when reinforcing with FRP [49]. The following sections will provide an overview of the most commonly used strengthening techniques worldwide.

2.2.1 Concrete jacketing

One of the most widely used and long-standing methods for rehabilitating concrete frames is adding concrete jackets with additional longitudinal and transverse reinforcement. This method requires more time and effort as new reinforcement needs to be added. Unlike other strengthening techniques that use steel elements, this method does not require specialized work demands. An advantage of this technique is that the increased stiffness of the structure is uniformly distributed, which is beneficial for the overall stability of the structure [50][51].

Adding joint transverse reinforcement to a concrete structure requires many labour-intensive steps, such as perforating the floor slab, drilling through the beams, and occasionally bending the reinforcement in place. The mass and volume are both increased while living space is diminished due to jacketing's effect on the size of the members. In addition to raising the total expense of the renovation, the construction operations themselves are disruptive to the building's tenants [50].

2.2.2 Steel jacketing

During the 1960s, engineers attempted to strengthen RC beams for the first time by connecting steel plates to the tension side of the beam from the outside [52]. While attaching steel plates to a beam did increase its flexural strength, this method had drawbacks, such as leaving the plate vulnerable to

environmental degradation mechanisms like corrosion. The weight of the steel plates also made it difficult and costly to install them [53][54][50].

2.2.3 Strengthening RC beams with FRP

The FRP laminate flexural strengthening technology became widely used. In the 1980s, the concept of using FRP laminates to repair and reinforce beams and slabs was introduced [55]. The basic idea behind the FRP strengthening method is to use the laminates on the tension side of the beam as an extra layer of reinforcement[56], [57][58]. FRP composite systems have proven to be a practical and cost-effective solution for strengthening structures due to their low cost, high strength-to-weight ratio, and resistance to corrosion [59].

Toutanji et al. in 2005 [60]used three, four, five, and six layers of CFRP sheet to strengthen the RC beam. The ultimate moment capacity was found to rise by 42.6%, 49.2%, 67.8%, and 70.2% over the control beam. When comparing the reinforcement with five and six layers of carbon fiber sheets, it is clear that there is no noticeable gain in strength.

Attari et al. in 2012 [58] discovered that a composite material made of glass fibers and carbon fibers worked well for strengthening concrete beams. While comparing the strengthened beam specimen to the control specimen, the strength capacity was shown to enhance by 114%.

The underside of a beam is often inaccessible due to obstructions such the suppression system, electrical cables, and ventilation ducts, making the implementation of retrofit solutions difficult and time-consuming. This means that it might be challenging to get the well-prepared concrete surface for the FRP application at the bottom of the structural element, or that access could be impossible due to logistical constraints. Applying FRP to the bottom might be especially challenging since it may need extra anchoring or equipment to support FRP laminates while an adhesive cure [61]. Moreover,

when a composite laminate is subjected to compression, there are specific possible problems, such as fiber micro-buckling, that need to be addressed [62].

Gunes et al . [63] revealed that wet conditions might significantly weaken the FRP-concrete connection over time. In only two weeks of exposure to moisture, more than half of the initial bond strength might be lost.

The temperature has a significant impact on the physical and mechanical characteristics of the resin components of FRP systems, and these qualities deteriorate at temperatures near and above their glass-transition temperature (Tg). Standard commercially available FRP systems have a (Tg) temperature between 60°C and 82°C [56]. Unfortunately, the use of FRP systems will not arrest the continued corrosion of existing reinforcing steel. FRP reinforcement should not be installed if steel corrosion is occurring or if the concrete substrate is being degraded [56].

2.3 Strengthening the RC element by UHPC overlay

This section presents the recent study of strengthening the RC element by UHPC.

Genedy in 2014 [53] conducted a study in which four RC beams were cast and subjected to four-point bending until failure. The purpose of the study was to investigate the flexural performance of a strengthening system for T-beams. Plate 2.1 illustrates the procedure, which includes removing the top 51 mm of the beam cover before attaching CFRP laminates to the existing concrete surface and casting UHPC overlay over the laminates. The load-bearing capability increased by 9.2 % after using the recommended strengthening method. In addition, the T-flexural beam's failure mode shifted to a shear failure mode. Nevertheless, the load capacity of the beam was not noticeably improved by using only the UHPC overlay to strengthen it.

As can be seen in Plate 2.2, the failure of the beam occurred at both loading locations because of debonding between the UHPC overlay and the conventional concrete surface. The UHPC overlay eventually became totally isolated from the base concrete portion as this debonding process spread laterally. Based on these findings, the suggested method may be useful for low- and medium-depth T-beams and slabs.

Plate 2.1: CFRP sheets and shear dowels installed [53].

Plate 2.2: Debonding of UHPC overlay [53].

Prem et al. in 2016 [27] UHPC overlays of 10, 15, and 20 mm in thickness were used to strengthen RC beams with reinforcement ratios of 0.57%, 0.89%, and 1.30%, respectively. Without deboning, the composite retrofitting beams are performed as a single unit under bending. With 10 mm of overlay, the damaged beams were restored to their original flexural capacity. For beams with 15 mm UHPC overlay reinforced with steel bars

of 0.57%,0.89%, and 1.3% increases load bearing capacity by 24%, 11.57%, and 10.60%.

Hussein and Amleh in 2015 [64] developed composite members consisting of UHPC/NSC and NSC/HSC RC beams without web reinforcement, as shown in Figure 2.1. The UHPC was placed on the tension side of the beam, surrounding the tension reinforcement, while the NSC/HSC was used on the compression side. To enhance the bond between the UHPC and the existing RC beam, stud connections or dowels were employed. According to the study, the shear strength of composite beams was 1.6 to 2.0 times higher than that of control beams. The addition of studs did not result in a significant increase in the shear strength of the composite beams because of the robust covalent bonds between the existing RC and UHPC layers.

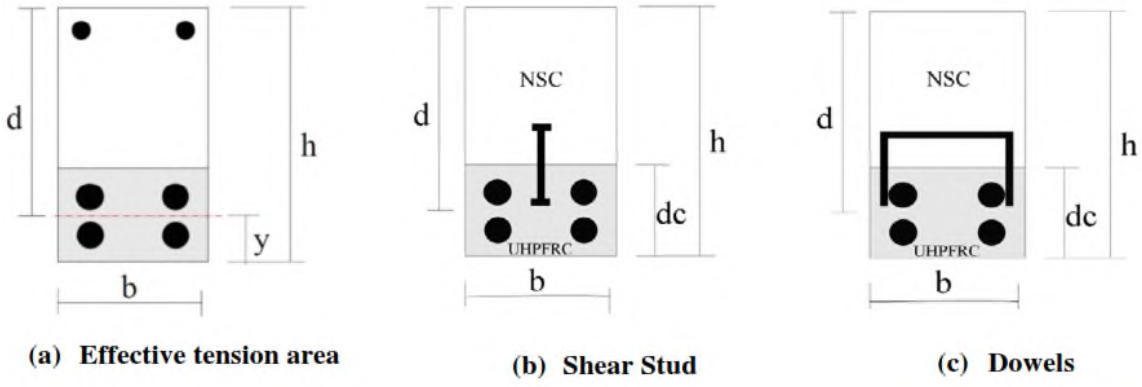

Figure 2.1. UHPC layers detail (a) Effective tension area (b) stud connection (c) shear connections [64].

Hor et al. [65] conducted an experimental study in 2017 to strengthen an RC slab using UHPC. Two different UHPC arrangements were used to reinforce the RC slab. In the first arrangement, the deteriorated concrete was removed, and UHPC of varying thickness was applied as a patch to repair the RC members. In the second arrangement, an additional UHPC overlay of 25-50 mm thickness was added to reinforce the RC members. Although the use of UHPC patch did not enhance the load-bearing capacity of the RC slab, all of the reinforced slabs demonstrated remarkable energy absorption

and ductility. Moreover, it was noticed that when the thickness of the UHPC layer is increased, the mechanism of failure transitions from shear failure to flexure failure. According to the data, the UHPC layer increased the total stiffness and delayed the onset of shear fractures. Plate 2.3 illustrates the failure mechanism of the patch and the overlay technique for strengthening.

In 2017 Murthy et al. [66] conducted a study where they used a UHPC laminate to repair a damaged RC beam. The main aim of this study was to examine how the addition of a thin UHPC laminate improves the pre damaged. The researchers strengthened the beams using a 10mm UHPC layer and subjected them to variations in pre-loading of 70%, 80%, and 90%, respectively. It was found that all pre-loaded and retrofitted RC beams had a maximum load-bearing capacity that was somewhat greater than the average maximum load of the control beam. Additionally, it was determined that the pre-loaded and retrofitted beams only required a 10mm UHPC laminate thickness to revert back to their behavior before pre-loading and retrofitting.

Tanarslan et al. [67] in **2017** did experimental work to investigate the performance of RC beams reinforced with UHPC laminate. There were two types of bonding used in the UHPC laminates' strengthening. Both methods of bonding UHPC laminate are depicted on Plate 2.4, with the first using epoxy glue and the second using mechanical anchoring. Also, the use of reinforcing bar in UHPC laminate was studied. The findings shown that using UHPC laminates, especially in the context of anchoring, is an efficient method for raising the RC beams' load bearing capability. The load-bearing capability of the UHPC-enhanced specimens was found to rise by at least 7% and by as much as 118%. The ultimate load of the laminate was increased by 73% when internal reinforcement was added in comparison to the load that was recorded when the laminate was not reinforced internally.

Plate. 2.3 Failure mode and cracking pattern of the tested specimens [65].

Plate 2.4. Bonding application for UHPC laminate [67].

Paschalis in 2018 [68], conducted an experimental and theoretical investigation of the structural behavior of a full-scale RC beam strengthened by UHPC. This study used six RC beams; the first two beams served as control, whereas the second two strengthened with the UHPC layer at the tension side. The others specimens were similar to the second one with a steel bar added to the UHPC layer. Before this method can be used in the real world, the interface between the new layer and the existing beam has to be roughened so that the aggregates can be seen. As shown in Figure 2.2, connecting bars were used to join the old and new reinforcement in this investigation. The test results showed that additional UHPC at the tension side resulted in a large increase of stiffness with a slight increase in the ultimate load However, adding a steel bar to the UHPC layer significantly increases the load carrying capacity (90% compared with the control specimen). Numerical findings show that the amount of layer reinforcement is a crucial factor in determining the enhanced beams' performance. Moreover, it seems that the quantity of reinforcement of the layer is more essential than the depth of the layer in terms of the maximum resistance to the applied stresses. Thus, the performance of the strengthened RC beam with a 30 mm layer and 16 mm steel bars is superior than the performance attained for strengthening with UHPC layers of 50 mm and 70 mm depths using 10 mm steel bars.

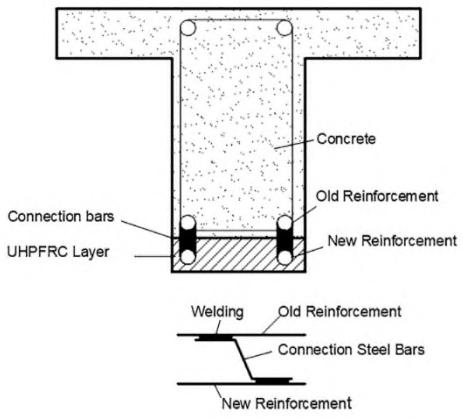

Figure 2.2 Application of UHPC layers in real practice [68].

The study conducted by **Zhang et al. in 2019** [69] provides valuable insight into the use of UHPC as a repairing material for damaged bridge decks. The experimental results demonstrated a significant improve the cracking and ultimate capacities of composites when placed UHPC at the tension face. This finding is particularly relevant for bridge decks, which are often subjected to heavy loads and harsh environmental conditions. By increasing the load-bearing capacity of the damaged deck, UHPC can help to extend the lifespan of the bridge and reduce the risk of catastrophic failure. Interestingly, the study also found that UHPC placed at the compression face did not improve the cracking capacity of the composite, but still increased the ultimate capacity by 30%. Another significant finding of the study was the delayed and restricted crack propagation in RC slabs that had been strengthened with UHPC.

Zhang et al. in 2020 [70]conducted a study to enhance the performance of damaged RC beams strengthened in flexural by adding a UHPC overlay. Thirteen RC beams were constructed in section and details shown in Figure 2.3, and various parameters were tested, including the degree of pre-damage of the tested specimens, and the improvement of the toughness of UHPC by a different method. The study found that the ultimate and cracking loads of strengthened specimens improved by 1.57 to 3.32 and 1.72 to 2.21 times, respectively. The reinforced UHPC layer successfully restricted cracks propagation. However, the degree of improvement in the flexural performance of UHPC-reinforced beams decreased with the severity of the RC beam's pre-damage. Moreover, the addition of steel wire mesh produced the most significant improvement.

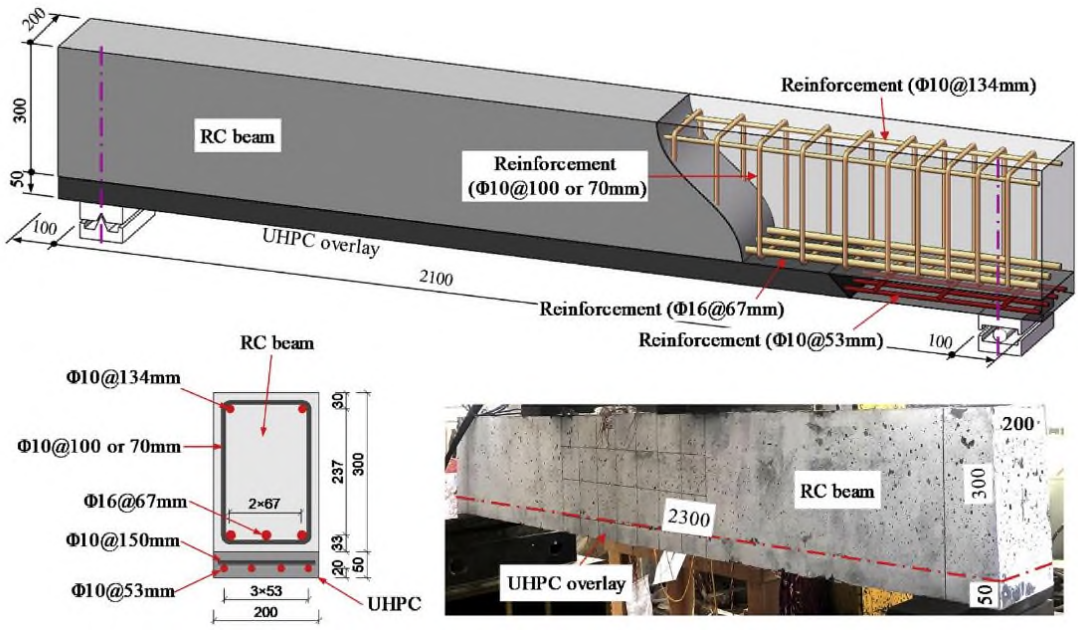

Figure 2.3 Detailed scheme for the test specimen [70].

Ismail and Hassan 2021 [71] conducted a study to investigate the response of a full-scale RC beam after being repaired with UHPC. The UHPC was used to replace a layer of NSC on the tension side of the beam. The study included the repair procedure with typical dimensions and compression pattern, as well as the reinforcement details, test apparatus, and results, as shown in Figure 2.4. According to the findings, the repaired beam exhibited enhanced ultimate load, ductility, and energy absorption when compared to the control beam. Despite the implementation of a substantial number of stirrups and surface roughening techniques to connect the original member with the repair material UHPC, the repaired beam failed rapidly due to shear-interface debonding, as depicted in Figure 2.4. These results demonstrate that while UHPC can effectively enhance the strength and durability of reinforced concrete structures, additional research is necessary to address challenges related to the bonding of UHPC with the existing concrete surface. Such findings highlight the need for continued research efforts to improve the effectiveness and long-term durability of UHPC-based repairs for concrete structures.

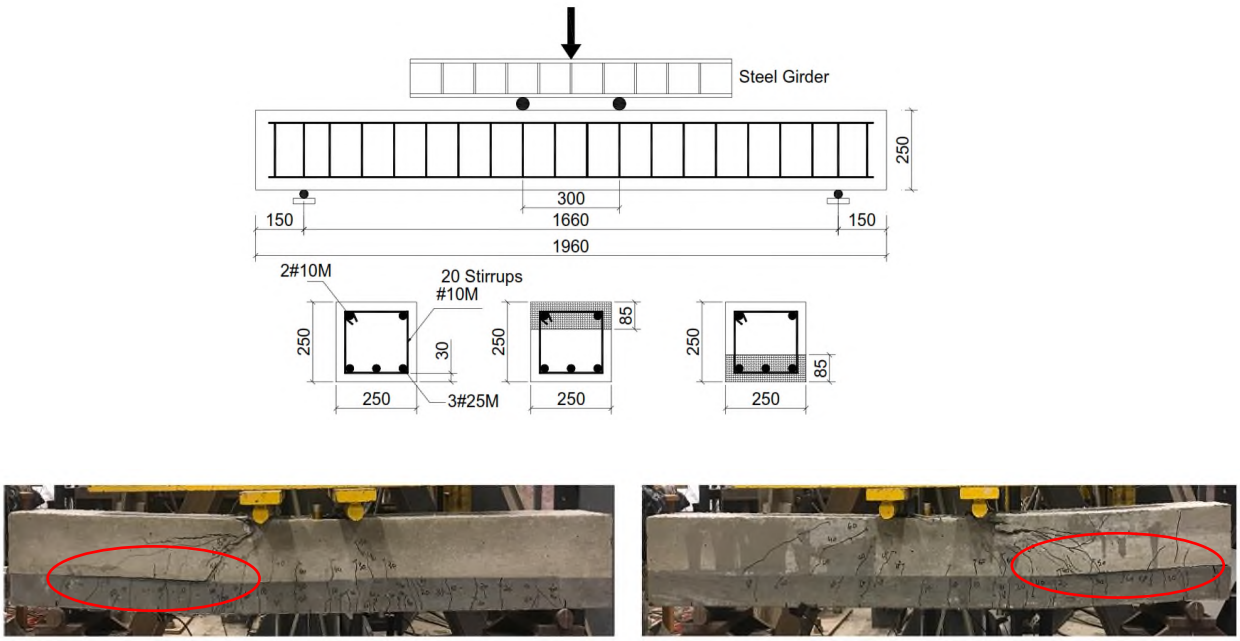

Figure 2.4 Test setup, reinforcement details, and typical cracking pattern [71].

To further elaborate on the study conducted by **Wei et al.** (2022) [72], the research aimed to investigate the potential for flexural cracking in a reinforced UHPC overlay on a bridge deck. The study was carried out under both static and fatigue loading conditions, which are common scenarios experienced by bridge decks in service. Despite the use of reinforcement in the UHPC overlay, the experimental findings showed that the failure of the overlay cannot be completely avoided, indicating the need for ongoing maintenance and repair. It is important to note that this study provides valuable insights into the limitations and challenges associated with the use of UHPC overlays for bridge deck rehabilitation, which can help inform future research and development efforts in this area

2.4 Debonding

2.4.1 Interfacial preparation

The interfacial behavior between the existing structure and the repair material has emerged as a critical factor in ensuring the structural integrity of the repaired structure. Recent research has highlighted the importance of

interfacial debonding in UHPC repairs, which can be minimized through proper surface preparation of the concrete substrate and quality control measures during UHPC application. Achieving an in-depth understanding of interfacial behavior is critical to ensuring effective interface preparation and reducing the risk of interface failure. Through an improved understanding of how interfaces behave, it may be possible to enhance the effectiveness of UHPC repairs and promote the long-term durability of reinforced structures [52][53]. The interface between two materials experiences both tensile and shear stresses that can lead to the sliding or splitting of the materials [75].

When replacing or strengthening existing concrete, it's best to use a comparable material. Unfortunately, that is not always the case and is seldom the best option. The two concretes are too far apart in age to be fully compatible for strengthening and restoration [76].

The researchers evaluated seven different approaches to preparing the interface for UHPC strengthening. These approaches included no preparation, rough preparation, rough preparation with epoxy adhesion, sandblasting, epoxy adhesion alone, rough preparation with studs, and studs alone [77].

Sandblasting and shot blasting are two surface preparation techniques with a reduced potential for microcracking, studies have shown that this bond is possible with a roughened, prepared amplitude of 0.125 inches or less in the concrete substrate Sandblasting and shot blasting are two surface preparation techniques with a reduced potential for microcracking, studies have shown that this bond is possible with a roughened, prepared amplitude of 0.125 inches or less in the concrete substrate [57][79][80].

According to many researchers in this field, there are three primary modes of failure observed in UHPC/NSC structures: cohesive failure within the

concrete substrate, adhesive failure at the interface, or a combination of both parts [81].

Plate 2.5. Debonding at the interface [67][82].

The bond between UHPC and the existing concrete can be evaluated using splitting tensile and slant shear tests. Tests conducted on smooth-surfaced cast-in-situ specimens revealed the lowest bond strength. Nonetheless, the slant shear test indicated the greatest bond strength when the concrete was prepared through sandblasting. On the other hand, the splitting tensile test indicated that the use of epoxy adhesives provided the strongest bond on a smooth surface of existing concrete. Conversely, the sandblasting of the concrete surface improved its roughness, enhancing its capacity to endure shear stress, and consequently yielding the highest bond strength during the slant shear test [81].

Recently, Hydrodemolition techniques are used in numerous UHPC overlay-strengthening projects. Hydrodemolition is the preferred removal method

for UHPC Overlays, and roughened surfaces with no microfractures create an ideal bonding surface with UHPC [83]. Plate 2.6 present the surface of the deck slab for NJ 57 over Hances Brook Bridge.

Plate 2.6 Hydrodilimiation of deck slab in practical [83].

2.4.2 Phased Construction Joints

UHPC overlays are often constructed in stages. An overlay is often put in place to keep traffic moving on a section of the bridge or because of the restrictions of the construction equipment. The transitions between stages of construction are marked by longitudinal joints as a consequence of this method. In addition, transverse construction joints may be required when there are large gaps between expansion joints. In such situations, it is essential to plan for and specify phased construction joints that are not only waterproof but also transmit stress. In order to achieve a strong link between the two UHPC phases, the hardened UHPC's surface must be properly prepared. As illustrated in Plate 2.7, one method for creating a strong link between hardened UHPC and fresh UHPC is to remove the solidified surface cement paste from the hardened UHPC and expose the fiber reinforcement. This outcome is attainable with the use of a set retarder and subsequent pressure washing or sandblasting [84].

Plate 2.7 Photo. Exposed fiber finish on a UHPC overlay construction joint [84].

2.5 Summary

1- One obvious drawback of concrete jacketing methods is the amount of effort required to complete the many steps involved. The mass and volume are both increased while living space is diminished due to jacketing's effect on the size of the members. Construction methods are disruptive to tenants, which might drive up the final cost of the renovation.

2- Steel plates attached externally to the beam were shown to be successful in flexural Strengthening, however, this method leaves the steel plate vulnerable to environmental degradation mechanisms like corrosion. The steel weight made it difficult and costly to set up these plates.

3- Logistically, it may be impossible to get access to the bottom of the structural member, where the concrete surface must be well-prepared for the FRP application. It was also discovered that extended exposure to moisture condition may result in considerable deterioration of the FRP-concrete bond strength and other issues when working with composite laminates subjected to compression. The resin components of FRP systems have physical and mechanical qualities that are affected by temperature and deteriorate at temperatures near and above their glass-transition temperature.

4- Strengthening flexural RC structures using UHPC has been a focus of research and development over the last years. The UHPC matrix is very dense and compact, which leads to great physical performance like reduced permeability and enhanced durability. Using UHPC to reinforce or repair RC structures has shown to be a successful and promising technology because of these qualities, especially when compared to more conventional methods.
5- Much attention must be paid to the debonding of the NC and UHPC layer, which may be prevented by roughening the beam and applying adhesives (epoxy).
6- As a consequence, it is important to undertake experimental investigations of the operation of the joints in the UHPC layer forced by the reality of the job (for instance, in roads, bridges, et.)

The present study aimed to enhance the flexural performance of RC beams by utilizing a thin UHPC overlay. A significant effort was dedicated to investigating the effects of construction joints in the UHPC overlay, which sets it apart from other studies. Additionally, the UHPC overlay was applied along the clear span of the beam to simulate the practical strengthening of the distance between the two supports. This differs from previous studies that applied the UHPC overlay along the beam. Moreover, the study examined the impact of UHPC reinforcement, including steel bars, GFRP bars, and steel mesh.

Chapter Three

Experimental Work

3.1 Introduction

The experimental program are described in this chapter. The materials, mix proportions, specimen preparation and curing, UHPC layer casting, and testing process are all described in depth, as well as the research methods utilized to achieve the goals outlined in chapter one.

Nineteen identical RC beams were tested under a four-point bending load; fifteen were strengthened with a UHPC overlay. Two specimens were made of NSC used as control specimens, and the other two, strengthened by 50 mm UHPC overlay, also served as control specimens, while the remind strengthened with 50 mm UHPC and investigated different factors, as discussed in the next sections. In the present study, two specimens were used as control specimens to know the accuracy of the results.

3.2 Identification of Specimens

Each strengthened specimen is designated in four parts to allow comparison and account. The first part (OS) refers to **O**verlay **S**trengthening. The second part represents the type of reinforcement in UHPC overlay (**N**=No reinforcement, **G**=GFRP reinforcement, **R**= steel rebar reinforcement, **M**= steel mesh reinforcement). While a third part represents the location of the construction joint in the UHPC layer (**0** =No joint, **1/2**=joint located at mid-span of overlay, and **1/3**=joint located at the third span of overlay)

respectively. Finaly, fourth part represents the shape of the construction joint in the UHPC layer (**K**=Key joint, **V**=Vertical joint). While the NSC specimens (control specimens) identified by C. Figure 3.1 illustrate the identification of the specimen.

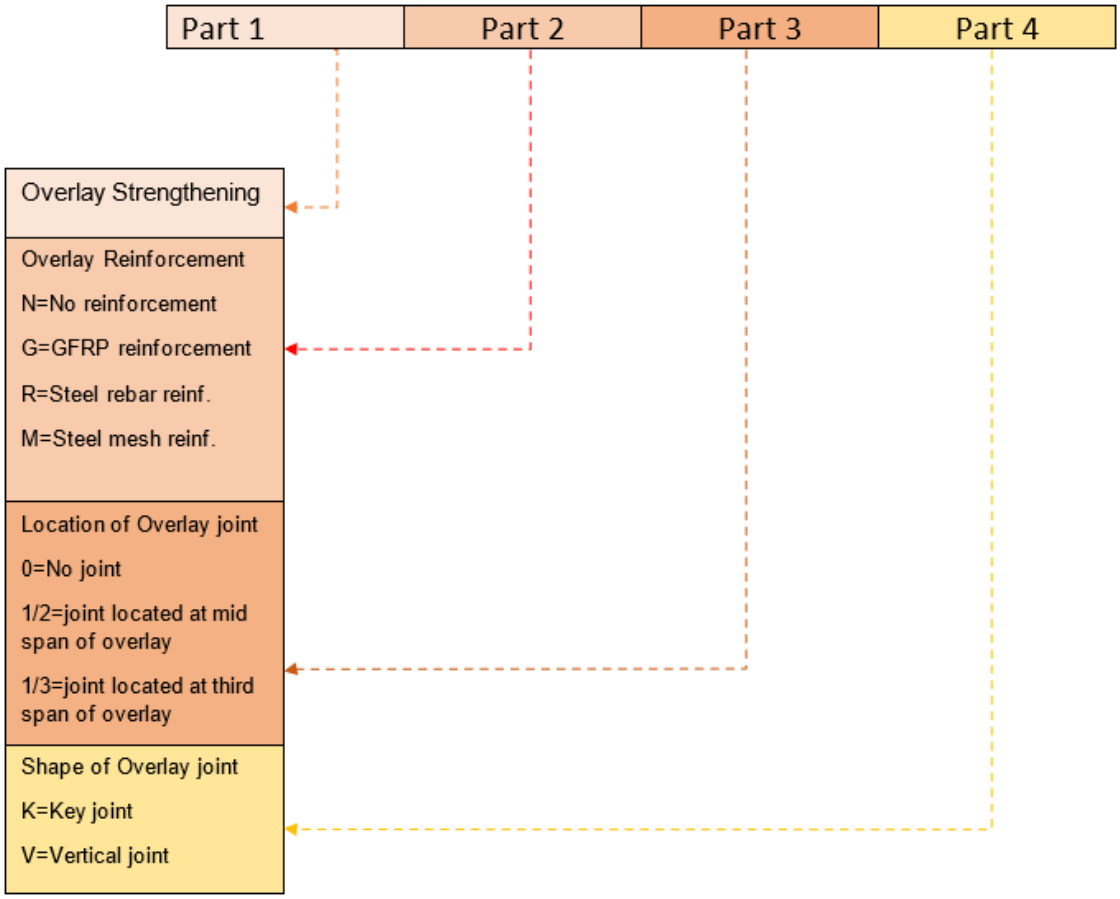

Figure 3.1 Specimens identification

3.3 Test matrix

The NSC beams were constructed according to ACI 318-19 [85], as shown in Appendix A, with a rectangular cross-section of 150 mm width, 200 mm total depth, and a total length of 2000 mm. 2Ø12mm was used as top and bottom reinforcement. However, Figure 3.2 illustrate the specimen details of the NSC beam (all dimensions are in mm).

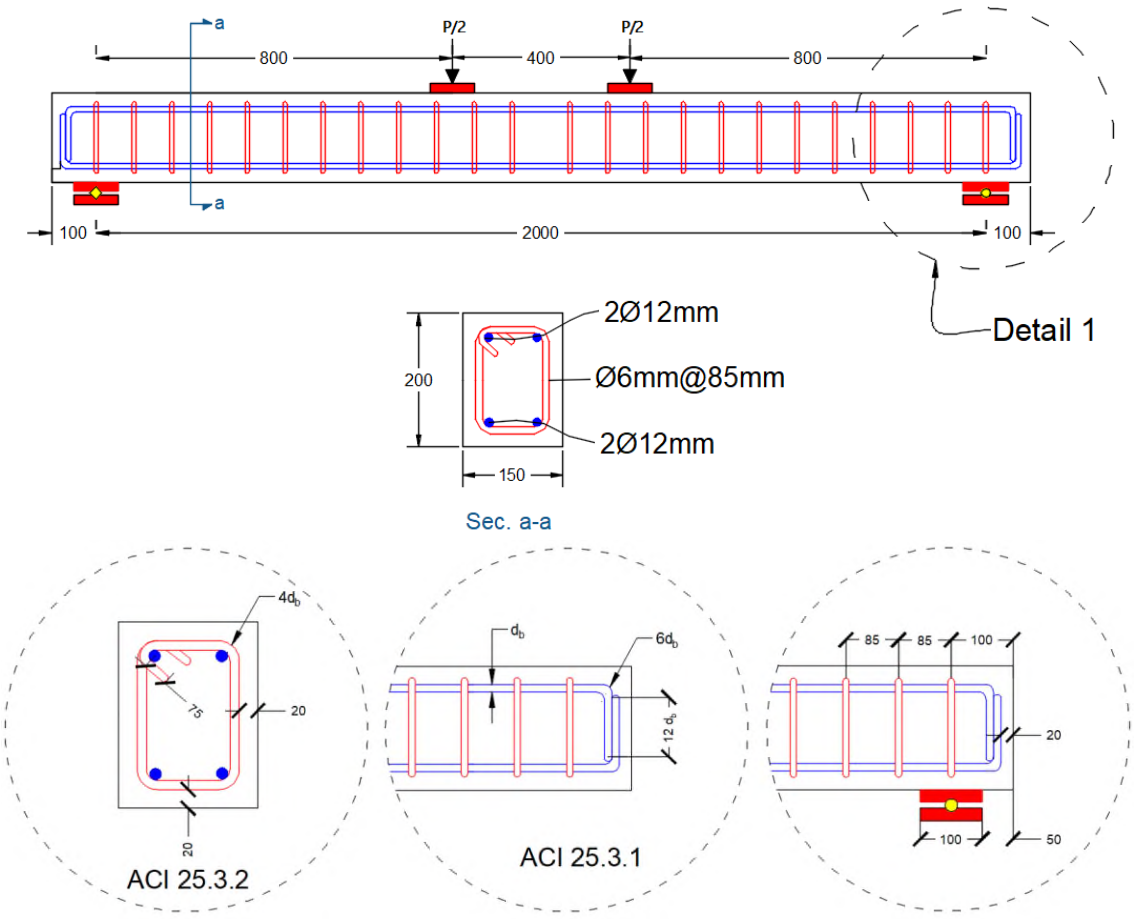

Figure 3.2 Reinforcement and geometrical details of NSC specimens.

As mentioned previously, two NSC beams served as control specimens, while the other two specimens were strengthened with a 50mm UHPC overlay to serve as control specimens also. In the present study, the UHPC overlay extended from face to face of supports to represent a practical case, as shown in Figure 3.3. Whereas most previous research utilized the UHPC

along the beam and extended throughout the supports, this is not true in practice.

The rest specimens were classified into two groups based on the shape of the construction joint in the UHPC overlay.

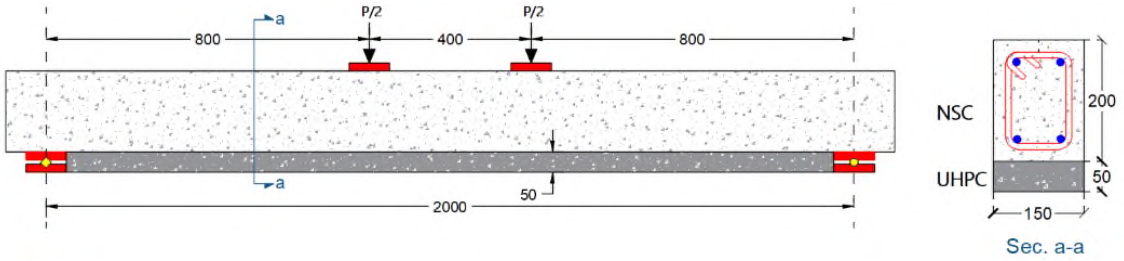

Figure 3.3. Strengthened specimen details.

3.3.1 K- Group

Seven specimens with a 50 mm UHPC overlay compensate the first group. The construction joint's position (middle of the span or the third span), the inclusion or absence of reinforcement in the UHPC overlay, and the kind of reinforcement were the independent factors. In this group, the key joint was used to limit shear flow and strengthen the bond. All the fine details of these specimens are shown in Figure 3.4.

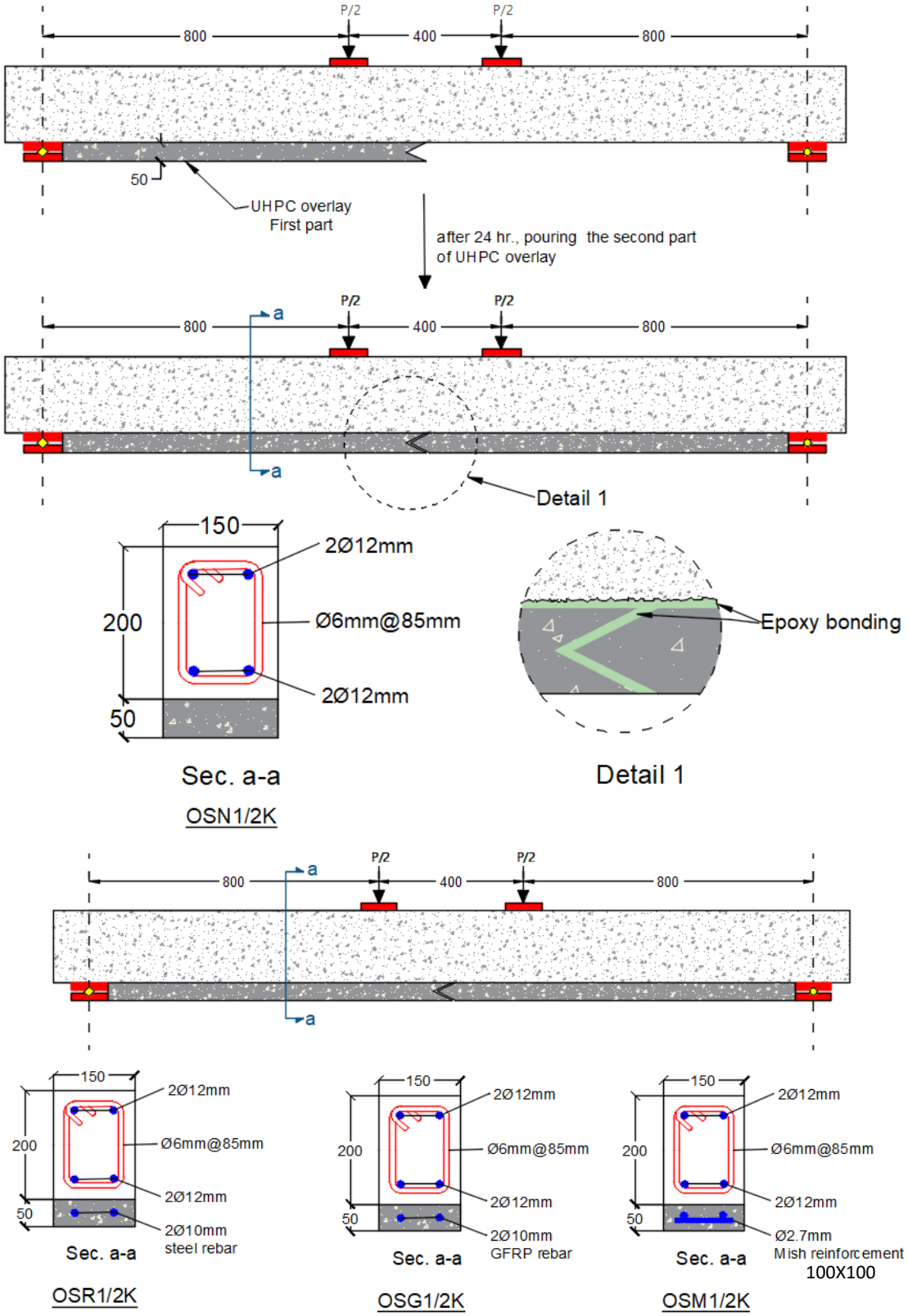

Figure 3.4 Geometry and reinforcement detail of specimens in K-group

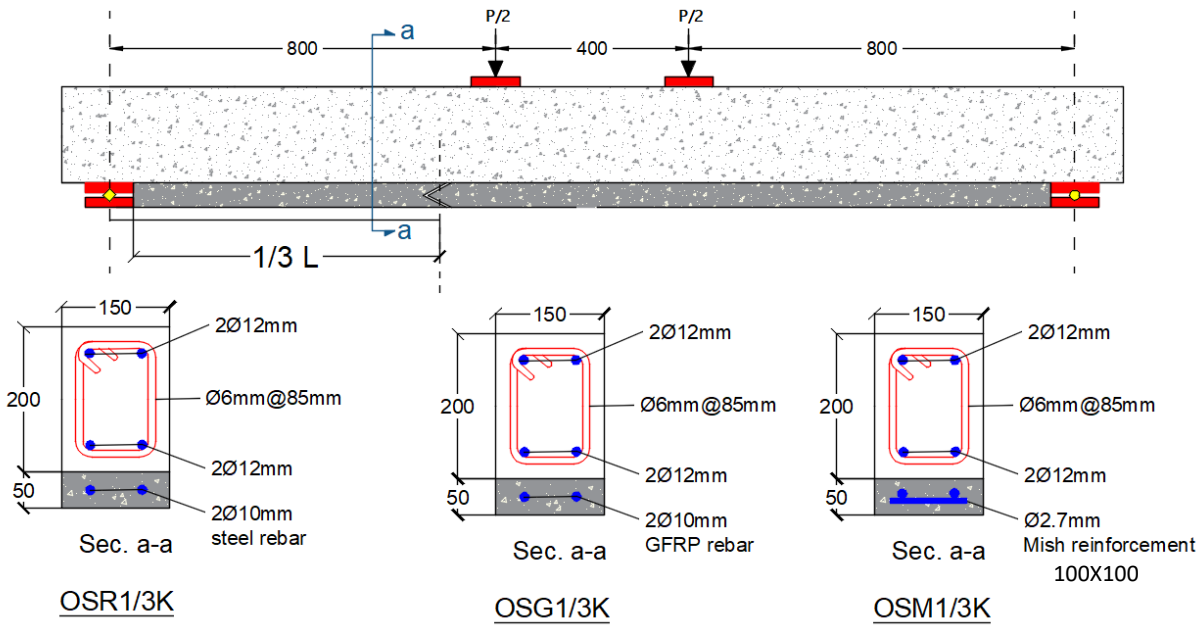

Figure 3.4 **Continued**, geometry and reinforcement detail of specimens in K-group

3.3.2 V-Group

Seven RC beams were strengthened with a 50 mm UHPC overlay, and the strengthening layer included vertical construction joints. The main variables were whether or not there was a construction joint in the UHPC overlay, whether or not reinforcement was used, what kind of reinforcement was used, where the construction joint was located (mid-span/third-span). Detail of the specimens in this group is shown in Figure 3.5.

Table 3.1 summarises the details and variables of tested RC beams in the present study.

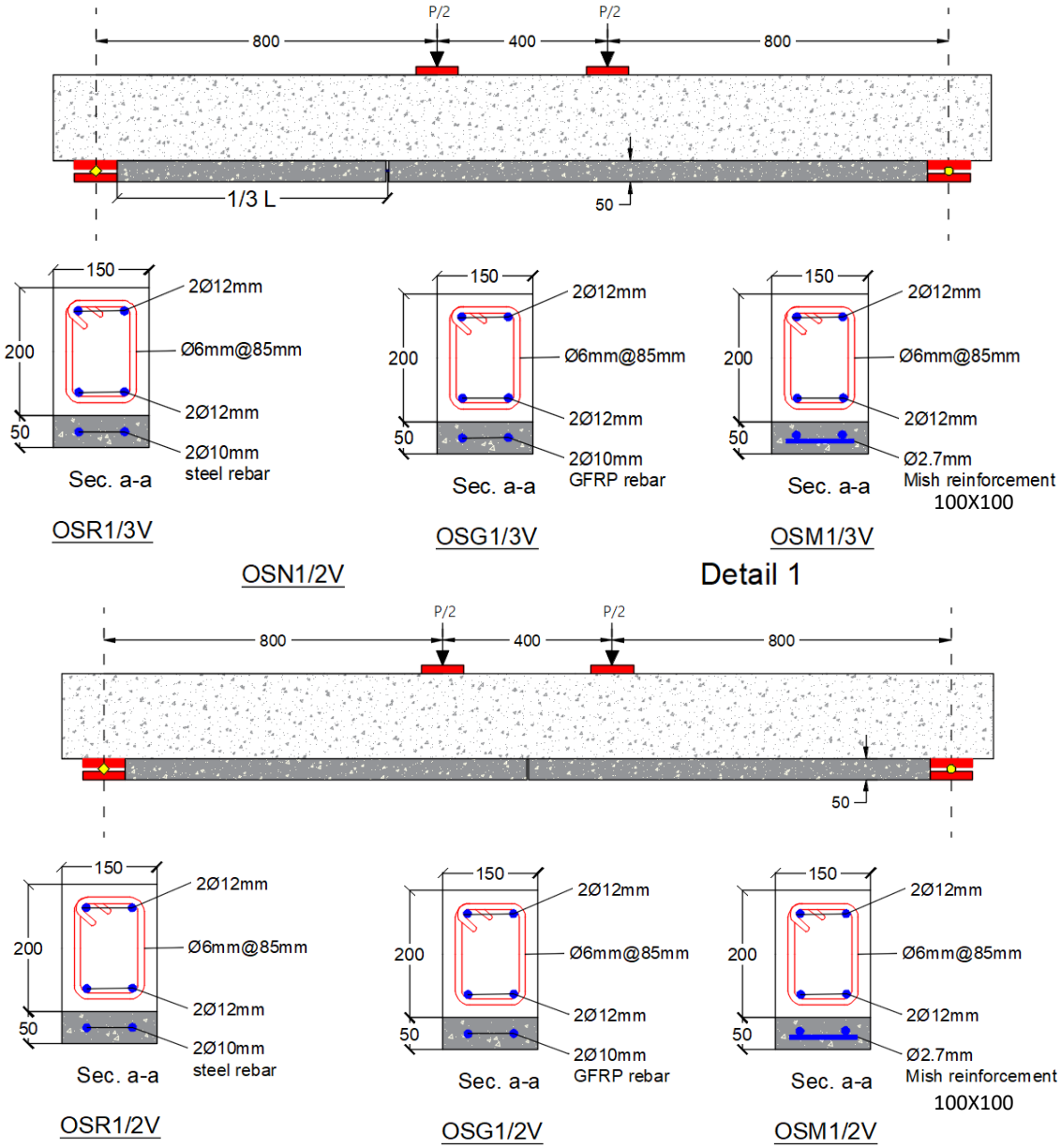

Figure 3.5 **Continoud**, Geometrical and reinforcement detail of specimens in V-group.

Table 3.1 presents a summary of details and variables of tested RC beams examined

No.	Designation	UHPC strengthening	Shape of joint	Location of joint	Type of UHPC reinforcement
1	C1	No	No	No	No
2	C2	No	No	No	No
3	OSN0	Yes	No	No	No
4	OSN0	Yes	No	No	No
5	OSM0	Yes	No	No	Mesh
6	OSN0.5K	Yes	Key	1/2	No
7	OSM0.5K	Yes	Key	1/2	Mesh
8	OSR0.5K	Yes	Key	1/2	Rebar
9	OSG0.5K	Yes	Key	1/2	GFRP
10	OSM0.33K	Yes	Key	1/3	Mesh
11	OSR0.33K	Yes	Key	1/3	Rebar
12	OSG0.33K	Yes	Key	1/3	GFRP
13	OSN0.5V	Yes	Vertical	1/2	No
14	OSM0.5V	Yes	Vertical	1/2	Mesh
15	OSR0.5V	Yes	Vertical	1/2	Rebar
16	OSG0.5V	Yes	Vertical	1/2	GFRP
17	OSR0.33V	Yes	Vertical	1/3	Rebar
18	OSG0.33V	Yes	Vertical	1/3	GFRP
19	OSM0.33V	Yes	Vertical	1/3	Mesh

3.4 Selection of materials and its fundamental characteristics

To ensure the production of adequate RC specimens, appropriate guidelines were followed during material selection, control, and ingredient proportioning processes. The experimental study thoroughly documented the materials used, including their sources, chemical composition, and physical properties. The study investigated two types of concrete: UHPC and NSC, and the properties of both fresh and hardened concrete, as well as the component mix and material quality, are detailed in the following sections.

3.4.1 Mix proportion of UHPC

The UHPC's exceptional strength is primarily caused by the high cement content, low water/cement ratio, silica fume, and well-graded components. Silica fume serves as a filler and a pozzolanic material in the UHPC mixture.

Micro steel fibers are added to reinforced the UHPC matrix. The addition of micro steel fibers to UHPC creates a composite material with improved properties, including increased tensile strength, ductility, and toughness. UHPC mixtures typically have a water/binder ratio of less than 0.2 [86]. With such a low water/binder ratio, however, UHPC needs a lot of superplasticizers to be practical.

In order to attain the required fresh and mechanical characteristics of UHPC, multiple trail mixes were conducted in the Engineering College laboratory at Al-Qasim Green University. The mixed percentage of UHPC shown in Table 3.2 was adopted in the current investigation based on many trail mix.

Because of its low water content, UHPC cannot be mixed using the same technique and time as NSC. It takes an average of 15 minutes to generate a homogenous UHPC mix, however, this might vary depending on the mixer type and the energy available to the mixer [86][87].

Table 3.2 The mix proportion of UHPC

Cement (kg/m^3)	Sand* (kg/m^3)	Silica fume (kg/m^3)	water/binder (%)	SP/binder (%)	Steel fiber (kg/m^3)
950	1050	190	15	3.5	157 (2%/m^3)

*Sand pass from sieve 0.6 mm

Plate 3.1. shows the preparation of material and mixing procedures. First, the dray material (cement, sand, and silica fume) was combined for 1-2 minutes. The liquid (water combined with superplasticizer) was progressively added and allowed for 12-15 minutes until the UHPC paste was flowable. The steel fiber was then progressively added to the UHPC paste and constantly mixed for 3-5 minutes until it was evenly dispersed throughout the paste. The UHPC is then ready to pour. The same procedure was used to cast the UHPC overlay of the full-scale RC beams with a high

shear mixer of 325 Liter capacity. Simultaneously, the flow test was conducted to ensure acceptable workability. The flow was examined based on ASTM 230 [88],[89]. It was found that the flow ranged between 230-240 mm. Plate3.2. illustrate the test procedure.

Pate 3.1 Preparation of material and mixing procedures.

Plate 3.2 Illustrate the flow test

3.4.1.1 UHPC constituent's material

3.4.1.1.1 Cement

Sulfate-resistant cement produced by the Lavarge Company in Iraq was utilized for this study. This cement is utilized in both UHPC and NSC. Tables 3.3 and 3.4 show the test result of the chemical analysis and physical conducted on the cement. This cement met I.Q.S.[90].

Table 3.3: Main components and chemical composition of AL-Jesr cement.

Chemical Composition	Percentage by Weight	Limit of IQSNo.5/1984
Lime (CaO)	61.25	-
Silica (SiO2)	19.78	-
Alumina (Al2O3)	3.41	-
Iron Oxide (Fe2O3)	4.8	-
Magnesia (MgO)	1.72	5.0
Sulfate (SO3)	2.29	2.8
Free Lime (free CaO)	0.914	-
Loss on Ignition (L.O.I.)	2.42	4.0
Insoluble Residue (I.R.)	0.85	1.5
Lime Saturation Factor (L.S.F.)	0.953	(0.66-1.02)%

Table 3.4: Physical properties of AL-Jesr cement

Physical Properties	Test Result	Limit of IQS NO. 5/1984
Specific Surface Area (Blaine Method) m2/kg	303	≥ 230
Initial Setting, (min)	1:10	≥ 45 min
The final setting, (min)	3:13	≤ 10 hrs
Compressive Strength at 3 Days (MPa)	17.39	>15
Compressive Strength at 7 Days (MPa)	27.06	>23

3.4.1.1.2 Fine sand

UHPC made with fine sand (passing 600 μm) has a sulfate concentration shown in Table 3.5. The sulfate levels complied with the specification (I.Q.S. No.45/1984) [91].

Table 3.5: The chemical properties of fine aggregate.

Properties	Test Results	Iraqi Specification No.45/1984
Sulfate Content	0.26	Max ≤ 5.0%

3.4.1.1.3 Micro Silica Fume (SF)

The ACI explains that silica fume is a form of silica that has undergone a thorough refining process, resulting in a non-crystalline structure. It is produced as a byproduct when manufacturing elemental silicon or silicon alloys using electric arc furnaces. It typically appears as a fine grey powder, resembling Portland cement or certain types of fly ash. Due to its highly reactive nature, silica fume is commonly used as a supplementary cementitious material in the production of high-performance concrete. Its addition to concrete mixes can improve the strength, durability, and resistance to various environmental factors such as freeze-thaw cycles and chemical attacks. Moreover, the use of silica fume in concrete production also contributes to sustainable development by reducing waste and carbon emissions associated with other industrial processes.There are two functions

for silica fume in the UHPC mixture. It may be used as a filler or pozzolanic material [22]. In the present study, a high-quality SF was used commercially named MasterRoc® MS 610 [21].

3.4.1.1.4 High Range Water Reducing Admixture

Master Glenium 54 [92] was used to develop the UHPC mix due to the high cementitious material content and low water to binder ratio. Master Glenium 54 is differentiated from conventional superplasticizers. This greatly improves cement dispersion. Produces steric hindrance at the outset of mixing, which controls the cement particle's ability to scatter and separate. Because of this technique, water use may be drastically cut down while early strength is increased in flowable concrete. Table 3.6 is taken from the manufacturer datasheet and details the product's physical and chemical characteristics.

Table 3.6 Typical properties High Range Water Reducing Admixture (HRWRA).

Form	Whitish to straw coloured liquid
Color	Grey
Density	0.55 - 0.7 kg/l
Chloride content	<0.1%

3.4.1.1.5 Micro Steel Fibers

In the current study, copper coated micro steel fibers were utilized as shown in Plate 3.3. These specific micro steel fibers were manufactured by Hebei YuSen Metal Wire Mesh, a company based in China [93]. Table 3.7 provides information on the characteristics of the steel fibers used, which conforms to the ASTM A820-96 standard [94].

Plate 3.3. photo of copper coated micro steel fiper

Table 3.7: Properties of Micro steel fiber.

Detected items	Diameter mm	Length mm	Tensile Strength	L/D
Standard Values	(0.2-0.25)	13± 10%	≥2850	30-100
Detected Values	0.2	13.1	3005	59

3.4.1.1.6 Water

In this study, all concrete mixes were prepared and cured using potable water sourced from the local water supply. The water used was free from organic matter, turbidity, and salts, ensuring that it did not contain any impurities that could negatively affect the properties of the concrete.

3.4.2 Normal Strength Concrete (NSC)

Ready NSC was supplied from a local concrete batching plant with a target compressive strength ($f_c^{`}$) equal to 30 MPa and slump of 15 mm. The cement used in NSC was the same type that was used in UHPC. While the other constituent materials were tested according to the Iraqi Standard Specification (IQS), as shown in tables 3.8, 3.9,3.10 and 3.11. The tables contain information regarding the various constituent materials used in the NSC, including their chemical properties, physical characteristics, and allowable limits.

Table 3.8 The physical properties of fine aggregate

Size of The Sieve(mm)	Cumulative Passing	Limits of IQSNo.45/1984 (Zone 2)
9.5	100	100
4.75	91.2	100-90
2.38	82.2	100-75
1.18	73.6	90-55
0.6	55.6	59-35
0.3	17.6	30-8
0.15	3.6	10-0

Table 3.9: The chemical properties of fine aggregate.

Properties	Test Results	Iraqi Specification No.45/1984
Fine Material Passing from Sieve (75 µm)	3.2	Max ≤ 5.0%
Sulfate Content	0.27	Max ≤ 5.0%

Table 3.10 The physical properties of coarse aggregate

Size of the Sieve (mm)	Cumulative Passing	Limits of IQ No.45/1984 a
37.5	100	100
20	97	100-95
9.5	39.4	60-30
5	3.4	10-0

Table 3.11: The chemical properties of coarse aggregate.

Properties	Test Results	Iraqi Specification No.45/1984
Fine Material Passing from Sieve (75 µm)	1	Max ≤ 3.0%
Sulfate Content	0.04	Max ≤ 0.1%

Plate 3.4 Insert pic for slump test and truck mixer.

3.4.3 Mechanical Properties of Reinforcement Bars

NSC beams and the UHPC overlay were reinforced using deformed steel bars of 10 mm in diameter for longitudinal reinforcement and 6 mm in diameter for transvers reinforcement. However, GFRP bars and steel mesh were used for reinforcing the UHPC overlay. The mechanical properties of these bars are listed in Table 3.12, based on test results and manufacturer datasheet value.

Table 3.12: Specifications and test results of steel reinforcing bars according to [95]

Material	Diameter (mm)	fy (MPa)	fu (MPa)
Steel	12	493	663
Steel	10	501	687
Steel	6	400	620
Steel mesh	2.7 (100X100)	277	277
GFRP[1]	10	….	827

[1] as per the manufacture datasheet

3.5 Casting Specimens

Before casting the specimens, the steel reinforcement was prepared based on section 3.3. Plate 3.5 illustrate the cast process. The following stages describe the process of casting:

1) Prepare the steel reinforcement of all specimens.
2) The twelve wooden molds were oiled on their inner side faces and laid flat on the ground.
3) A plastic spacer was used to position the reinforcement inside the molds such that all sides would be covered by 20 mm.
4) A modified hydrodelimination technique mentioned in section 2.4.1, was used to roughen the tension surface of specimens [83]. The modification was by coating the bottom of the mold with a plasticizer before pouring the normal concrete into the molds, to delay the hardening of the concrete. Resulting in saving time and roughening the surface with less water pressure.
5) After that, concrete was poured into molds and vibrated well.
6) At the same time, the samples of concrete were taken in the form of cubes, cylinders, and prisms to evaluate the mechanical properties.
7) A day after casting, the specimens were taken out of their wooden molds and reversed so that the tension side was facing outward. Washing away the concrete with a high-pressure water jet exposed the aggregate, which roughened the tension side and strengthened the connection between the UHPC and NSC.
8) The samples were cured in a water tank, while beams were covered with damp burlap and let to dry out. Casting prose is shown in Plate 3.6.

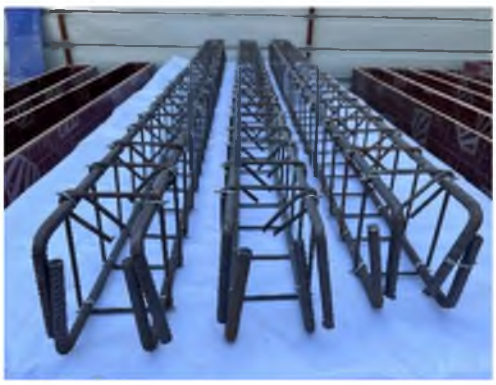

a)steel bar reinforcement detail

b) paint the mold by oil

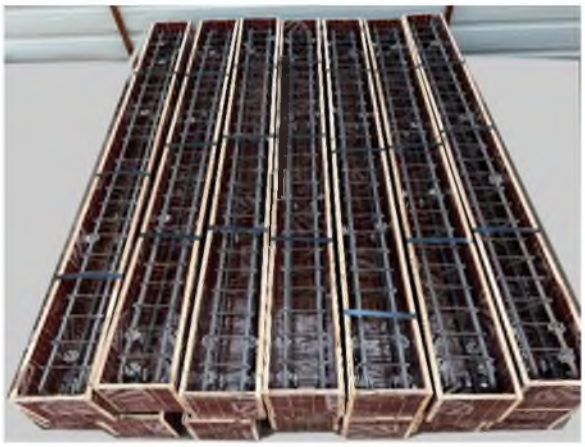

c) preparing models for casting

d) ensure concrete cover

e) Concrete pouring

Plate 3.5 illustrate the casting prosses.

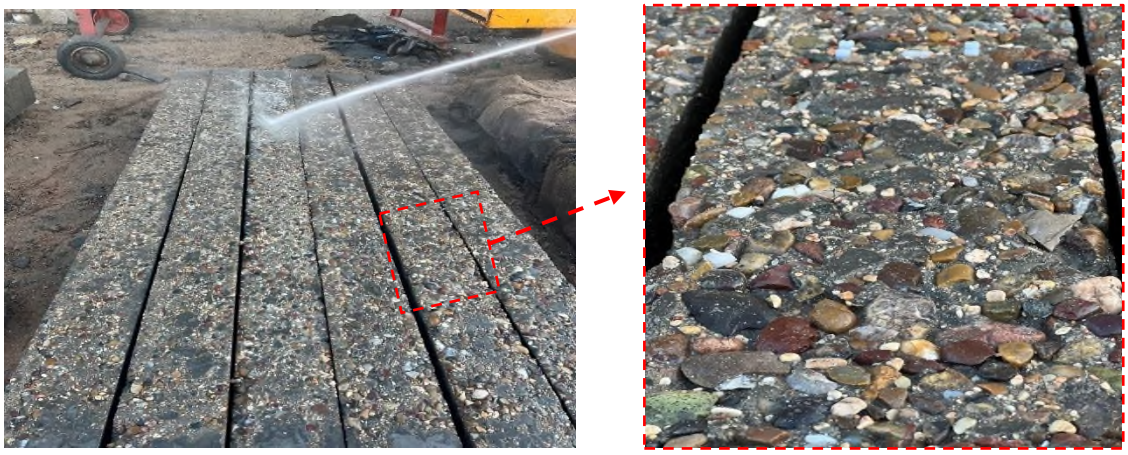

a) Water-jetting b) Rough surface

c) Casting the sample d) Curing the sample

Plate 3.6 Illustrate rough surface and curing.

3.6 Strengthening the specimens with UHPC overlay

Following their casting, the specimens underwent a curing process for a total of 28 days under carefully controlled conditions. Once the curing process was completed, the tension surface of the specimens was subjected to a water jetting treatment to clean the surface and remove any contaminants that may have accumulated during the curing process. Afterward, the surface was dried using a vacuum air system to ensure that it was completely free of

moisture, which could compromise the bond between the NSC and UHPC layers.

Before casting the UHPC layer, a commercially available epoxy bonding agent called Netbond EP [96] was used as per the manufacturer's recommendations. The bonding agent was left to set for approximately 2 hours. The first UHPC layer, which had a thickness of 50 mm, was then cast according to the configuration specified in the previous section. After waiting for 24 hours, the second UHPC layer was cast in the same way. The specimens were then left to cure for approximately 28 days. It is noteworthy that UHPC samples in cube, prism, and cylinder shapes were all cast at the same time. Plate 3.6 provides an illustration of the strengthening procedure that was carried out using the UHPC overlay.

a) Clean surface b) install mold c) Preparation epoxy d) Coating epoxy

g) casting UHPC layer

h) casting part 2 i)Casing cubic &cylinder j)shape joint

Plate 3.7 Illustrates the strengthening procedure using the UHPC overlay.

3.7 Testing Procedure

3.7.1 Test setups

On the day preceding the test, the surface of the beam specimen was thoroughly cleaned and coated with light-colored paint. Next, the beam was positioned in the testing location and checked for levelness before securing the LVDT in place. During the testing process, the primary characteristics of the structural behavior of the specimens were recognized at each stage of loading. Each test recorded important information such as the initial occurrence of a crack, the amount of displacement at the midpoint of the span, the rate of crack growth, the maximum load applied, and the type of failure that ultimately occurred.

In Plate 3.8, the configuration of the tested specimens is shown. For all tests, a four-point bending test configuration was used. The two supports of the beams were separated by 2000 mm. Two concentrated loads spaced 400 mm apart were applied to each beam until it collapsed. When the applied load decreased below 80% of the test peak load, the test ended. The load was applied using a 500 kN hydraulic actuator with a 0.5 kN/sec loading rate. To measure the applied load, a load cell with a 300 kN capacity was used. A vertical linear variable differential transducer was used to measure the vertical mid-span displacement (LVDT). In order to monitor the relative slip between the UHPC layer and the NSC, three horizontal LVDT were also mounted to the sides of both the normal concrete beam and the UHPC layer.

In order to monitor the specimen's deformation using a digital image correlation (DIC), half of one side of the specimen was also marked with black ink as illustrated in Plate 3.9.

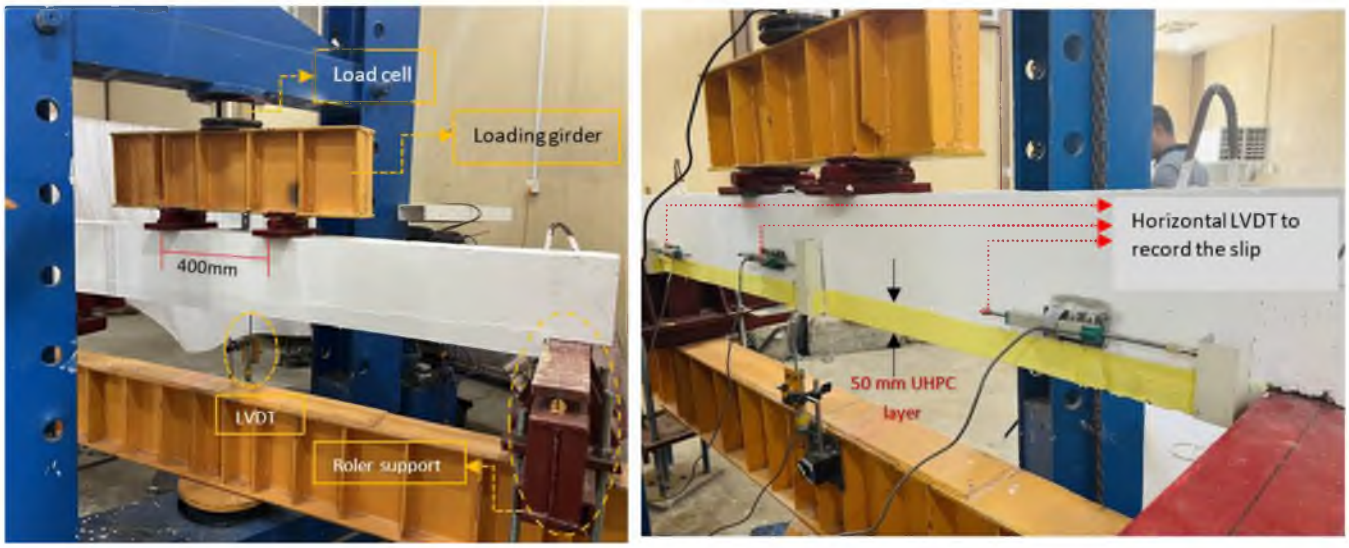

Plate 3.8 Test setup and loading condition

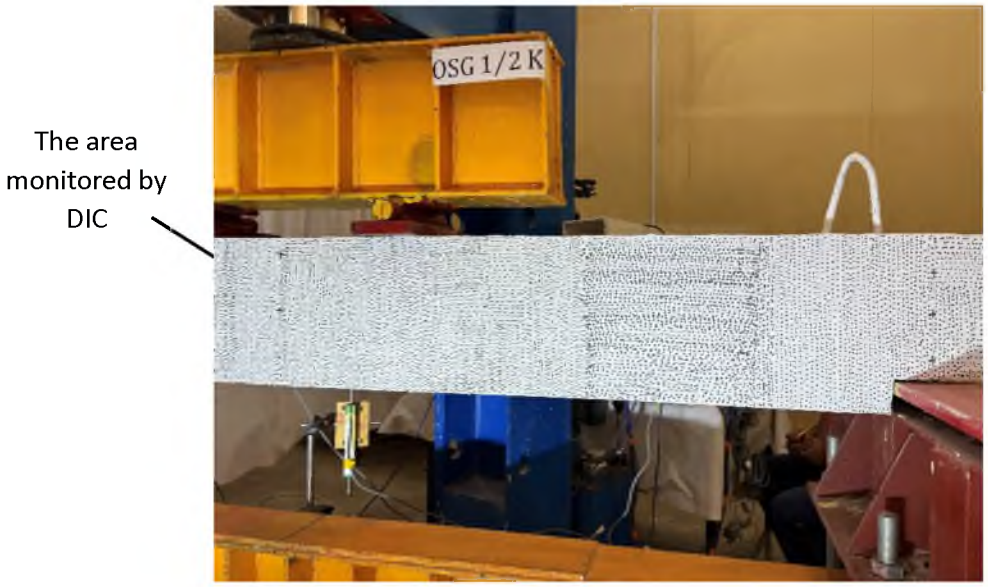

Plate 3.9 A digital image correlation (DIC).

3.8 Mechanical Properties of Concrete

3.8.1 Mechanical properties of UHPC

3.8.1.1 Compressive Strength ($f_c^{`}$)

One of the key technical characteristics of concrete that may provide a general idea of its quality is its compressive strength. Based on references [97]–[101] the compressive strength of the UHPC cube is very close to that resulted from testing the cylinder sample, therefore a cube with sides of 50 mm was utilized to assess the compressive strength of UHPC According to ASTM C109 [102]. A universal testing device with a 1900 kN capacity was used to determine the compressive strength with loading rate loading rate of 0.75 MPa/sec as suggested by ASTM C1856 [103]. The average compressive strength of 60 samples was 138.18 MPa, the standard deviation was 4.55MPa. Plate 3.10 presents the test method and failure mode of the tested cube.

Plate 3.10 The test method and failure mode of the tested cube

3.8.1.2 Splitting Tensile Strength

ASTM C496 [104] was used to assess the splitting tensile strength of UHPC. Six cylindrical UHPC specimens measuring 100x200 mm were fabricated

for the testing process. The testing machine was set up by placing the specimens between its bearing blocks, with two bearing wooden strips. universal testing machine of 1900 kN capacity was used to examine the specimen as depicted in Plate 3.11. The splitting tensile strength was 13.82 MPa, with a standard deviation of 0.99 MPa.

Plate 3.11 Splitting tensile strength test.

3.8.1.3 Modulus of Rupture

Nine samples of UHPC prisms (100×100×400 mm) were tested according to ASTM C78 [105] to calculate the modulus of rupture. Four-point loading was applied to the prisms in a testing machine with a 1900 kN capacity (as seen in Plate 3.12). The standard variation in the modulus of rupture was 1.43 MPa, with a strength of 18.23 MPa.

Plate 3.12: Flexural strength test and machine

3.8.1.4 Direct Tensile Test

To estimate the direct tensile strength of UHPC, recommended dog-bone-shaped specimens outlined by Qiao et al. [106] were utilized. To maintain a quasi-static condition during testing, a low loading rate was employed, as suggested by Qiao et al. [106]. A universal testing machine with 1000 kN capacity was used to conduct the test at AL-Mustaqbal College. LVDT has been installed at the center of the dog-bone specimen along the loading path to record the change in length. The applied load and change in length were recorded simultaneously by two cameras. Plate 3.13 illustrates the test preparation. The average value direct tensile test of three specimens was 9.86 MPa. Figure 3.6 present the tensile strength vs strain of UHPC. Table 3.13. summarizes the average value of mechanical properties of UHPC.

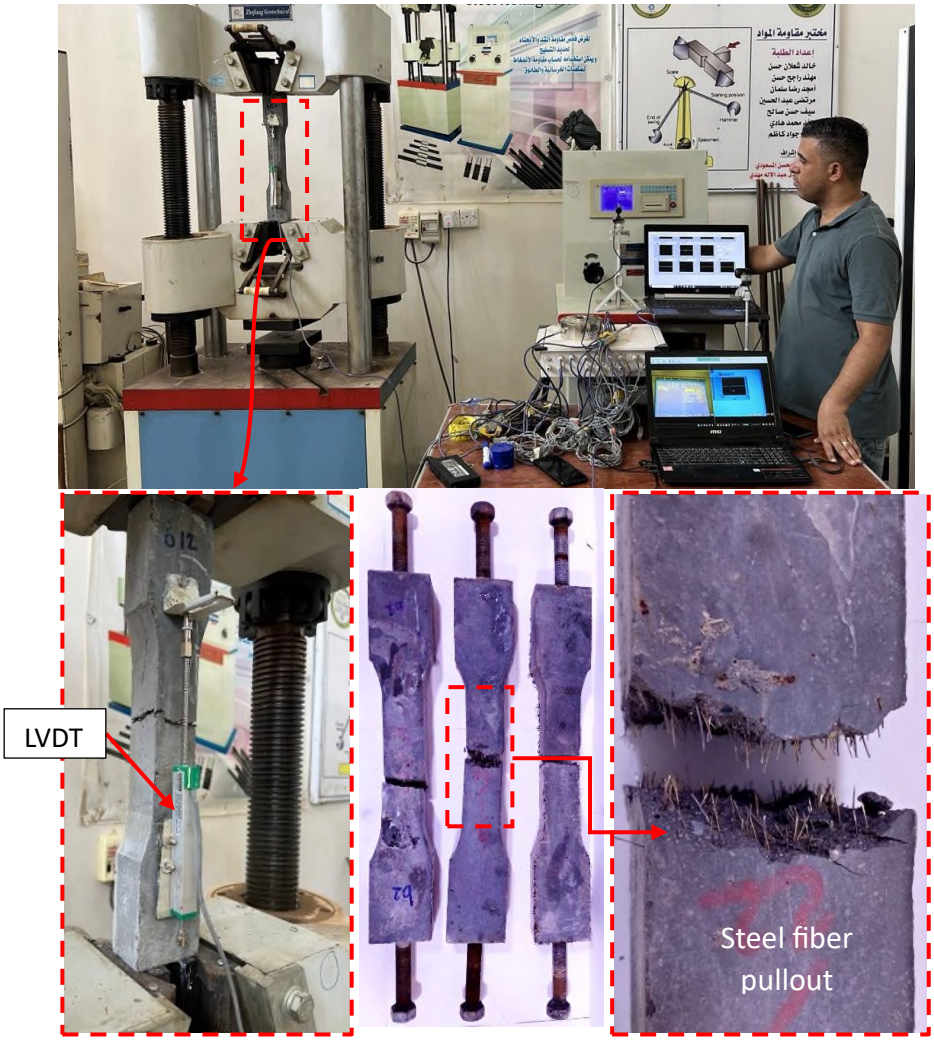

Plate 3.13 Illustrates the test preparation

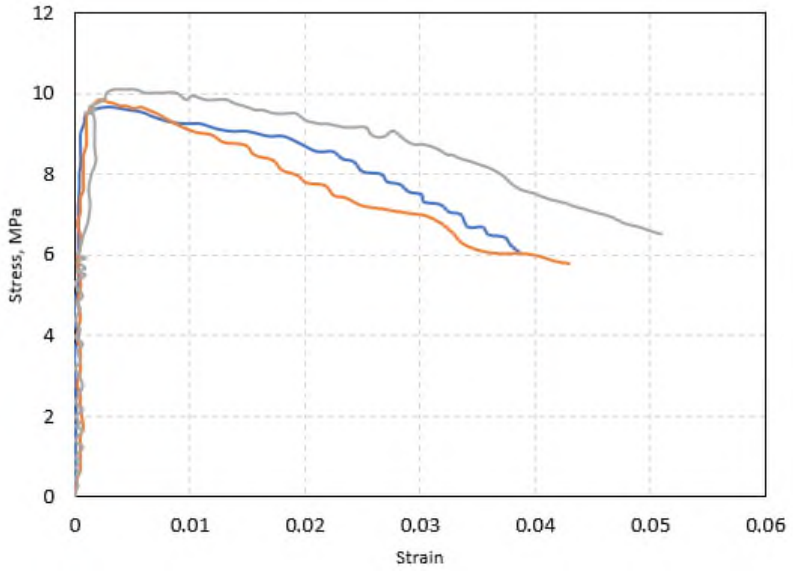

Figure 3.6 Present the tensile strength vs strain of UHPC.

Table 3. 13 Test results of UHPC Mechanical properties

Type of test	Test method	Value
Compressive strength	ASTM C109 [107] ASTM C1856 [103]	138.31MPa
Modulus of rupture (f_r)	ASTM C78 [105]	18.23MPa
Splitting tensile strength (f_t)	ASTM C496 [104]	13.82 MPa
Direct tensile test (f_D)	Zhou and Qiao [106]	9.86 MPa

3.9 Mechanical properties of NSC

3.9.1 Compressive strength

To create the NSC sample, molds with dimensions of 150 × 150 × 150 mm were utilized. The tests were conducted in the laboratories of the University of Babylon's Department of Civil Engineering using 2000 kN universal machine, as demonstrated in Plate 3.14. The results of the concrete cube compressive strength test are presented in Table 3.13. The average compressive strength of 24 sample was 38.28 MPa with a standard deviation of 2.39 MPa. These values indicate that the NSC models were able to achieve the expected strength requirements for their intended use.

Plate 3.14 Compressive strength testing machine

3.9.2 Splitting tensile strength

The splitting tensile strength is a crucial mechanical characteristic that is considered in structural design. In order to estimate the splitting strength of cylindrical concrete specimens with dimensions of 150 × 300 mm baced on ASTM C496 [104], as illustrated in Figure 3.15. The test results revealed an average splitting tensile strength of six samples was 3.22 MPa, with a standard deviation of 0.45 MPa.

Plate 3.15 The test result of splitting tensile strength

3.9.3 Flexural strength (modulus of rupture)

The modulus of rupture test is a method to estimate the flexural strength of concrete. In this test, a three-point bending setup is used to evaluate the specimen's ability to withstand bending stress. The specimens used in this study were12 samples of 100mm × 100mm × 400mm in size, and the test was conducted using a universal testing machine, as shown in Plate 3.16. The results of the modulus of rupture test are presented in Table 3.14, with an average value of 5.14 MPa and a standard deviation of 0.4 MPa.

Plate 3.16 The modulus of rupture test.

Table 3. 14 Test results of NSC Mechanical properties

Type of test	Test method	Value
Compressive strength (cube)	BS EN 12390-3[108]	38.28 MPa
Modulus of rupture (f_r)	ASTM C78/C78M[105]	5.14 MP
Splitting tensile strength (f_t)	ASTM C 496 [104]	3.22 MPa

Chapter Four

Results and Discussions

4.1 Introduction

This chapter discusses the results of tests performed on 19 RC beam specimens. The specimens were classified as either K-group or V-group, based on the construction joint shape.

The importance of the various experimental factors was explored by comparing the results of the various experiments. Maximum load-bearing capacity, crack and failure mechanism, bond slip between the existing concrete and UHPC overlay, and load-displacement relationships were the key value used for assessment. Ductility, stiffness, and energy absorption were estimated using the predicted load-displacement relationships and compared.

4.2 Failure mode and cracking pattern

4.2.1 Crack pattern and failure mode of control specimens

The first visible crack appeared in the control specimen (C) at load 12 kN under the point load. As the load increased, new flexural cracks developed along the beam. When the load level reached 25 kN, the cracks propagate along the depth of the section and widened. Finally, the area between the two-point load was crushed at 63 kN, and the load dropped slowly. As

expected, the failure mode was a pure flexural failure. This is exactly what happened for the second control specimen. Plate 4.1 present the Failure mode and cracking pattern of control specimens (C1 and C2).

Also, two specimens OSN0 were also examined, and the results showed a similarity in the behavior and failure mode. Strengthening the specimen using unreinforced UHPC layer (OSN0) delays the appearance of the first crack, increases the stiffens, and increases the ultimate load by about 11%. The first visible crack appears at load level 25 kN. As the load increases, an additional crack is generated but less than what was observed in normal strength control specimens. The UHPC overlay shows multi-hairline cracks along with the UHPC layer. Finally, the specimens failed in flexural mode. Plate 4.2 presents the failure mode and cracking pattern of UHPC control specimens.

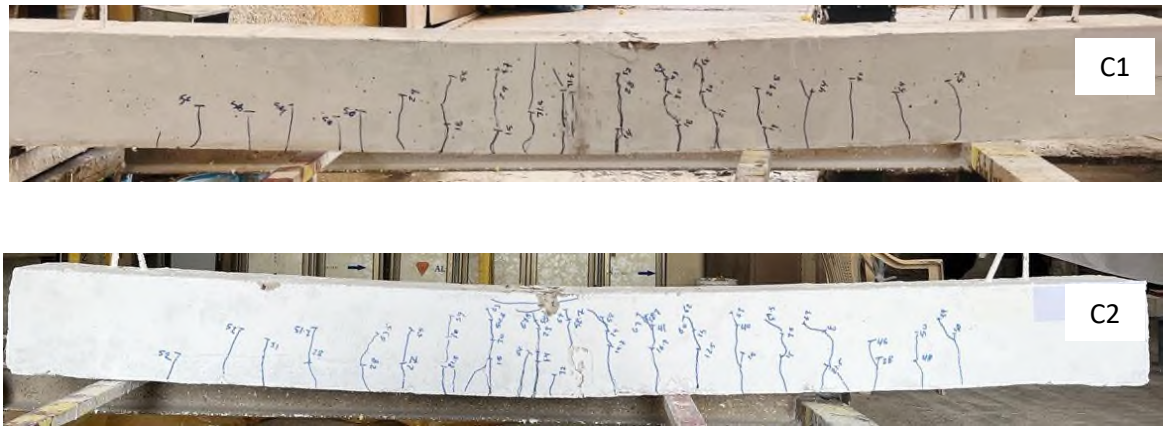

Plate 4.1 the crack pattern and failure mode of both NSC beams (C1 and C2)

Plate 4.2 the crack pattern and failure mode of both strengthened beams OSN0.

The load-deflection response of specimens C1 and C2 are shown in Figure 4.1. The average response to load-deflection is shown by the dashed line. The selection of two specimens with the same features allows researchers to assess the validity of their study, and it is evident from Figure 4.1 that both specimens exhibit the same behavior.

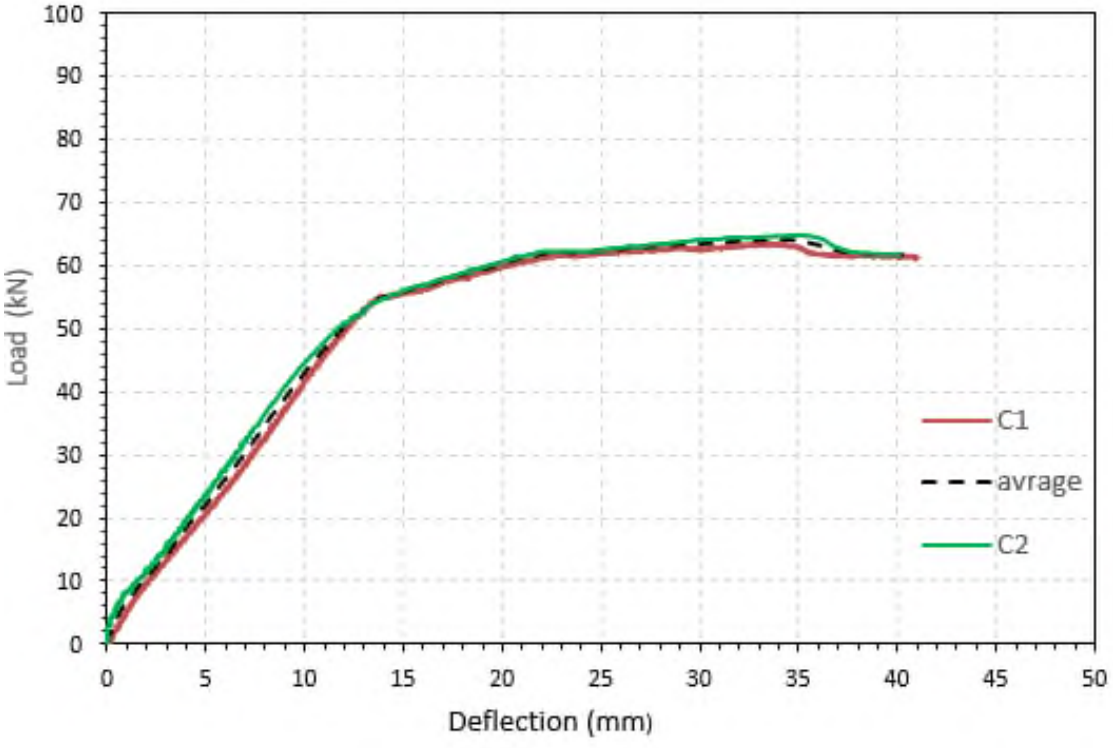

Figure 4.1 Load-deflection response of control specimen (C).

The load-deflection response of the control specimen can be divided into three parts. The first part behaves in linear responses till yield at approximately 55 kN; after that, the specimens show strain hardening till the ultimate load of 63 kN. Then the compression zone is crushed and the load drop slowly.

Although the failure of control specimen (C) is similar to OSN0, the load-displacement response differs from NSC specimens, as shown in Figure 4.2. The behavior of OSN0 was stiffer than the NSC specimen due to the UHPC strengthening layer. In addition, the yield point was not observed clearly as in NSC specimens.

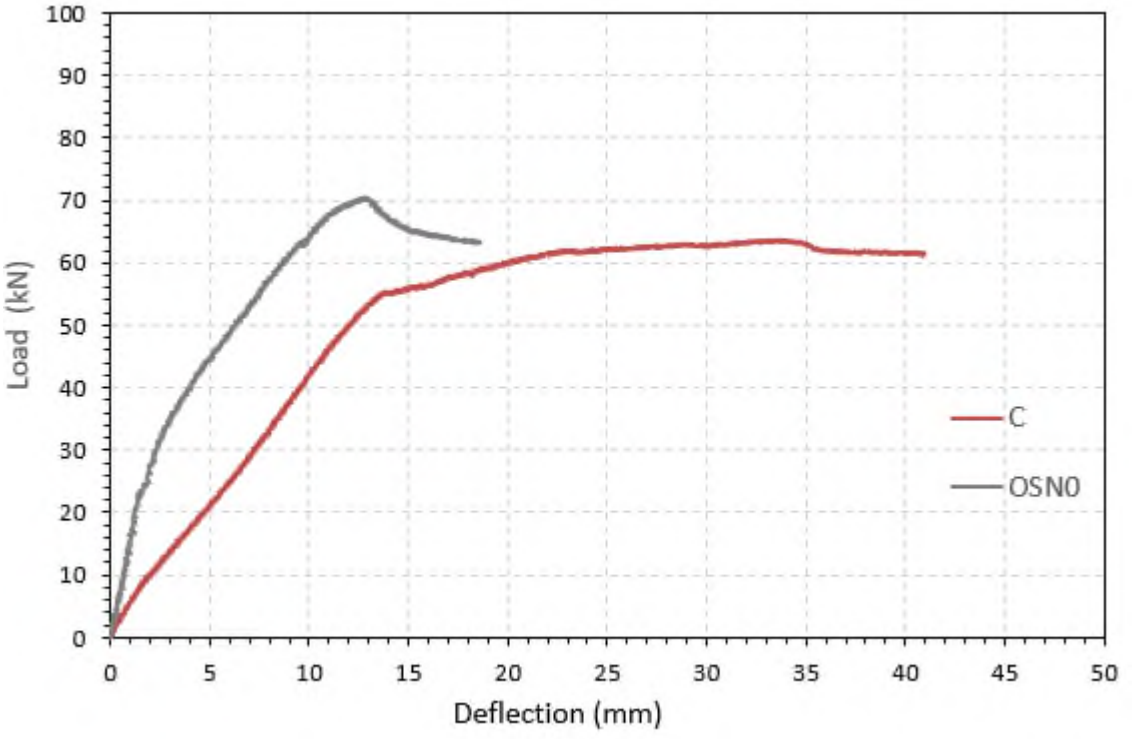

Figure 4.2 Comparison of the OSN0 specimen's load-deflection response to that of the control specimen.

4.2.2 Crack pattern and failure mode of the K-group

Figure 4.3 presents the failure prosses of the tested specimens that were monitored by the DIC technique. The tested specimens exhibited two types of failure modes. The first type was a pure flexural failure, which controlled

the behavior of the control beam, as well as the specimens that were strengthened with an unreinforced UHPC layer or reinforced with steel mesh. In this mode of failure, the beam developed multiple flexural cracks at the maximum tension stress zone, which extended throughout the depth of the beam as the load increased, as depicted in Figures 4.3(a),(b), and(c).

Another failure mode was observed in the beams that were strengthened with a UHPC overlay reinforced by steel bars/GFRP bars, which was concrete cover separation. In this mode of failure, flexural cracks appeared along the beam, and a diagonal crack was formed at the corner of the support just before the sudden cover separation occurred. It is noteworthy that concrete cover separation occurred away from the UHPC-NSC interface due to the strong bond that exists between the two materials.

The presence of a joint in the UHPC overlay diminished the effectiveness of the strengthening method even with using a key joint. due to the crack opening at the interface of the joint and propagating upward rabidly.

The specimen OSN0.5K shows similar behavior to NSC specimens (control specimens), with significantly improving the stiffness. The first crack was noted at 9 kN in the interface of the construction joint. No significant cracks were observed in the UHPC overlay until the final stage, this indicates that the UHPC overlay work effectively. With increasing the applied load, the first crack propagates horizontally 20 mm away from the interface between the UHPC and normal concrete and then behaves similarly to the control specimen, as shown in Plate 4.3.

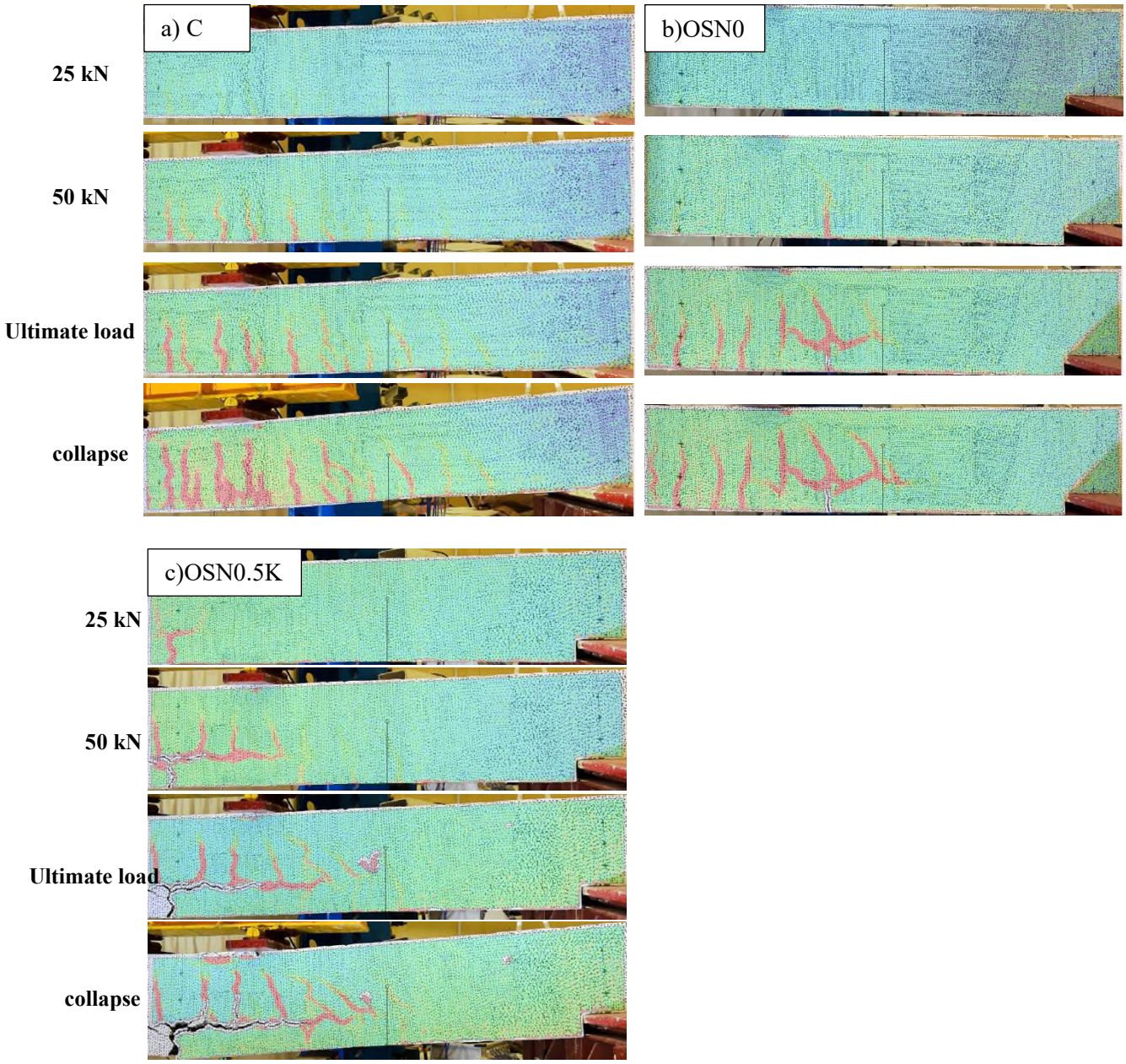

Figure 4.3 Failure process of selected specimens in K-group.

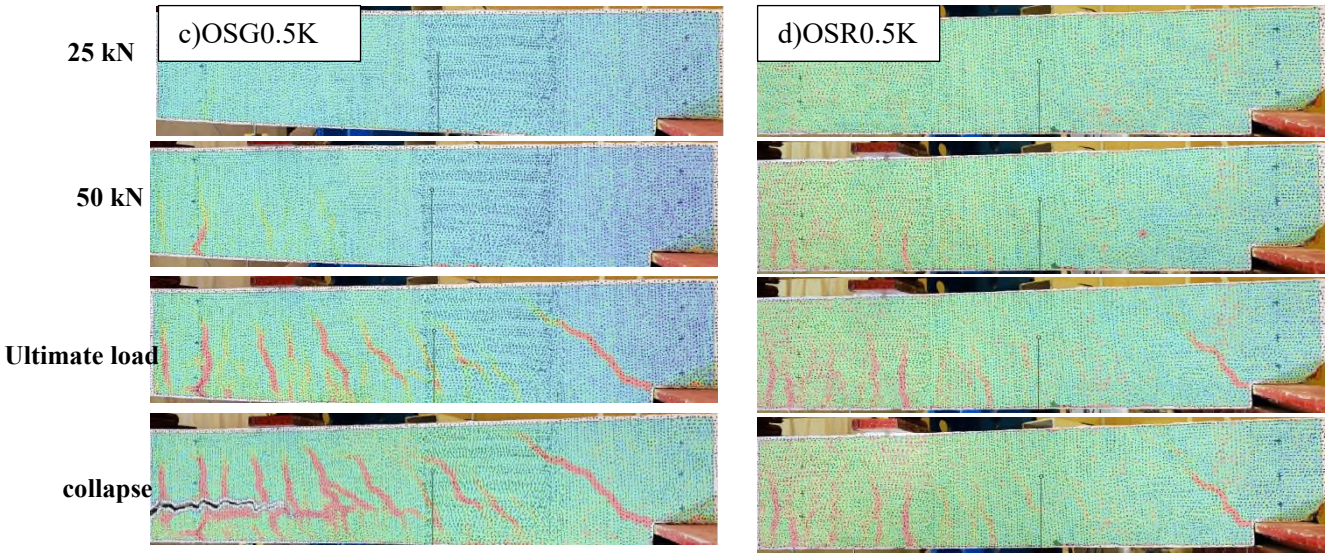

Figure 4.3 continued

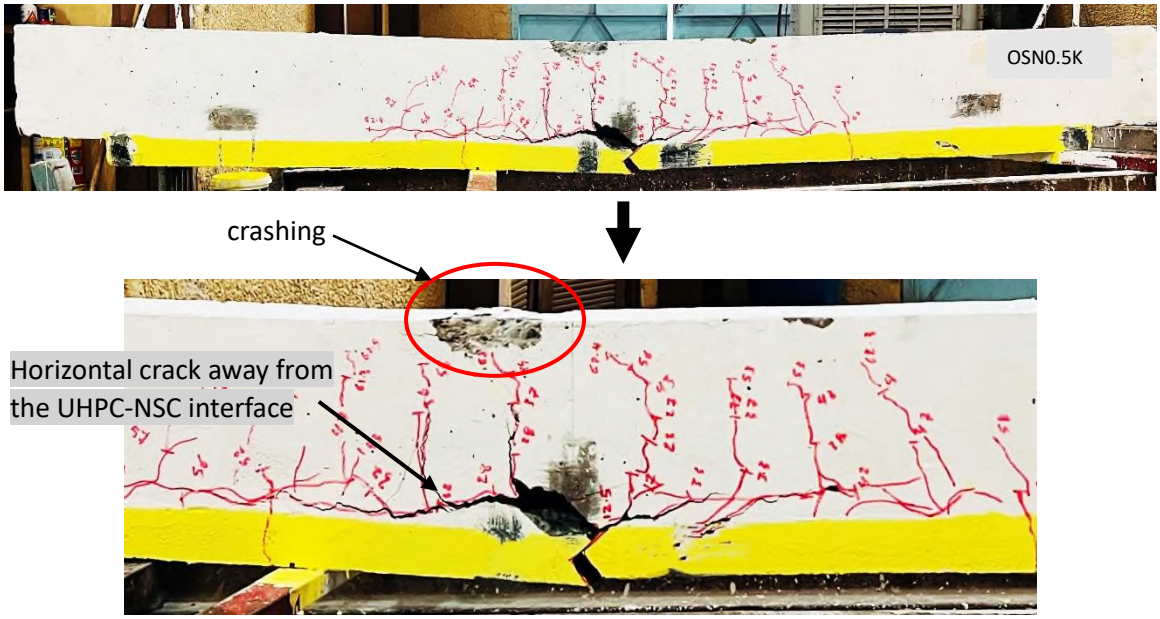

Plate 4.3 The crack pattern and failure mode of specimen OSN0.5K.

Adding steel mesh to the UHPC overlay with the key joint shows a slight improvement as shown in the behavior of the specimen OSM0.5K. This may be due to insufficient reinforcement used in the UHPC overlay. The first crack appeared at the key joint interface at 17.5 kN. As the loading prosses, the crack at the joint interface propagates and extends horizontally to the left

and right side. After that, the flexural cracks generated along the beam and started from the horizontal cracks. Finally, the specimen failed in flexural mode after the load reached 66.64 kN. Plate 4.4 show the crack pattern of specimen OSM0.5K.

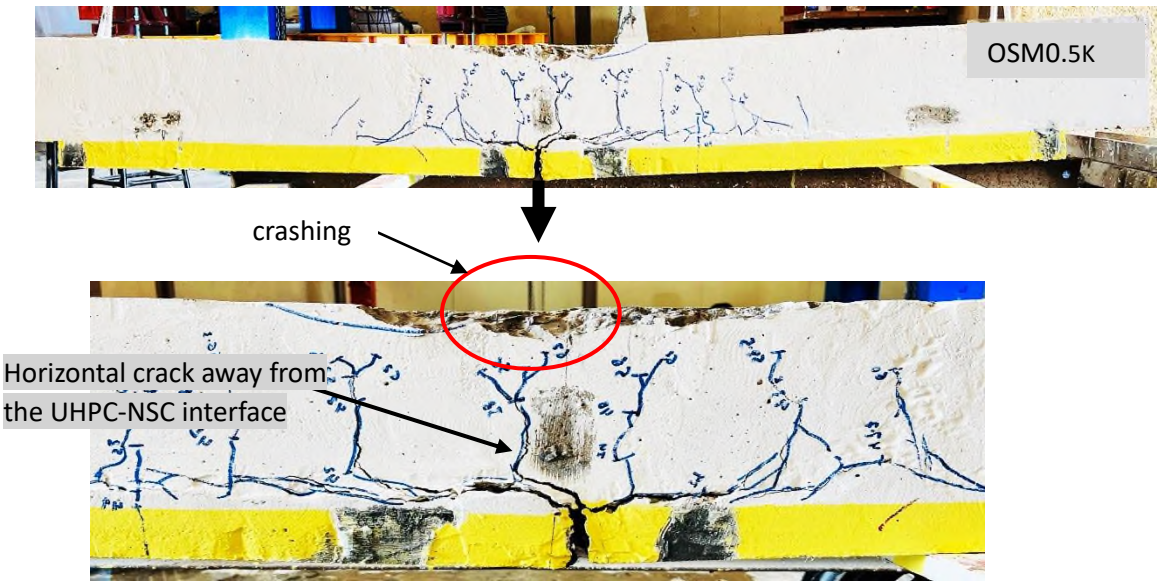

Plate 4.4 The crack pattern and failure mode of specimen OSM0.5K.

However, utilizing a steel bar or GFRP bar to reinforce the UHPC overlay even with the construction joint in the middle and third span of the specimens (OSR0.5K, OSR0.33K, OSG0.5K and OSG0.33K) improves the performance of the strengthening technique by increasing the load-bearing capacity, stiffness and eliminating the cracking width as well as the flexural crack distributed along the span. It was noted that the specimens reinforced GFRP had a higher ultimate load than the specimens reinforced steel rebar, and the load-bearing capacity was higher when the construction joint moved away to the third span.

Generally, the first crack was observed at the joint interface. The flexural crack was generated along the UHPC overlay and distributed at a distance equal to 100 mm. The result indicated that reinforcing the UHPC overlay by

both steel bar/GFRP diminishes the effect of the construction joint in the UHPC overlay. It is clearly shown that a sudden failure mode controls the specimens strengthened with reinforced UHPC overlay through a concrete cover separation due to the high bond stress concentration at the ends of the UHPC layer. The separation was generated 20 mm away from the bonding interface due to the perfect bond between the NSC and UHPC overlay. However, most previous research extended the overlay over the support, and this would provide anchorage and prevent the concrete form separation. In practice, this is not true. Thus, care should be taken when using this technique in strengthening by providing mechanical anchorage at the ends of UHPC overlay or using a CFRP warp to prevent brittle failure. Plate 4.5 shows the failure mode and cracking pattern of OSG0.5K, OSG0.33K, OSR0.5K, and OSR0.33K.

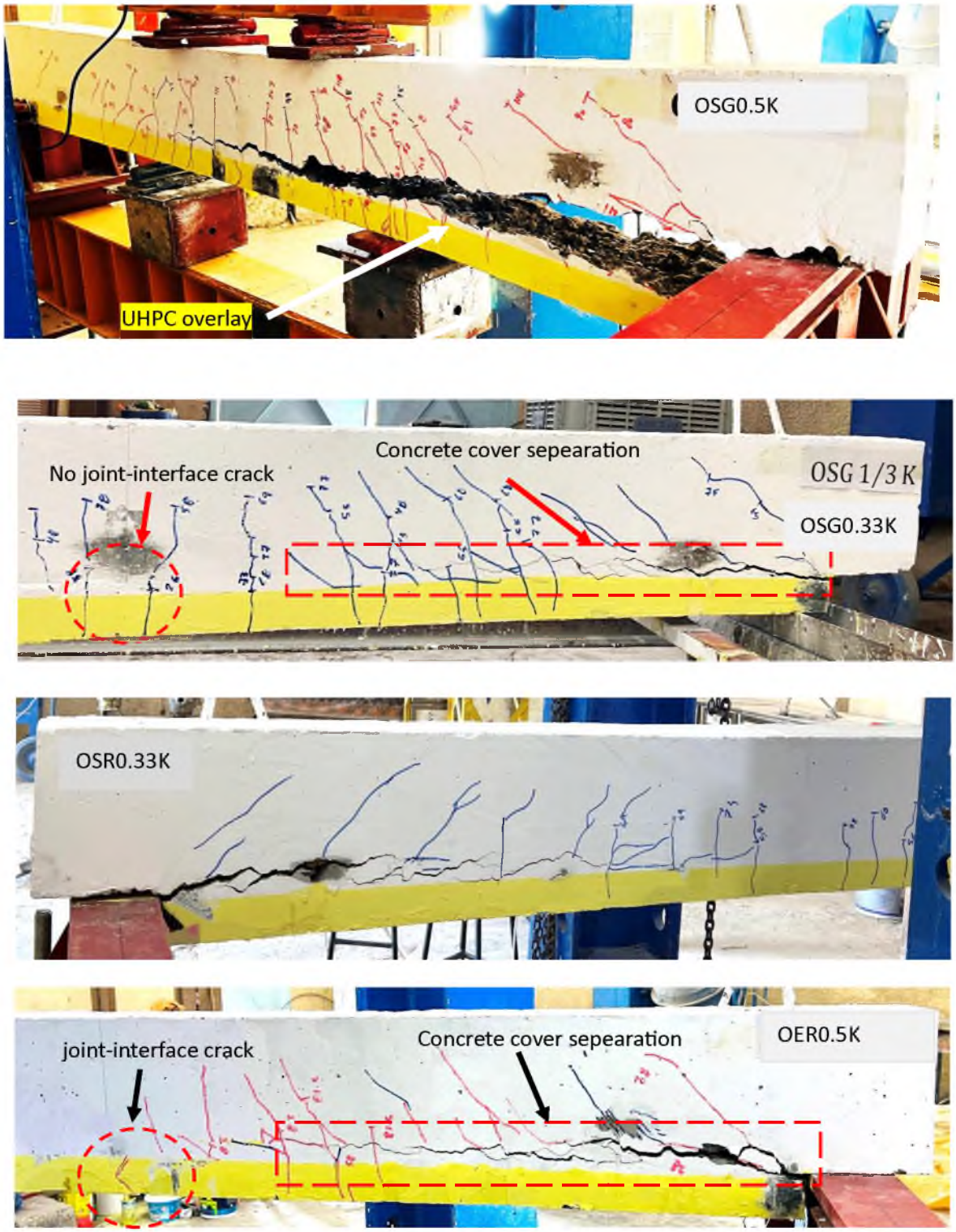

Plate 4.5 Shows the failure mode and cracking pattern of the tested specimens OSG0.5K, OSG0.33K, OSR0.5K, and OSR0.33K.

Constructing the joint in the third span showed better performance than that in the mid-span ,despite it being under the combined effect of shear and moment. The specimens with a construction joint at the third show increase in load-bearing capacity by about 11 % compared with that of mid-span construction joint for both steel bar and GFRP reinforcing cases. Moreover, utilizing GFRP in reinforcing UHPC overlay shows an increase in the load-bearing capacity of about 7.8 % with respect to that reinforced with a steel bar for both mid-span and third-span construction joint cases. This is may be due to the compatibility between the UHPC and GFRP because they have an approximately similar modulus of elasticity. However, specimens with UHPC overlay reinforced by steel bar show more rapid failure than others. Finally, Table 4.1 presents the main experimental results. The percentage of increase in ultimate load (Pu) compared to the control specimen is represented by the value between the brackets in the column of ultimate load (Pu).

4.2.3 Crack pattern and failure mode of the V-group

In this group, the variables were similar to that in the K-group, except the joint shape was vertical rather than key construction joint in the K-group. Figure 4.4 illustrates the failure proses of selected tested specimens in this group. The tested specimens show approximately similar behavior to that in K-group.

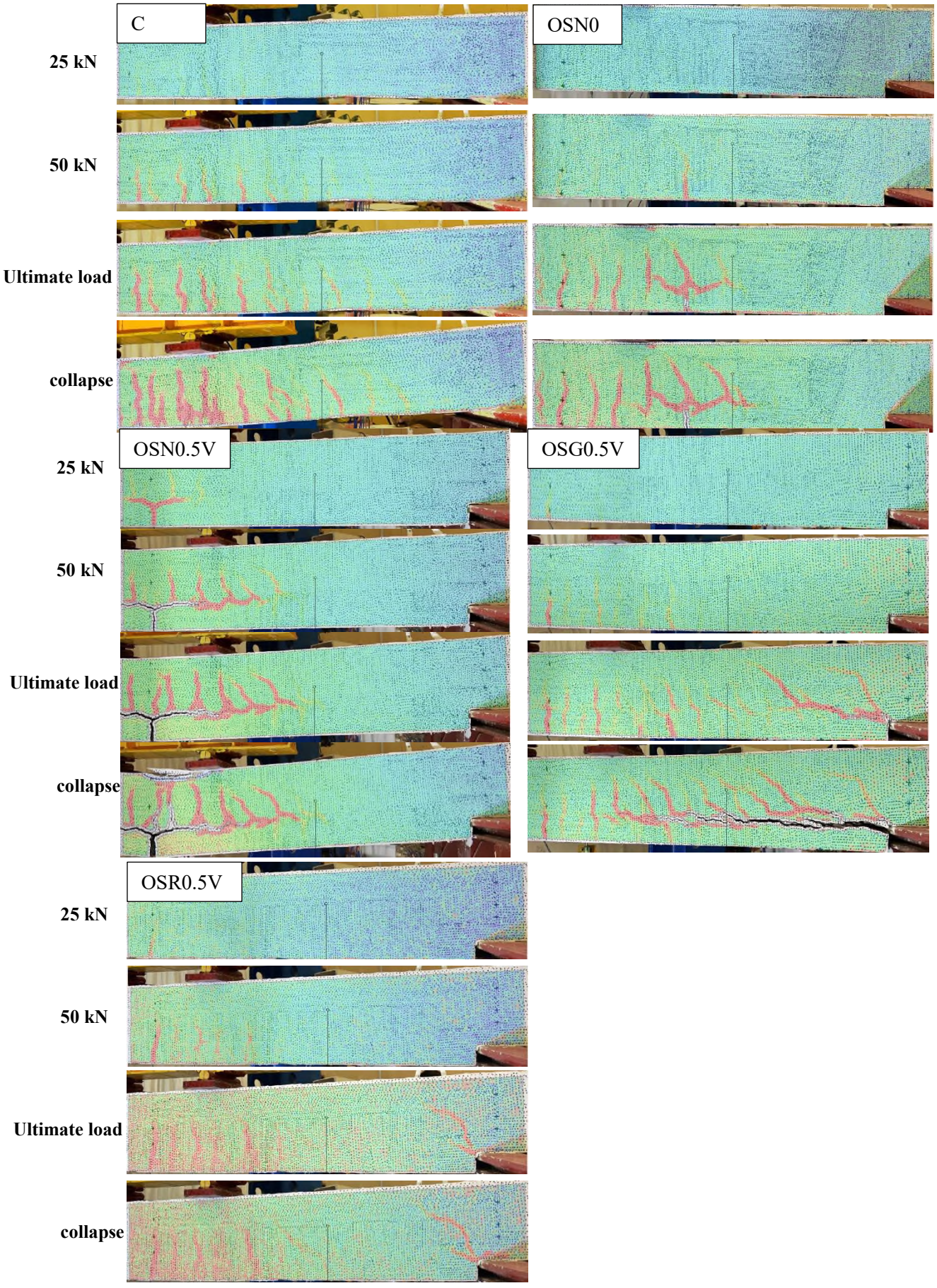

Figure 4.4 Failure process of selected specimens in V-group

The specimen OSN0.5V shows similar behavior to the OSN0.5K specimen, and this means the increase of shear flow area during the key joint shape did not improve the behavior significantly compared with the vertical joint.

The first cracking occurred at 9 kN in the joint interface of the OSN0.5V specimen. Then, the crack propagates to 10-20 mm through the NSC and extends horizontally, as shown in Plate 4.6.

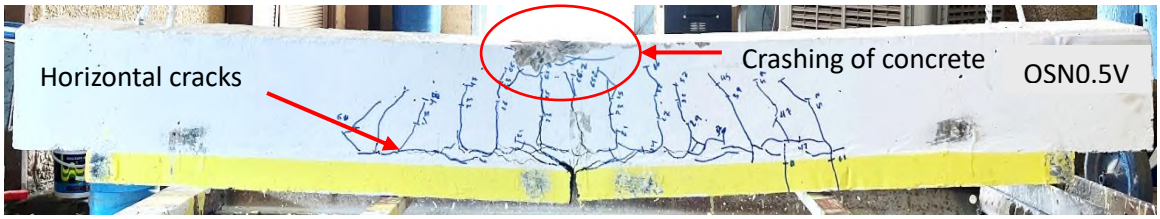

Plate 4.6 presents the failure mode and cracking pattern of specimens OSN0.5V.

Its clear from Plate 4.6 that very few cracks were noted in the UHPC overlay, indicating that the UHPC overlay did not contribute to resisting the tension force due to the crack localization at the joint interface. Finally, the specimens failed by flexural mode after crashing the loading area. Adding steel mesh to the UHPC overlay, as in OSM0.5V shows similar behavior to that strengthened with unreinforced UHPC overlay, as shown in Plate 4.7.

Plate 4.7 present the failure mode and cracking pattern of specimens OSM0.5V.

Reinforced the UHPC overlay by steel bar/GFRP bar shows better load-bearing capacity and stiffness behavior. The flexural cracks developed along the UHPC overlay. The effect of the construction joint was diminished. No horizontal cracks were observed as in the previous strengthened specimens

in this group. A diagonal crack was generated at the edge of the strengthening overlay immediately before sudden failure due to concrete cover separation. The crack pattern and failure mode were similar to than in k-group, as shown in Plate 4.8.

Table 4.1 present the experimental result in term of first crack load, ultimate load and failure mode. Comparing the V groups, it is clear that the cracks generated in the vertical joint earlier than that generated in specimens with key joints, as illustrated in Table 4.1. However, the strengthened specimens with construction joints both key/vertical collapsed in similar failure mode at approximately similar ultimate load.

Table 4.1 present the experimental result in term of first crack load, ultimate load and failure mode

Group K				Group V			
Specimens ID	First crack load (kN)	Pu (kN)	Failure mode	Specimens ID	First crack load (kN)	Pu (kN)	Failure mode
C	12	63.437 (Nill)	Flexural				
OSN0	25	70.431 (11)	Flexural				
OSM0	45	77.68 (22.5)	Flexural				
OSN0.5K	9	62.45 (-)	Flexural	0SN0.5V	9	66.772 (5.25)	Flexural
OSM0.5K	17.5	66.641 (5)	Flexural	OSM0.5V	12.5	63.128 (Nill)	Flexural
OSR0.5K	24.6	83.559 (31)	Concrete cover separation	OSR0.5V	15	74.32 (17.15)	Concrete cover separation
OSG0.5K	23	89.87 (41.6)	Concrete cover separation	OSG0.5V	13	80.171 (26.4)	Concrete cover separation
OSM0.33K	23.5	68.818 (8.5)	Flexural	OSM0.33V	8	70.37 (11%)	Flexural
OSR0.33K	35	78.137 (23%)	Concrete cover separation	OSR0.33V	25	83.05 (30.92)	Concrete cover separation
OSG0.33K	18	88.697 (40)	Concrete cover separation	OSG0.33V	17.7	89.506 (41.1)	Concrete cover separation

The value between two bracts represents the increase/decrease in ultimate load concerning the control specimen.

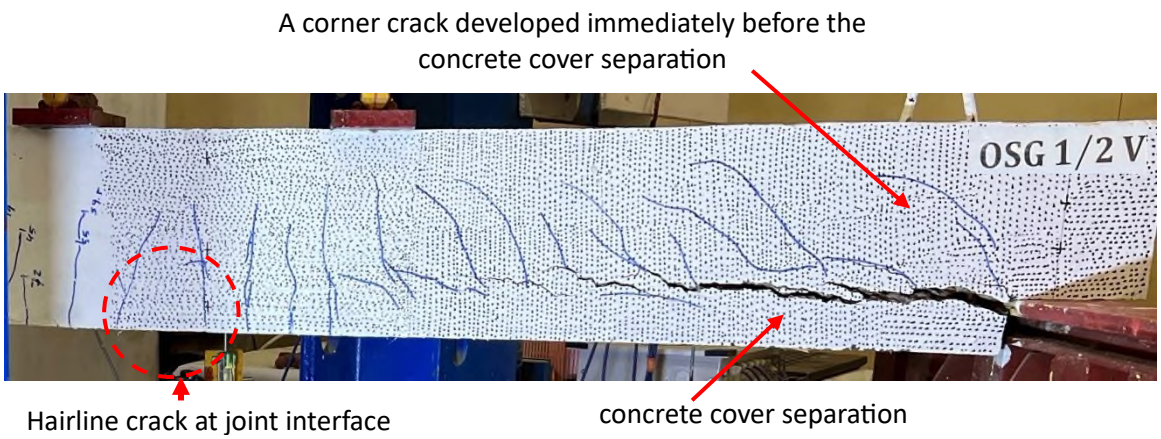

Plate 4.8 present the failure mode and cracking pattern of specimens OSG0.5V, OSG0.33V, OSR0.5V, and OSR0.33V.

4.3 Load-deflection response

4.3.1 Load-deflection response of the K-group

Figures 4.5 to 4.9 present the load-midspan displacement for the tested specimens in the k-group. Two different behavior are noted based on the load-deflection response. The first behavior governed the specimens C, OSN0.5K, and OSM0.5K. In this case, the load-deflection response is divided into three stages. The first stage was approximately linear up to yielding at 55 kN as shown in Figure 4.5, followed by strain hardening up to ultimate. After that, the load dropped slowly.

The second response governed the OSR0.5K and OSG0.5K. In this case, they behaved appropriately linearly till the ultimate load followed a sudden drop in the ultimate load due to sudden failure; one can note this clearly in Figures 4.7 and 4.8.

At the first stage, the specimens OSN0.5K, and OSM0.5K show stiffer behavior to control specimens (C) till yield; after that, these specimens behave similarly to control specimens. The presence of construction joint in the UHPC overlay diminishes the benefit of the UHPC overlay.

However, reinforcing the UHPC overlay by steel bar/GFRP bar show significant improvement in the stiffness, ultimate load and diminish the effect of the construction joint, as shown in Figure 4.8 to 4.9.

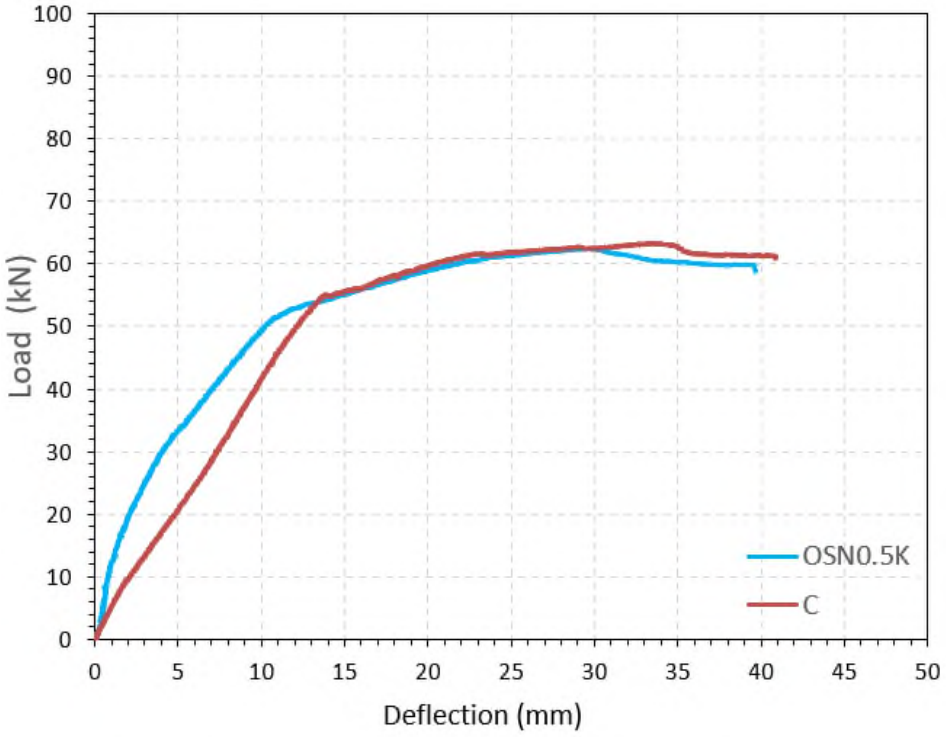

Figure 4.5 Load – deflection curve for specimen OSN0.5K

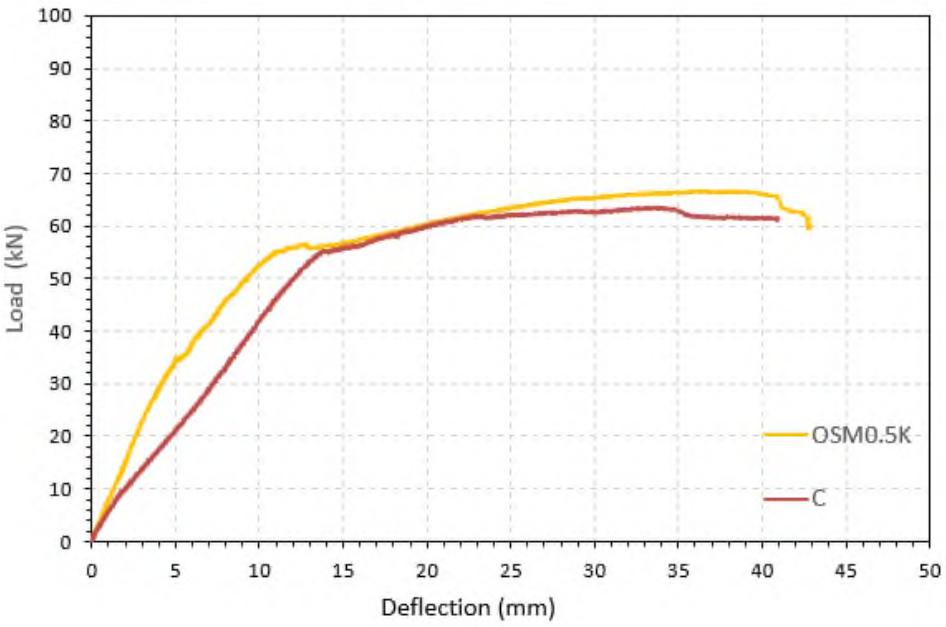

Figure 4.6 Load-deflection curve for specimen OSM0.5K.

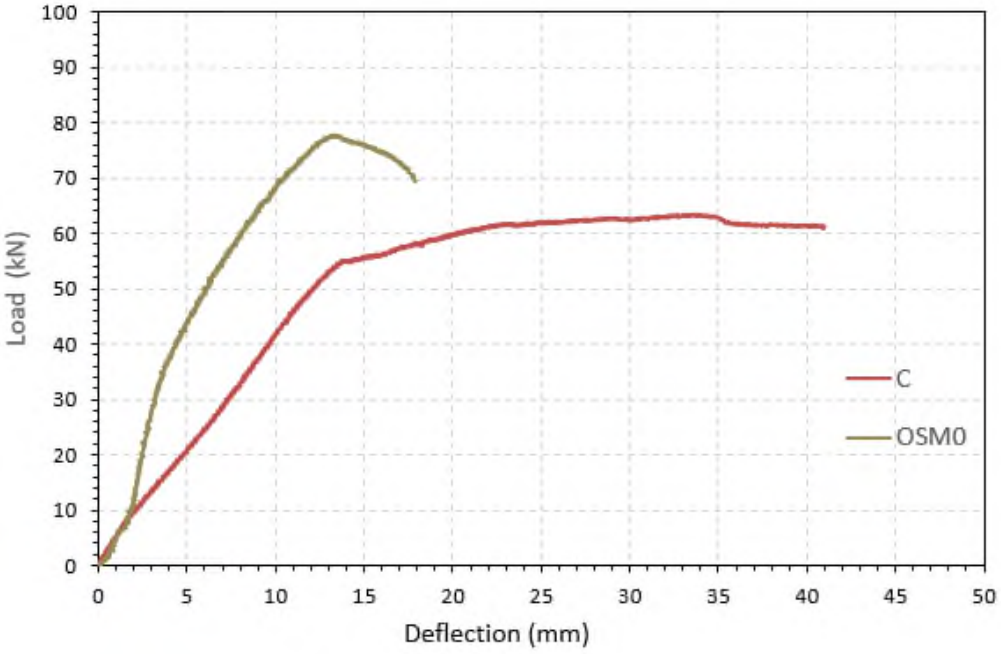

Figure 4.7 Load – deflection curve for specimen OSM0.

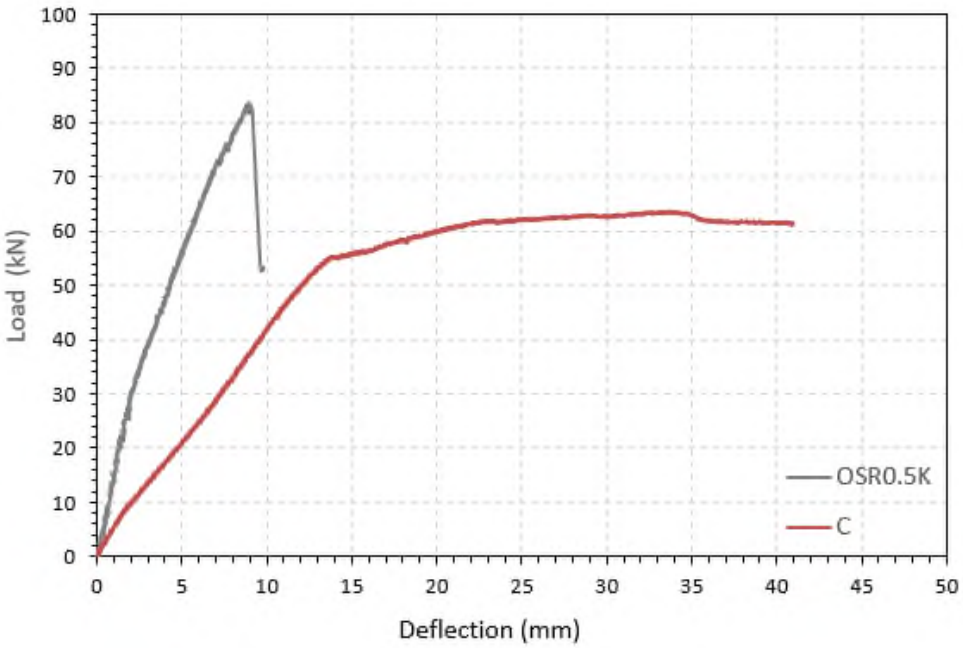

Figure 4.8 Load – deflection curve for specimen OSR0.5K.

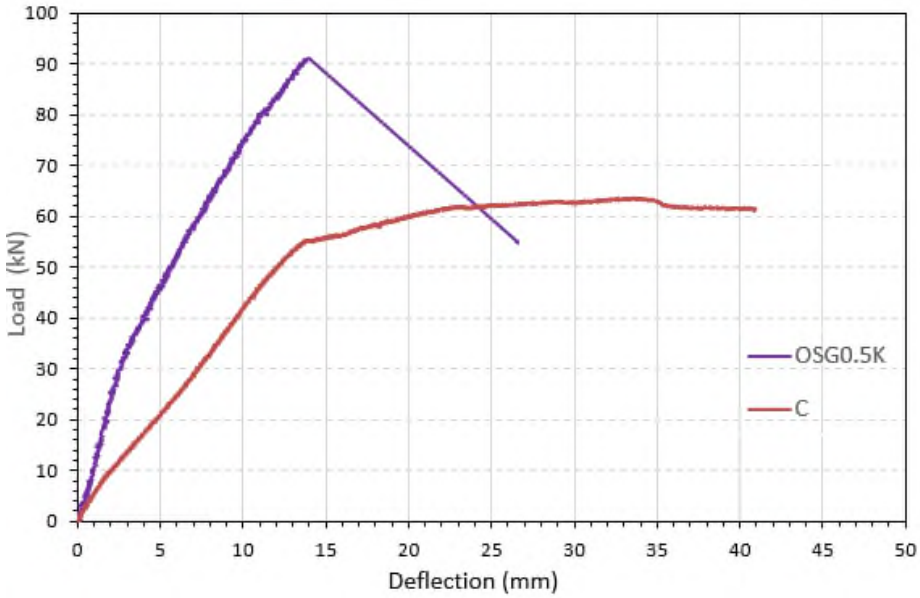

Figure 4.9 Load-deflection curve for specimen OSG 0.5K.

Figures 4.10 and 4.11 present a comparison between the beam strengthed by UHPC with a construction joint at midspan and that moved the construction joint to the third span.

The specimens (OSG0.5K and OSR0.5K) with a construction joint at the third span show similar behavior to that with a construction joint at the third span. This may be due to the presence of steel/GFRP bars diminishing the effect of the construction joint and changing the location of the joint show no significant effect.

However, moving the joint away from the beam center for the beam-strengthened UHPC layer reinforced with steel mesh show enhancement in term of initial stiffness and ultimate load. As shown in Figure 4.12.

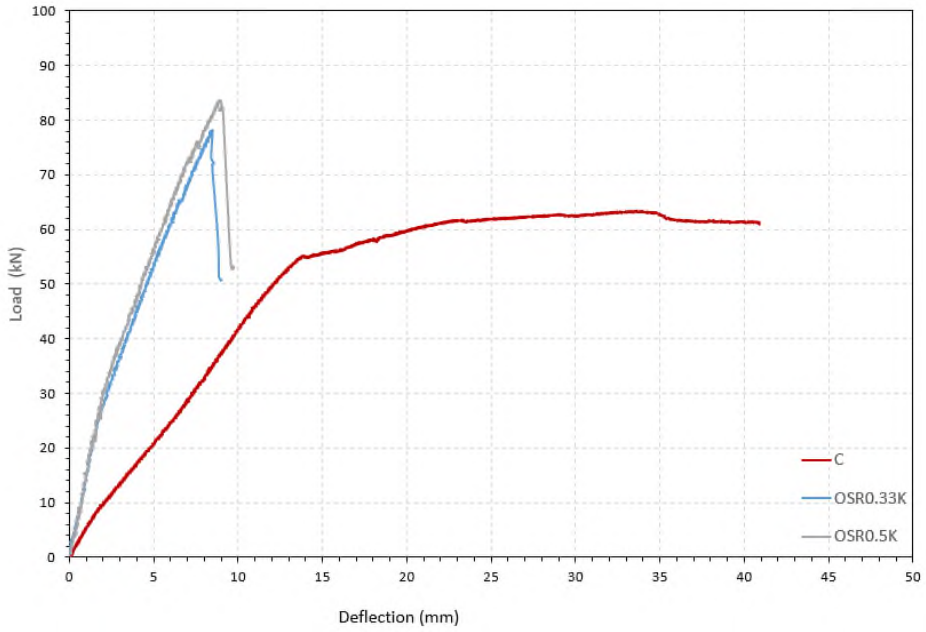

Figure 4.10 Present a comparison between the Load-deflection curve for specimens OSR0.5K, OSR0.33K, and C.

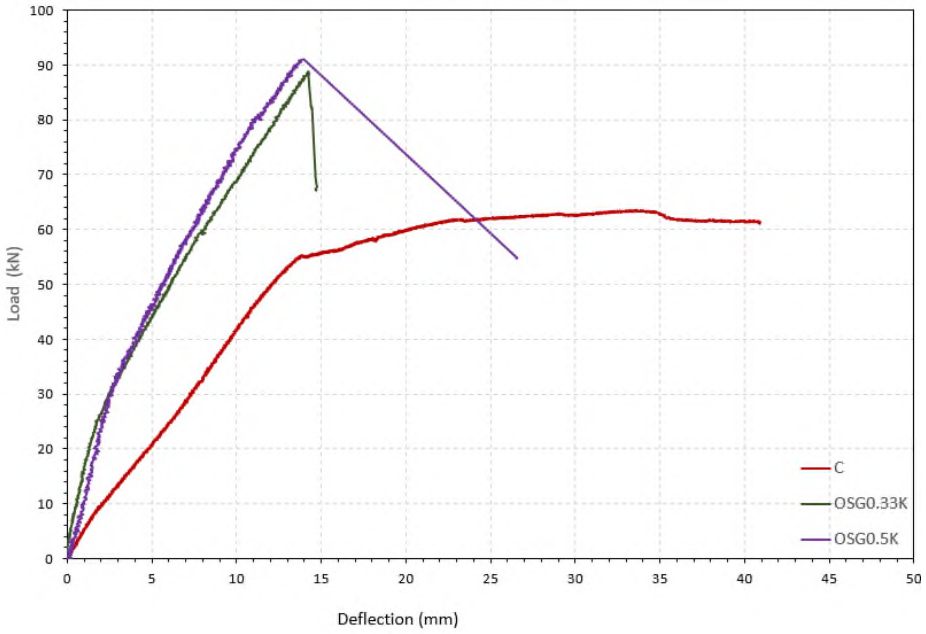

Figure 4.11 Present a comparison between the Load-deflection curve for specimens OSG0.5K, OSG0.33K, and C.

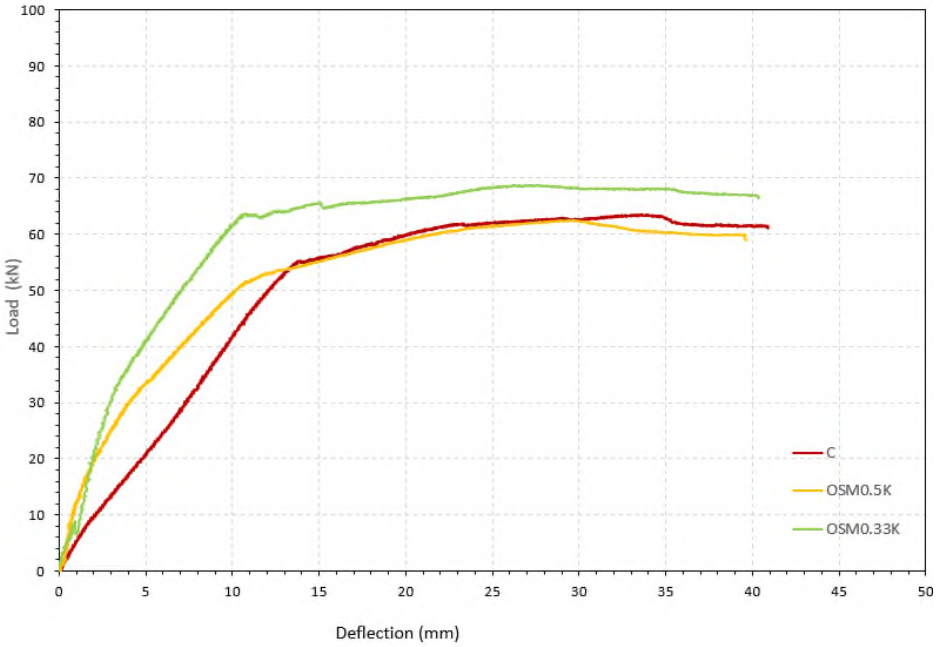

Figure 4.12 Present a comparison between the Load-deflection curve for specimens OSM0.5K, OSM0.33K, and C.

4.3.2 Load-deflection response of the V-group

Similar to the k-group, two load-deflection responses were observed. The first one is similar to the control specimen, which behaves linearly up to yielding, followed by strain hardening till the ultimate load, and then the load drops slowly. This response governs the behavior of specimens OSN0.5V, OSM0.5V and OSM0.33V, as shown in Figures 4.13 to 4.15.

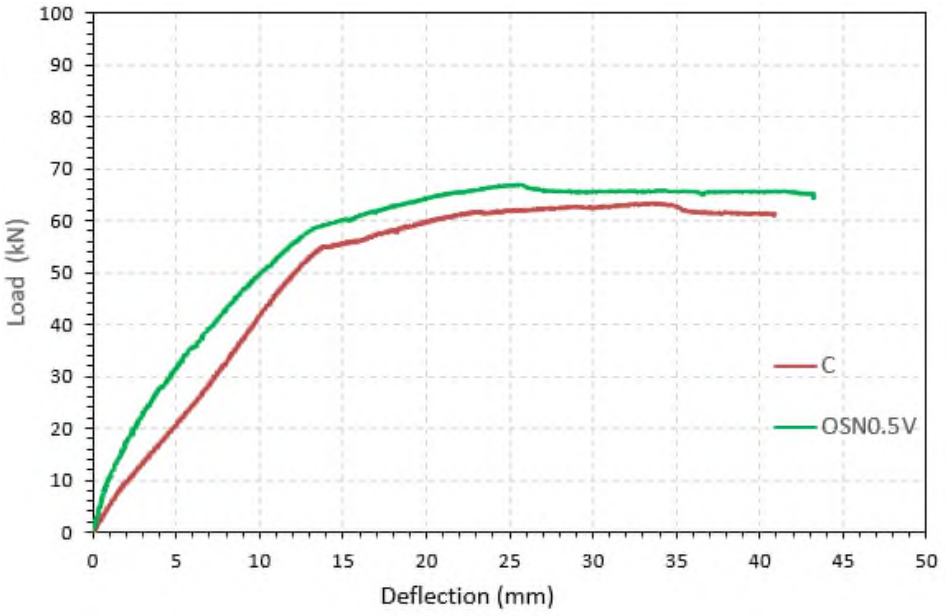

Figure 4.13 Load-deflection curve for specimens OSN0.5V.

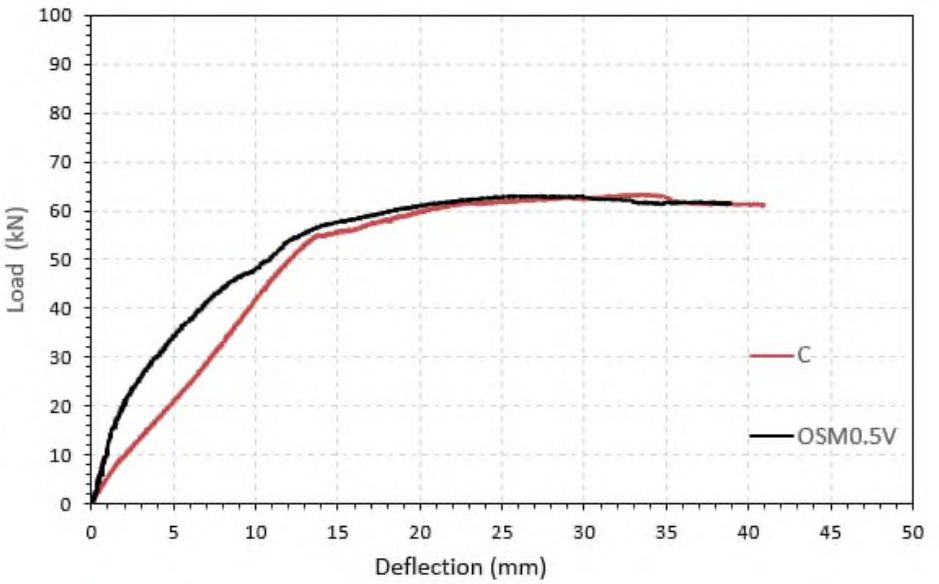

Figure 4.14 Load – deflection curve for specimen OSM0.5V.

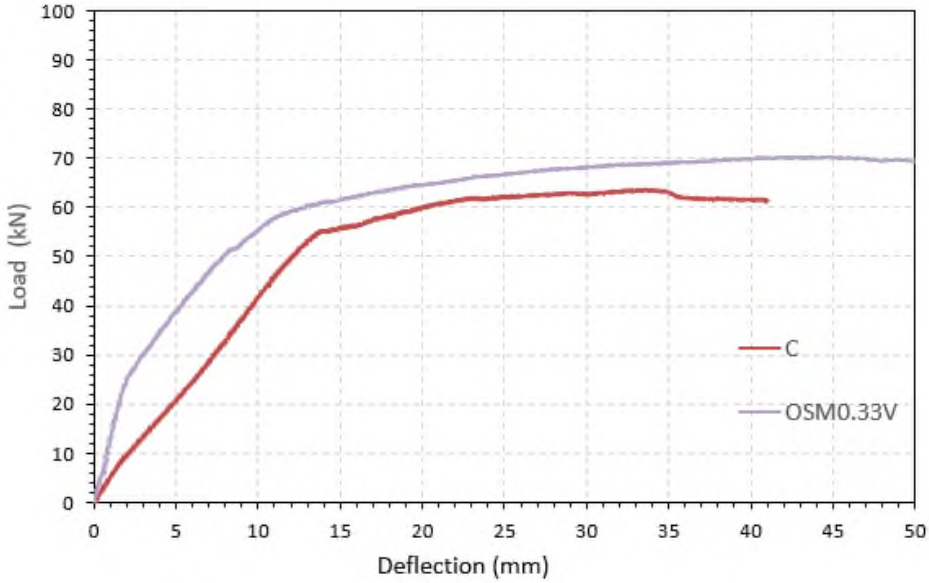

Figure 4.15 Load – deflection curve for specimen OSM0.33V.

The other load-deflection response behaves approximately linear up to the ultimate load, followed by sudden failure due to concrete cover separation. This response governed the behavior of specimens with overlay reinforced with GFRP/Steel bar as shown in Figures 4.16 to 4.18.

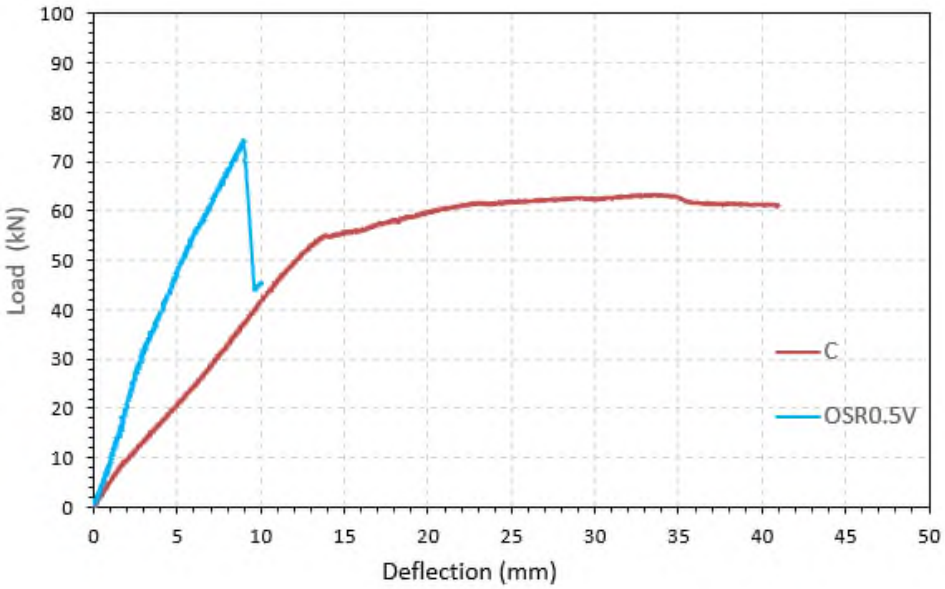

Figure 4.16 Load – deflection curve for specimen OSR0. 5V.

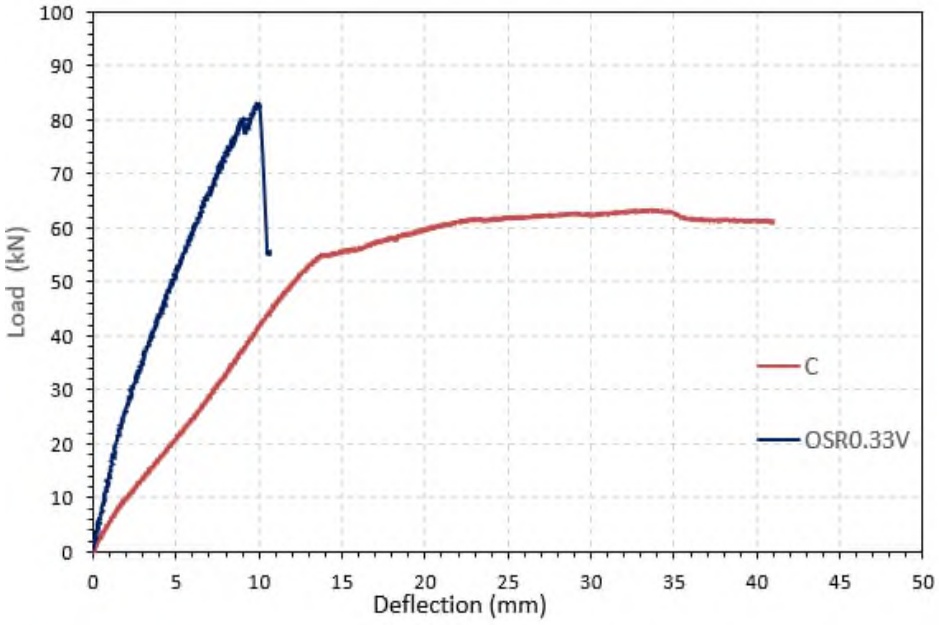

Figure 4.17 load-deflection curve for specimen OSR0.33V

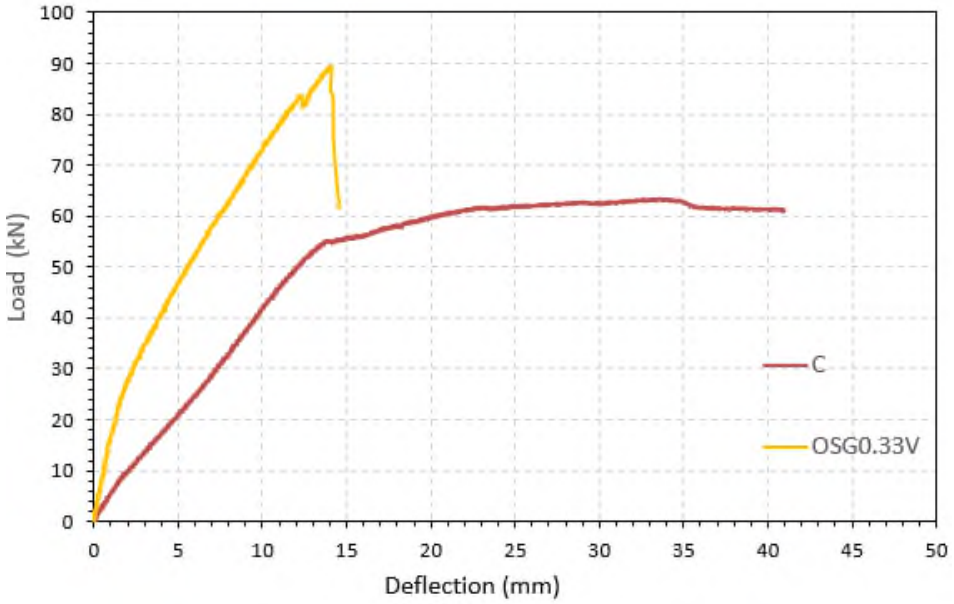

Figure 4.18 Load – deflection curve for specimen OSG0.33V.

The specimens OSN0.5V and OSM0.5V show a significant increase in initial stiffness with a slight increase in ultimate load. Moving the construction joint to the third span rather than the mid-span show 11% increase in ultimate load.

Reinforcing the UHPC overlay by GFRP/steel bar show improvement in stiffness compared with the control specimen and shows a 17.15 % and 26.4 % increase in the ultimate load for specimens OSG0.5V and OSR0.5V, respectively, compared with the control specimen.

Figures 4.19 and 4.20 present a comparison between the strengthened specimens with mid-span construction joint and third-span construction joint for a different type of UHPC reinforcement. One can note that moving the construction joint away from the mid-span shows a slight increase in the stiffens and ultimate load. While the ultimate load for specimens 0SM0.33V, OSG0.33V and OSR0.33V increased about 11%,13.77%, and 14.7%, respectively, in comparison with specimens that have a joint in the middle.

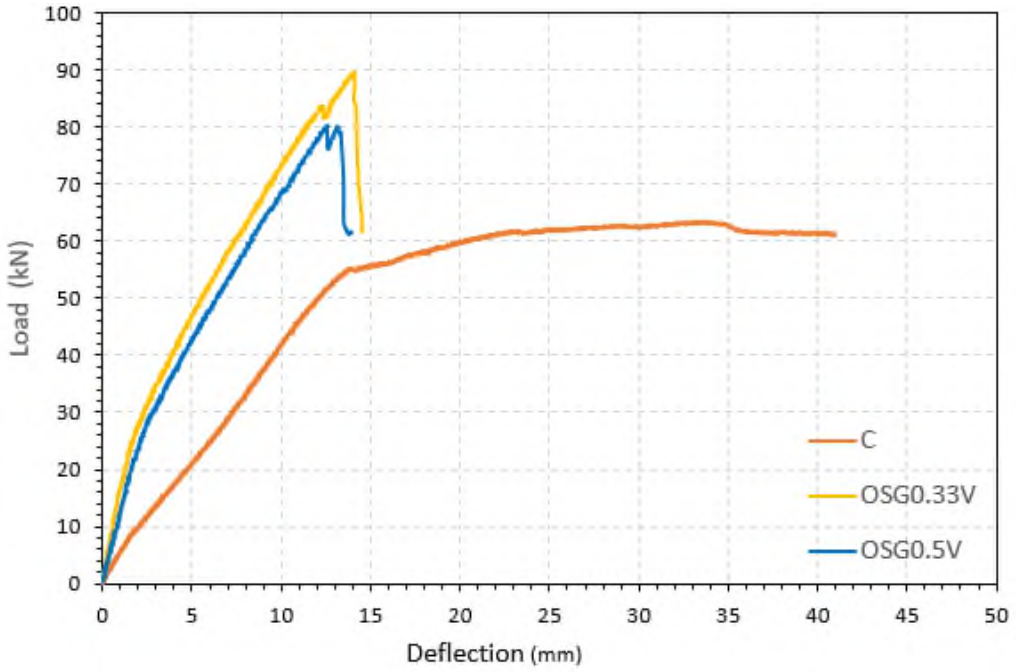

Figure 4.19 Compares the load-deflection curve for tested specimens OSG0.5V, OSG0.33V, and C.

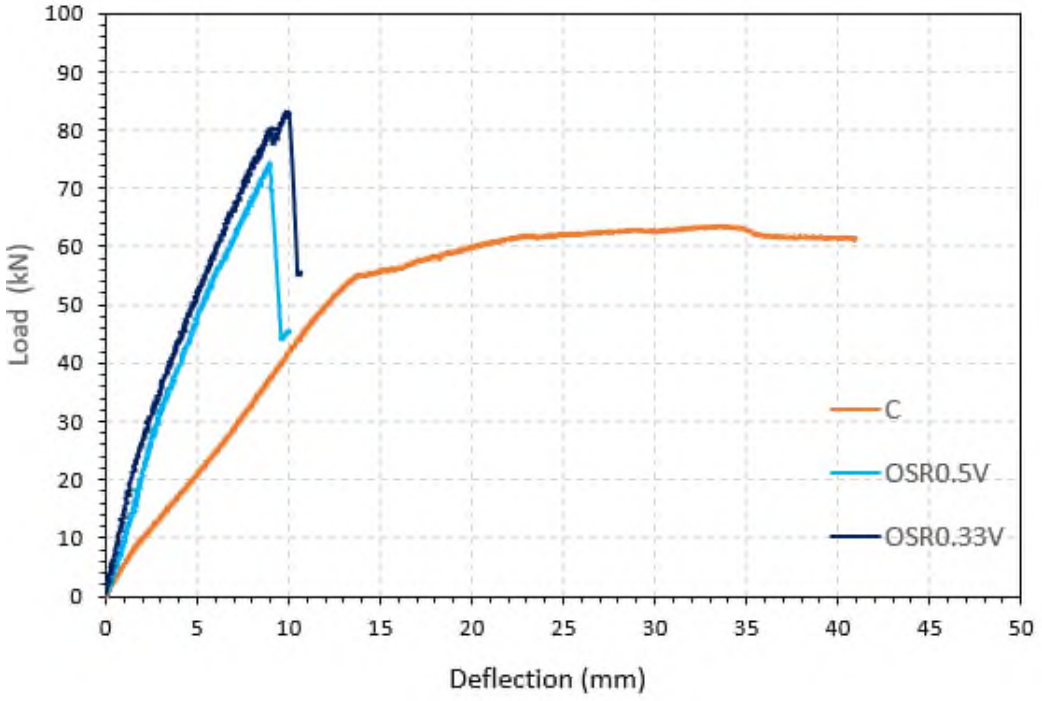

Figure 4.20 Compares the load-deflection curve for tested specimens OSR0.5V, SR0.33V, and C.

Again, GFRP shows better performance than steel bar in reinforcing UHPC overlay in terms of ductility and ultimate load, as shown in Figures 4.21 and 4.22. The specimens OSG0.5V and OSG0.33V shows ultimate load of about 9.25% and 10.18% greater than OSR0.5V and OSR0.33V, respectively.

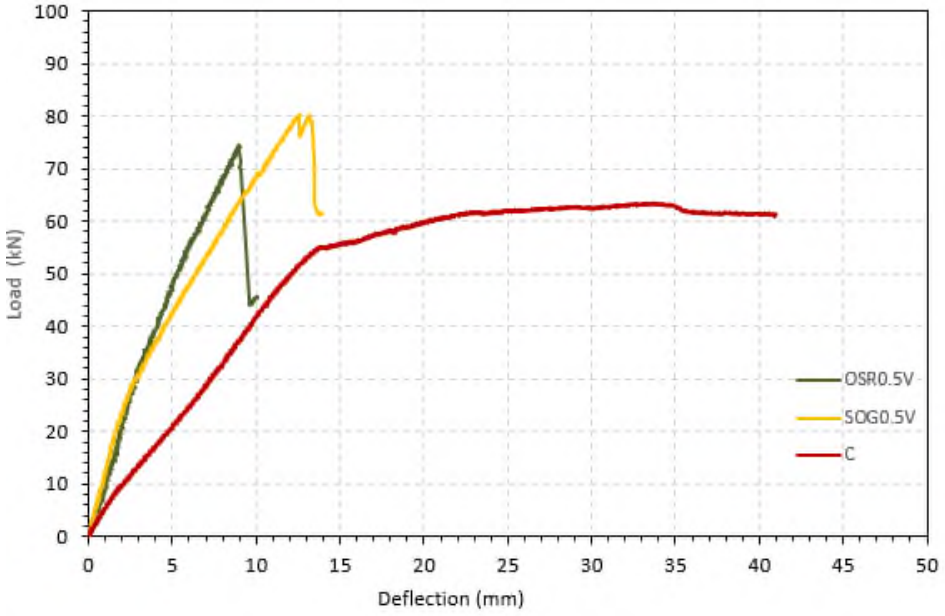

Figure 4.21 Comparison of the Load-deflection curves for the OSR0.5V, OSG0.5V, and C specimens.

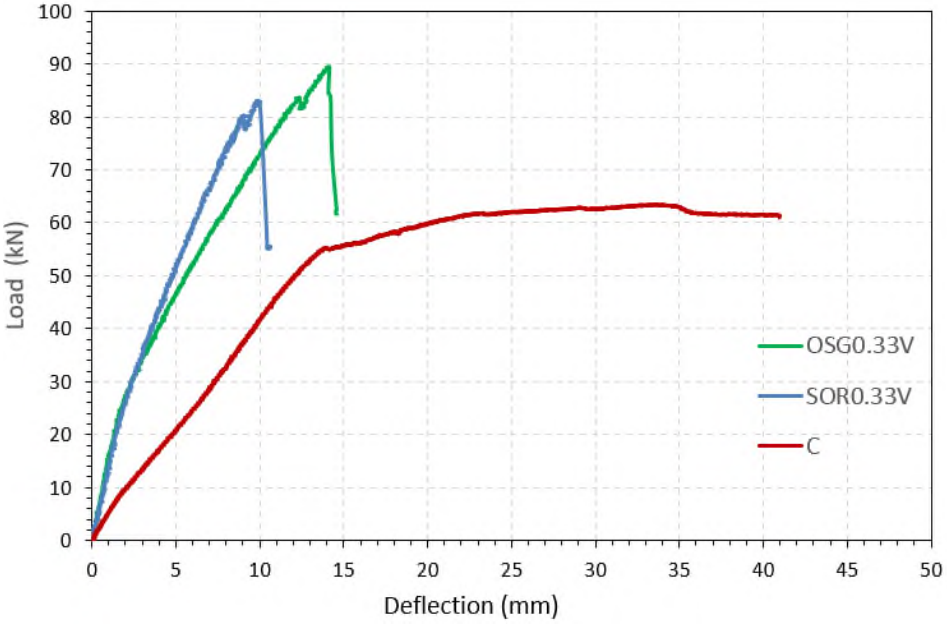

Figure 4.22 compares the load-deflection curves of the tested specimens OSR0.33V, OSG0.33V, and C.

4.3.3 Comparison between the k-group and the V-group

Figures 4.23 to 4.28 show a comparison between the load-deflection response of K-group and V-group. Both groups show similar behavior, and the difference in ultimate load did not exceed 10%. This is may be due to the

effect of reinforcement in the UHPC overlay. It was found that the presence of GFRP/steel bar diminishes the effect of construction joints in the UHPC overlay. Therefore, it is practical to use V-joint rather than K-joint.

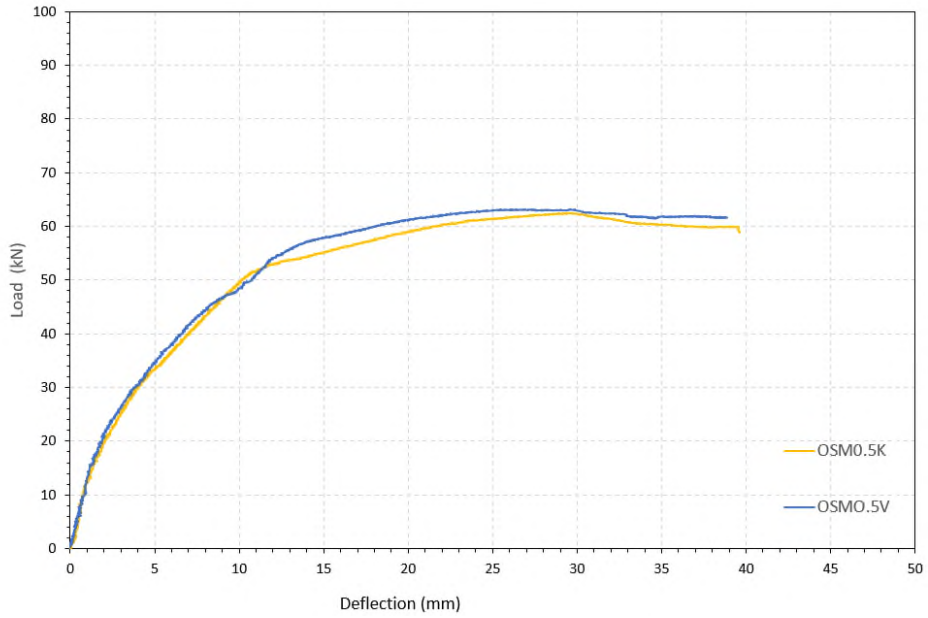

Figure 4.23 compares the Load-deflection curves for the tested specimens OSM0.5K and OSM0.5V.

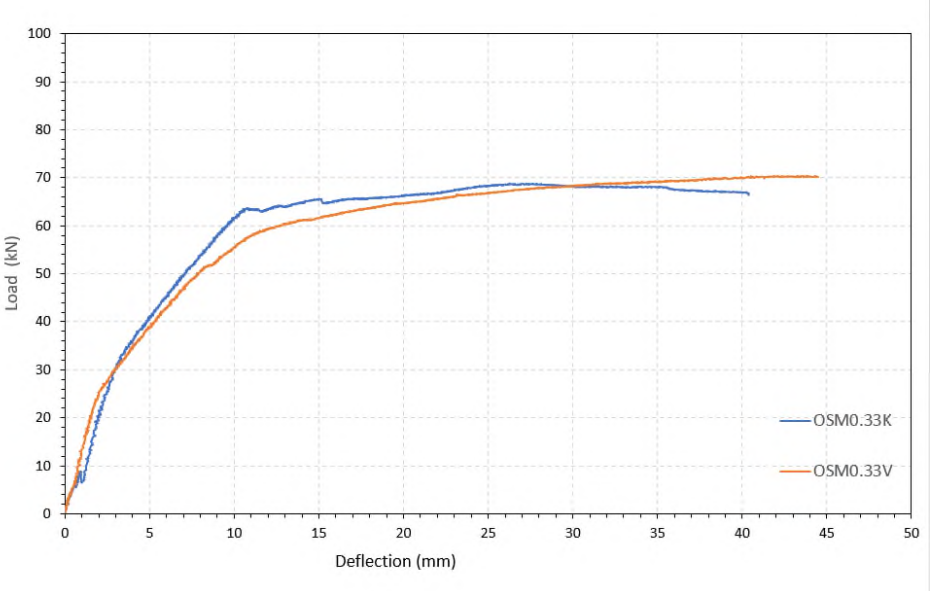

Figure 4.24 compares the Load-deflection curves for the tested specimens OSM0.33K and OSM0.33V.

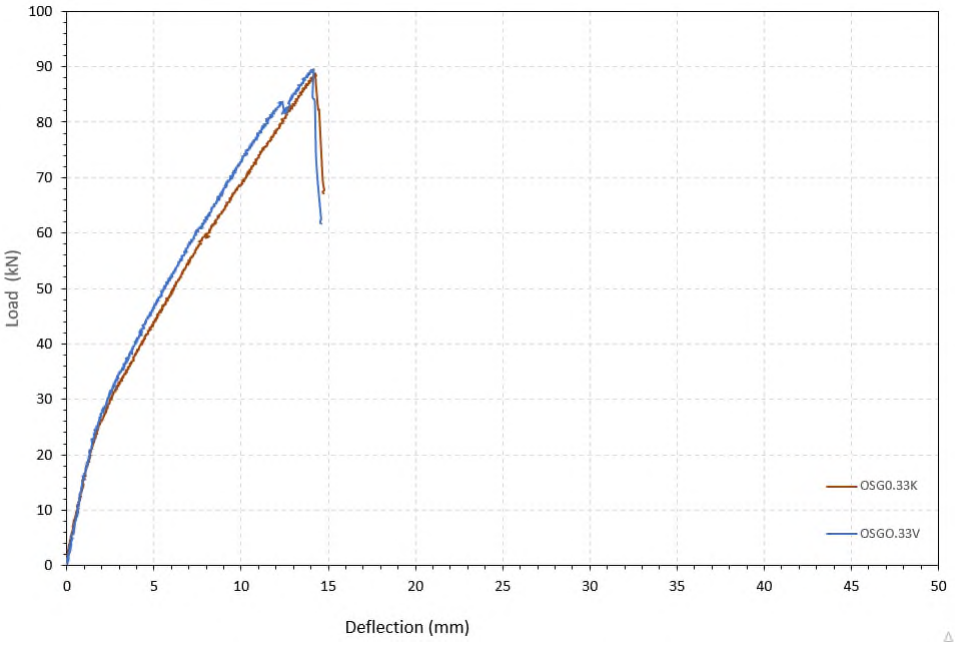

Figure 4.25 compares the load-deflection curves of the tested specimens OSR0.5K and OSR0.5V.

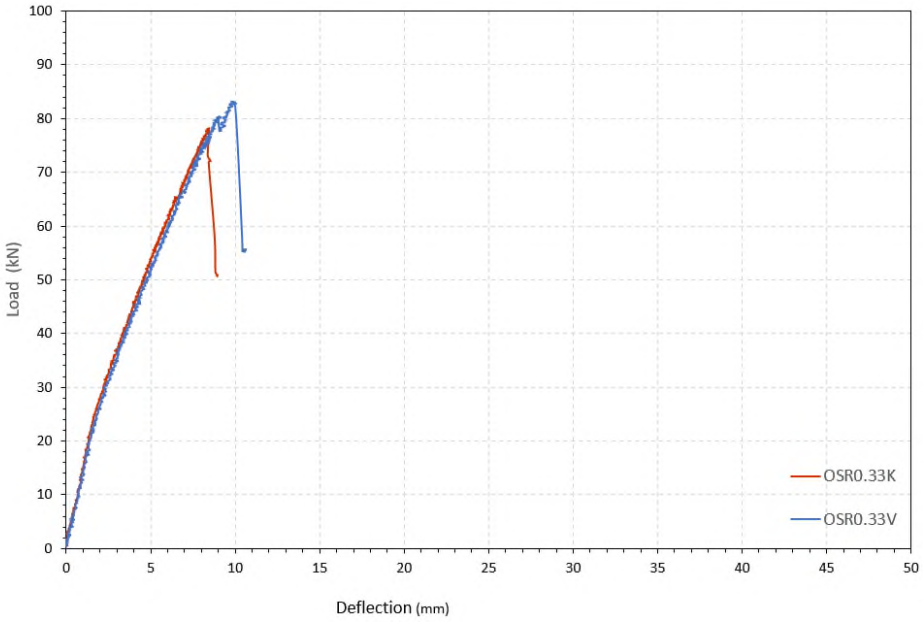

Figure 4.26 compares the Load-deflection curves for the tested specimens OSR0.33K and OSR0.33V.

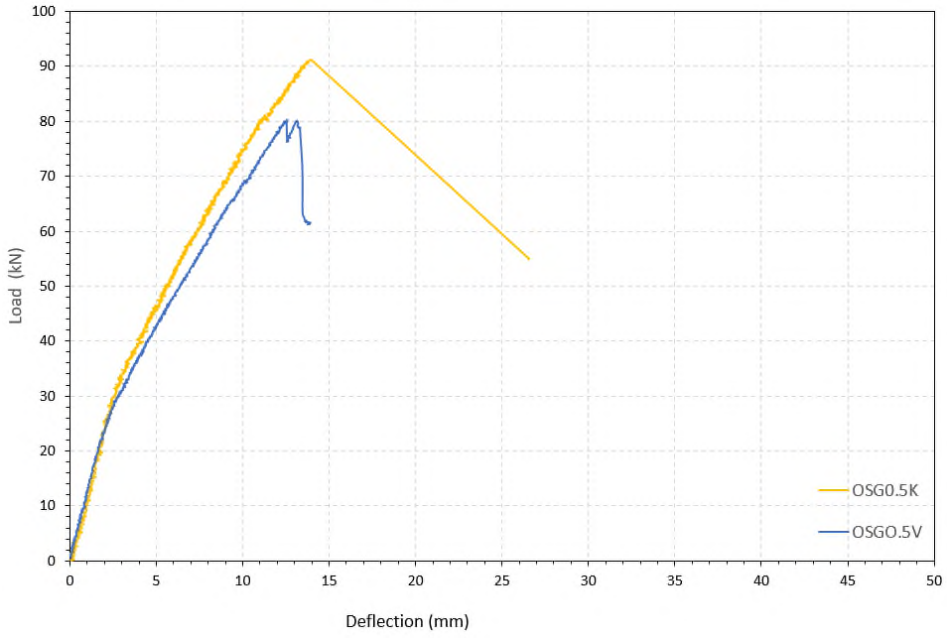

Figure 4.27 Load-deflection curve for tested specimens (OSG0.5VandOSG0.5K)

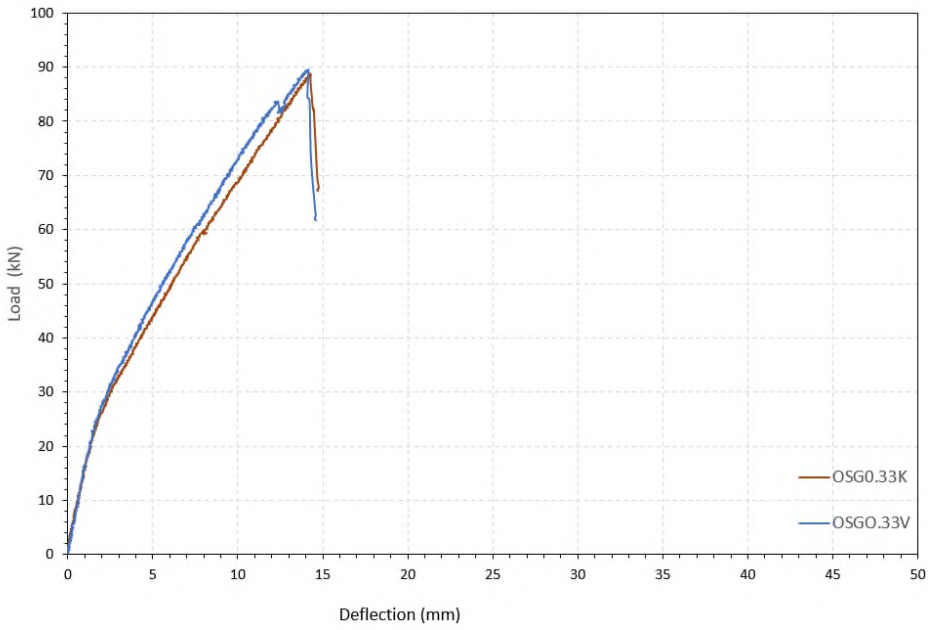

Figure 4.28 Load-deflection curve for tested specimens (OSG0.33VandOSG0.33K).

4.4 Discussions

4.4.1Ductility

Ductility is defined as the capacity to undergo inelastic deformation before failure [109]. Also, it can be defined as the reserved load-carrying capacity from the yield point to the ultimate load-carrying capacity. The ductility index is defined as the ratio of ultimate displacement to yielding displacement [110]. The ultimate displacement (Δ_u) corresponding to the ultimate load. However, (Δ_y) was calculated based on Park [111]. Figure 4.29 presents the component of the ductility index.

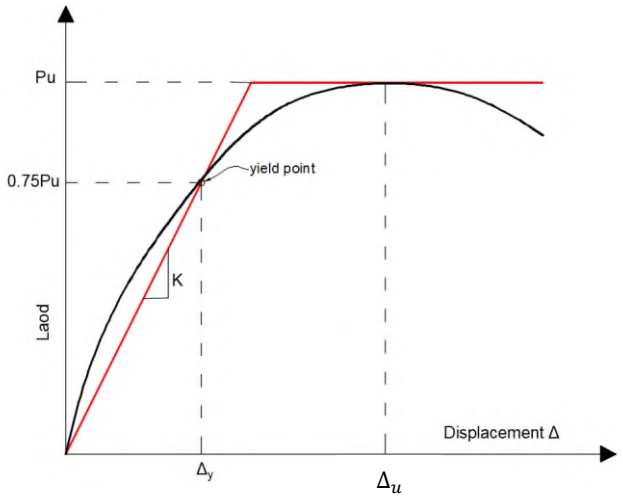

Figure 4.29 Determination procedures of ductility component and initial stiffness [111].

Figure 4.30 illustrates the ductility index of all tested specimens in this group compared to the control specimen (c). Its observed that specimens OSN0.5K, OSM0.5K and OSM0.33K show a ductility index higher than control specimens by about (22, 36 and 33) % respectively. In comparison, the other strengthened specimens show less ductility index.

The ductility index of strengthened specimens in the V-group was similar to that in the k-group. Figure 4.31 shows the ductility index of the tested specimens in the V-group.

In the present study, most of the strengthened specimens by UHPC overlay show less ductility index than normal strength concrete beams. There are

mainly two reasons behind this; first, the generation of multiple main cracks in the tensile zone of the control specimen (as shown in Plate 4.1), making the deflection at the ultimate load higher, thus giving a high ductility index. The strengthened beams have a higher tensile strength at the tension face, and only one main crack developed in the UHPC overlay resulting in less deformation. The second reason is that the strengthened specimens with reinforced UHPC overlay failed suddenly by concrete cover separation at the ends of the layer due to high stress concentration before reaching its full capacity.

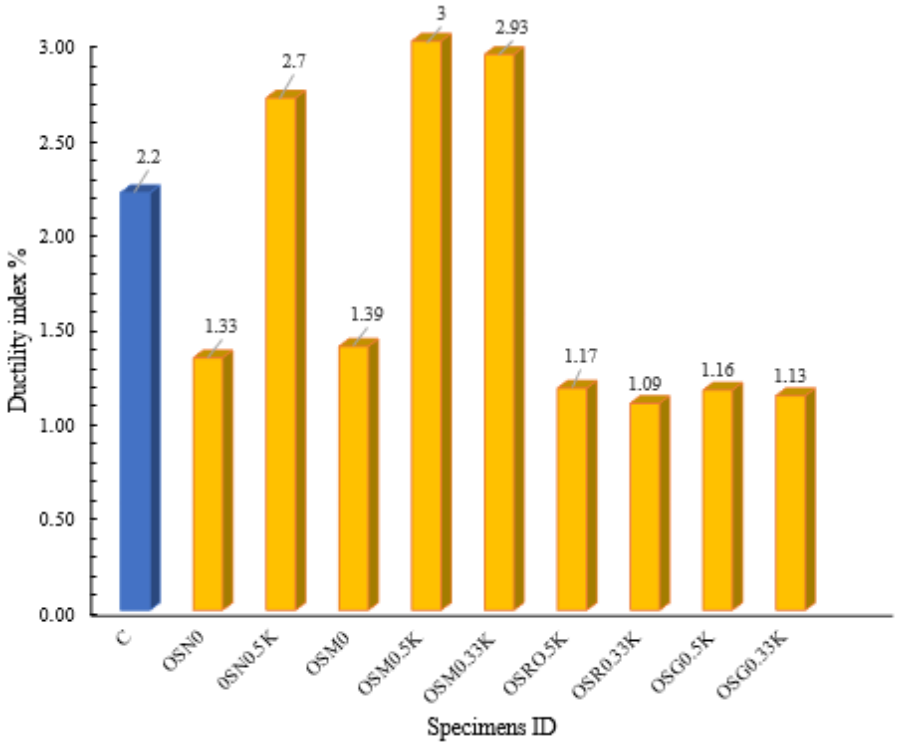

Figure 4.30 The ductility index of the tested specimens in K-group.

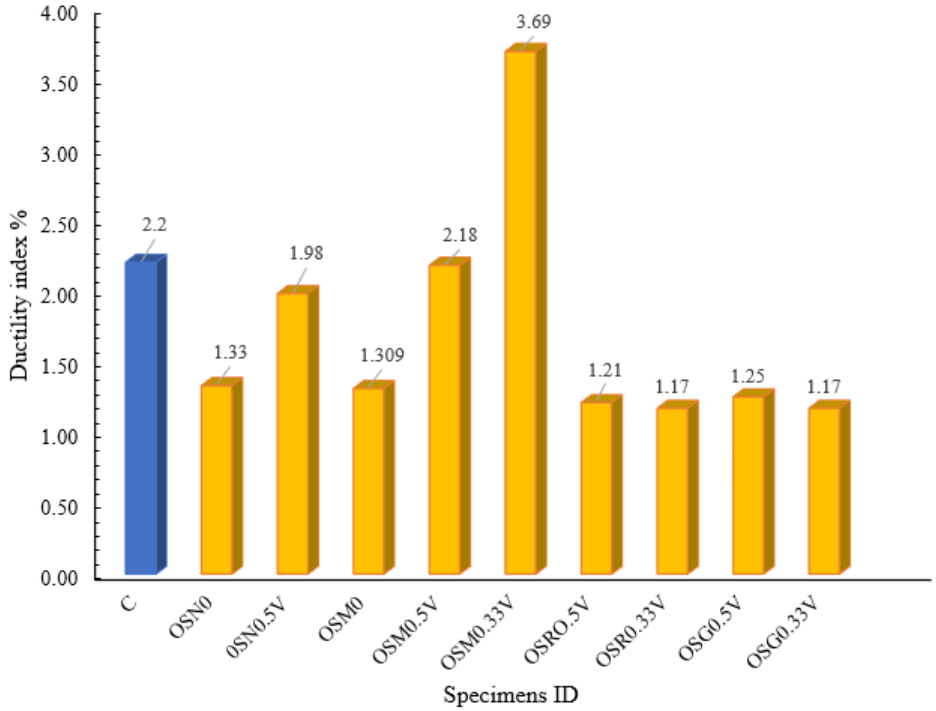

Figure 4.31 The ductility index of the tested specimens in K-group.

4.4.2 stiffness

The present study calculated the initial stiffness for the strengthened beams and compared with the control specimen. The initial stiffness was estimated by using the secant of the force versus displacement passing through the point at which the applied force reaches 75% of the ultimate load [112], as shown in Figure 4.29.

Figures 4.32 and 4.33 present the initial stiffness for both groups compared with the control specimen. It's clear from the Figures that the type and percentage of reinforcement. As compared to the control specimen, using a plain UHPC overlay enhances the initial stiffness by roughly (80)%. The presence of the construction joint (K/V) decreases the initial stiffness by about (33) % compared to that without the construction joint. Reinforcing the UHPC overlay by steel mesh show similar behaviour to that strengthened with plain UHPC overlay.

Reinforcing the UHPC overlay with a steel bar improves the initial stiffness significantly, even with the presence of a construction joint. In this case, the initial stiffness show (78) % higher than the control specimen for both types of joint. However, utilising the GFRP bar in reinforcing the UHPC overlay shows an initial stiffness of about (30%) higher than the control specimen. One can note that the initial stiffness for the case of utilising GFRP bar is less than the case of utilizing steel bar by about (38%). This is mainly due to the modules of elasticity for steel bars about four times that of GFRP. It's clear that utilize steel bar/GFRP bar diminishes the effect of construction joint and shows no effect on stiffness. Therefore, the shape and location of the construction joint do not affect the behaviour of strengthened specimens in term of initial stiffness.

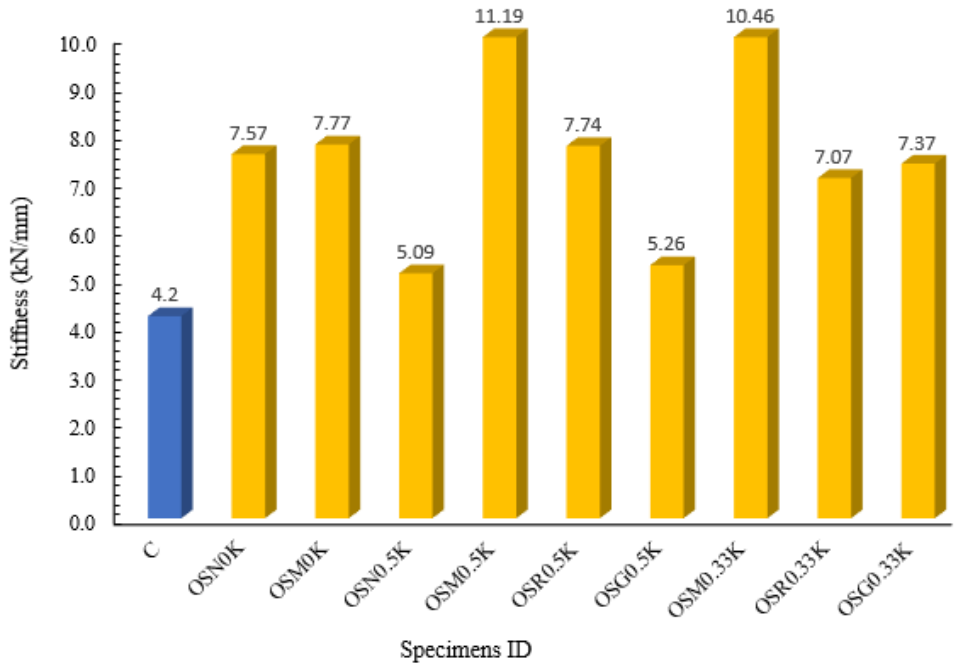

Figure 4.32 The initial stiffness of the tested specimens in K-group.

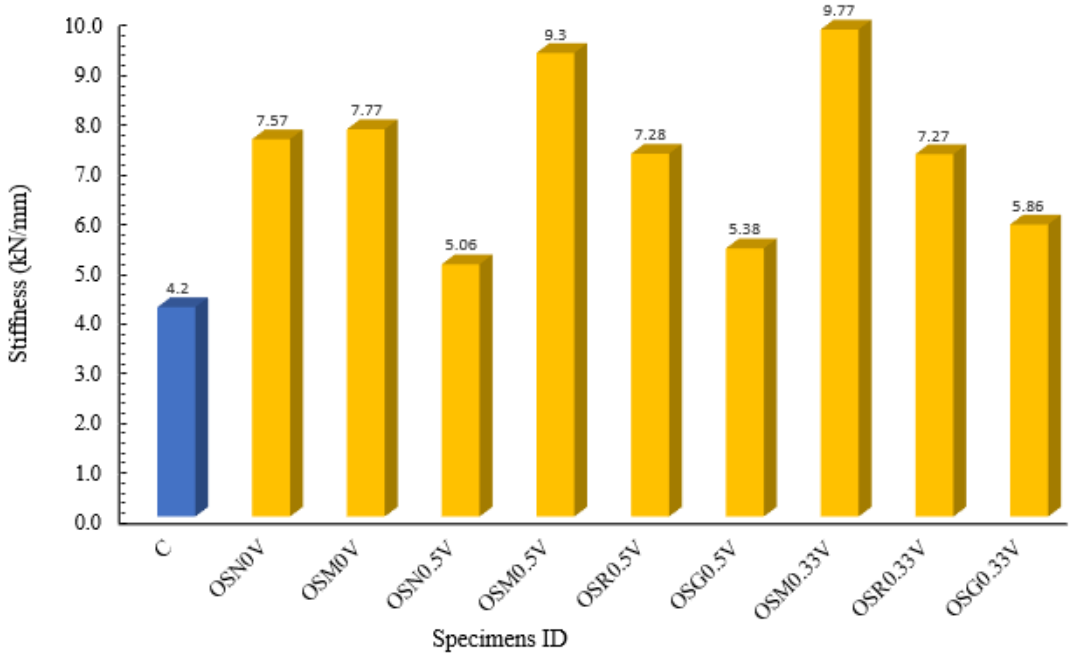

Figure 4.33 The initial stiffness of the tested specimens in V-group.

4.4.3 UHPC overlay slippage at the NSC interface

One of the most issues in this strengthening technique is the debonding between the UHPC overlay and the NSC beam. Epoxy resin was used to increase the contact between the two surfaces after roughing the NSC surface by water jetting under high pressure. As mentioned in section 3.5 and 3.6, two LVDTs were used to record the slip between the NSC and UHPC overlay. No significant slip was recorded at the interface between the normal concrete and UHPC. Figures 4.34 and 4.35 presents the relation between the slip and the applied load it's clear that no displacements are recoding by LVDT and the reading shown in Figures represents a noise. Based on the Figures 4.34 and 4.35, and experimental observation, it is fair to say the bond between the two types of concrete is perfect.

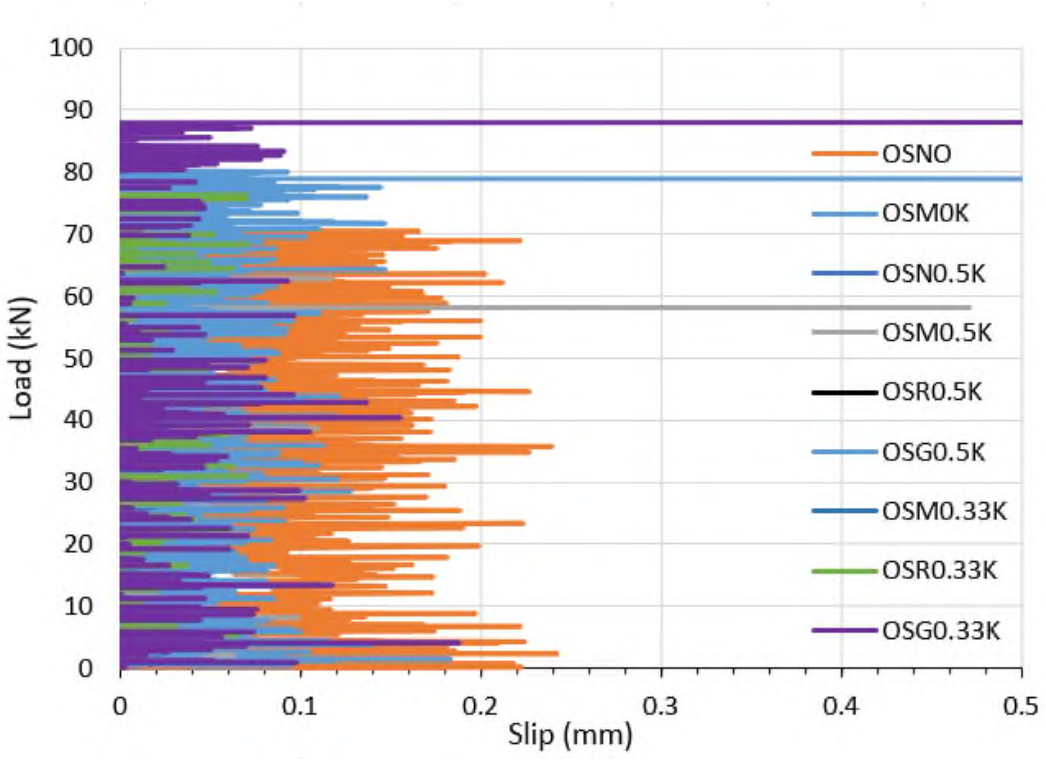

Figure 4.34 presents the relation between the slip and the load in the K group.

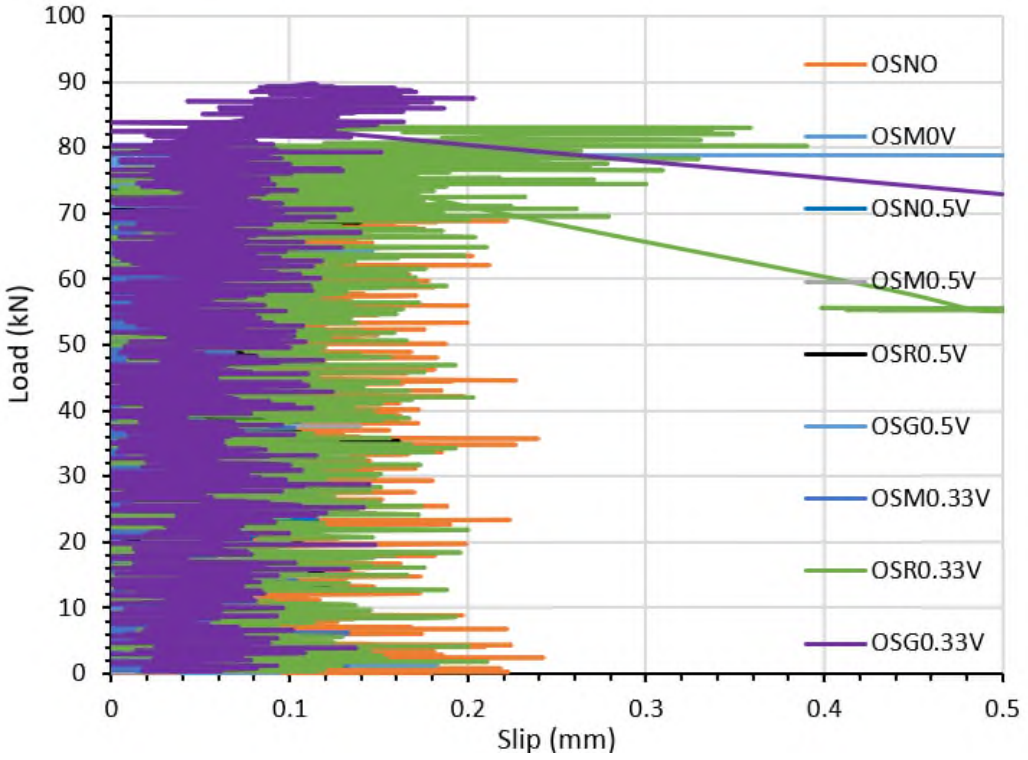

Figure 4.35 Presents the relation between the slip and the load in the V group.

4.5 Theoretical Modeling of a UHPC-Overlaid Reinforced Concrete Beam

Shirai et al. [113] in 2020 employed force equilibrium to calculate the moment capacity of an RC beam strengthened with UHPC overlay. Figure 4.36 shows the methodology used, which involves determining the forces and moments acting on the beam and ensuring that they are in equilibrium. This approach allows for an accurate determination of the moment capacity of the strengthened beam and can be used to optimize the design of UHPC strengthening systems for RC beams.

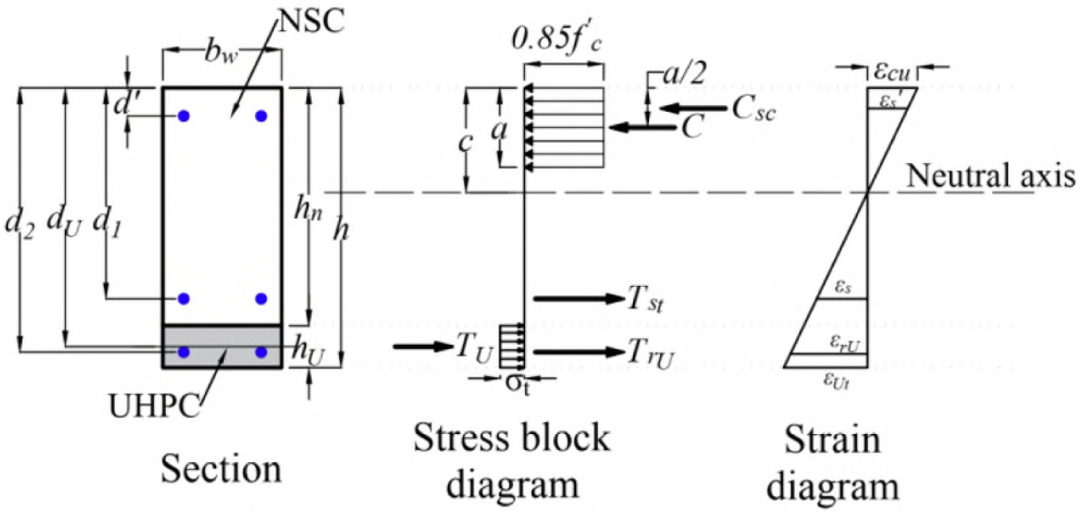

Figure 4.36 The force and strain distribution in a section of a reinforced UHPC-overlaid RC beam [113].

$$M_n = A_s\sigma_s\left(d-\frac{a}{2}\right)+A_u\sigma_t\left(d_u-\frac{a}{2}\right)+A_{ru}\sigma_{ru}\left(d_{ru}-\frac{a}{2}\right) + A'_s\sigma'_s\left(\frac{a}{2}-d'\right) \ldots\ldots\ldots\ldots\ldots\ldots\ldots\ldots\ldots\ldots (Eq.\,4.1)$$

And

$$a=\frac{A_s\sigma_s+A_u\sigma_t+A_{ru}\sigma_{ru}-A'_s\sigma'_s}{0.85\,f'_c b_w} \ldots\ldots\ldots\ldots\ldots (Eq.\,4.2)$$

To ensure the applicability of Eq.4.1, Majid et al. [114] plot a relation between the predicted (*Pu*) from Eq. 4.1 and those found from finite elements (*FE*), as shown in Figure 4.37. Different types of reinforcement were used in the UHPC overlay. It shows good agreement with the mean ($P_{FE}/P_{redicted}$) equal to 1.104 and a standard deviation of 0.2.

Table 4.2 presents a comparison between the predicted values and experimental data collected from various scientific studies presented in the literature. The comparison showed a good agreement between the two, with an average ratio of predicted to experimental values of 1.07 and a standard deviation of 0.15. It is worth noting that the experimental data available at the time of the study were limited.

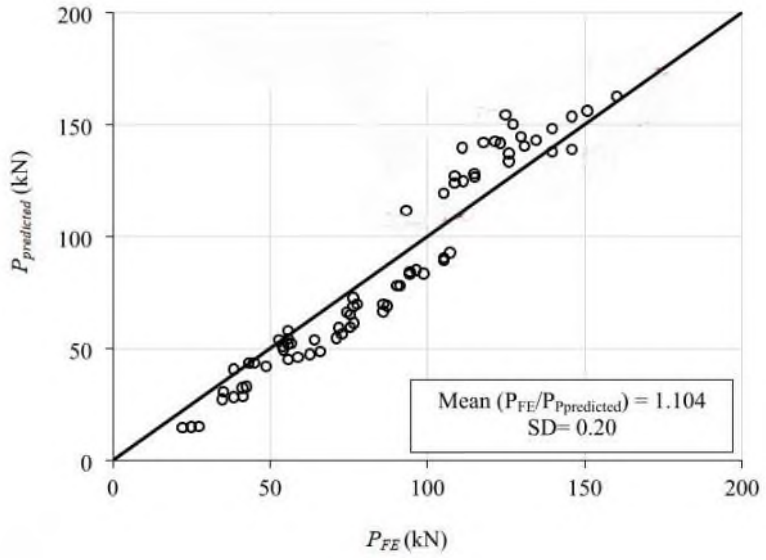

Figure.4.37 Predicted load vs. corresponding FE [114].

Table 4.2 Predicated beam flexural capacity based on Eq. 4.1 vs experimental results ($P_{redicted}$/ $P_{Exp.}$).

NO.	Refenes	$P_{redicted}$	$P_{Exp.}$	($P_{redicted}$/ $P_{Exp.}$)
1	Paschalis [68]	93.93	103.5	0.9
2		63.61	55.3	1.15
3	Lampropoulos [115]	86.76	84	1.03
4		142.23	126	1.12
5	Yin hor [116]	73.17	73.47	0.99
6		105	77.97	1.34
7	Tanarsla[117]	59.53	52.58	1.13
8		81.12	94.27	0.86

Table 4.3 compares the experimental result found in the present study and that predicted by Eq. 4.1. It was found that the estimated value by equation 4.1. shows good agreement for specimens strengthened by plain UHPC overlay/UHPC overlay with mesh reinforcement. Whereas the equation shows overestimate value for specimens strengthened by UHPC overlay reinforced by steel bar/GFRP bar. This is may be due to the strengthened beams failed by concrete cover separation without reaching their full flexural capacity and the reinforcement bar in the UHPC overlay didn't reach yield. Therefore, it is fair to estimate the beam flexural capacity of specimens strengthened by UHPC overlay based on Eq. 4.1 after ensuring no concrete cover separation will occur.

Table 4.3 Compares the experimental result found in the present study and that predicted by Eq. 4.1.

NO.	Specimens	$P_{redicted}$	$P_{Exp.}$	($P_{redicted}$/ $P_{Exp.}$)	Failure mode
1	OSR	131.63	79.76	1.65	Concrete cover separation
2	OSG	146.43	87.06	1.68	
3	OSN0	85.026	70.43	1.2	Flexural
4	OSM0	89.091	77.68	1.15	

Chapter Five

Conclusions and Recommendations

5.1 Conclusions

The aim of this study was to examine the effectiveness of using ultra-high-performance concrete (UHPC) overlays for strengthening reinforced concrete (RC) beams. The experiment was extensive in scope and involved applying the UHPC overlay to the tension side of the RC beams along the clear span. The UHPC was applied in two stages to simulate actual construction practices and create a construction joint. Several key variables were taken into account during the experiment, including the type of UHPC reinforcement (steel mesh, steel bar, and GFRP bar), the shape of the construction joint (key joint/V-joint), and the location of the construction joint (third span and mid-span). Based on the results of the experiment, the following conclusions can be made:

1. To further elaborate, the use of UHPC overlay demonstrated a remarkable improvement in the stiffness of the RC beams. The enhancement in stiffness of around 75% highlights the effectiveness of UHPC overlay as a strengthening method for RC beams.

2. It can be concluded that there was an excellent bond between the two materials, i.e., the pre-existing NSC and UHPC, as there were no instances of slip observed at the interface until the point of failure.
3. The existence of a construction joint in the UHPC overlay diminishes the effectiveness of the strengthening techniques utilized.
4. Although the addition of a steel mesh layer to the UHPC overlay resulted in a slight improvement in the performance of the strengthened beams, with a marginal increase in ultimate load and a delay in the appearance of flexural cracks, the percentage of steel reinforcement was insufficient to improve the behavior of the RC strengthened beam when compared to using an unreinforced UHPC overlay.
5. The reinforcement ratio in the UHPC overlay is an important parameter that has considerable importance on the performance of the strengthened beams. The result indicated that reinforcing the UHPC by 2Ø10 mm steel bar increases the load-bearing capacity by a range between (17.5-31%) and stiffness by about (78%) compared with the control specimen.
6. The thinness of the UHPC overlay leads to a minimal UHPC cover thickness, which can result in less protection for the reinforcement. To address this issue, the present study utilized GFRP bars as reinforcement for the UHPC overlay due to their high resistance to environmental conditions. The results indicate that the use of GFRP as reinforcement for the UHPC overlay led to an improvement in the performance of the strengthened specimens, as evidenced by an increase in load bearing capacity by approximately 40% and stiffness by approximately 30%. Additionally, the appearance of flexural cracks was delayed, further indicating the positive impact of using GFRP bars as reinforcement for the UHPC overlay.
7. The inclusion of steel or GFRP bars to reinforce the UHPC overlay reduces the impact of construction joints, which means that the behavior

of the strengthened specimens using reinforced UHPC overlay is not affected by the shape or location of the construction joint. Therefore, if a construction joint is required in the UHPC overlay, it is recommended to use a vertical joint.

8. The beams strengthened by UHPC reinforced by steel bar/GFRP bar failure due to concrete cover separation at the ends of UHPC overlay before the strengthened beams reach their full capacity. This represents a big issue; therefore, care should be taken when using this technique in strengthening the beams.

5.2 Recommendation

1. Its recommended to anchorage the ends of UHPC overlay throughout full warp by CFRP laminate or mechanical anchorages.
2. Experimentally investigate the optimum thickness of the UHPC overlay corresponding to the optimum reinforcement ratio in the UHPC overlay.
3. Application of this technique of strengthening on the pre-damaged beams and investigation if this technique improves the performance of beam exposed to a high degree of damage.
4. Numerically simulate the behavior of the strengthened beam by finite element model.

[1] M. M. A. Kadhim, A. Jawdhari, W. Nadir, and L. S. Cunningham, “Behaviour of RC beams strengthened in flexure with hybrid CFRP-reinforced UHPC overlays,” *Eng Struct*, vol. 262, no. May, p. 114356, 2022, doi: 10.1016/j.engstruct.2022.114356.

[2] V. Matsagar, *Advances in structural engineering: Materials, volume three*. Springer India, 2015. doi: 10.1007/978-81-322-2187-6.

[3] S. H. Buch and D. M. Bhat, “Comparative modelling of infilled frames:A descriptive review and analysis,” in *Advances in Structural Engineering: Materials, Volume Three*, Springer India, 2015, pp. 2169–2184. doi: 10.1007/978-81-322-2187-6_166.

[4] Y. Huang, S. Grünewald, E. Schlangen, and M. Luković, “Strengthening of concrete structures with ultra high performance fiber reinforced concrete (UHPFRC): A critical review,” *Construction and Building Materials*, vol. 336. Elsevier Ltd, Jun. 20, 2022. doi: 10.1016/j.conbuildmat.2022.127398.

[5] A. H. Al-Saidy, H. Saadatmanesh, S. El-Gamal, K. S. Al-Jabri, and B. M. Waris, “Structural behavior of corroded RC beams with/without stirrups repaired with CFRP sheets,” *Materials and Structures/Materiaux et Constructions*, vol. 49, no. 9, pp. 3733–3747, Sep. 2016, doi: 10.1617/s11527-015-0751-y.

[6] A. H. Al-Saidy, H. Saadatmanesh, S. El-Gamal, K. S. Al-Jabri, and B. M. Waris, “Structural behavior of corroded RC beams with/without stirrups repaired with CFRP sheets,” *Materials and Structures/Materiaux et Constructions*, vol. 49, no. 9, pp. 3733–3747, Sep. 2016, doi: 10.1617/s11527-015-0751-y.

[7] E. S. Júlio, F. Branco, and V. D. Silva, “Structural rehabilitation of columns with reinforced concrete jacketing,” *Progress in Structural Engineering and Materials*, vol. 5, no. 1, pp. 29–37, Jan. 2003, doi: 10.1002/pse.140.

[8] Y. Zhu, Y. Zhang, H. H. Hussein, and G. Chen, “Flexural strengthening of reinforced concrete beams or slabs using ultra-high performance concrete (UHPC): A state of the art review,” *Engineering Structures*, vol. 205. Elsevier Ltd, Feb. 15, 2020. doi: 10.1016/j.engstruct.2019.110035.

[9] G. Martinola, A. Meda, G. A. Plizzari, and Z. Rinaldi, “Strengthening and repair of RC beams with fiber reinforced concrete,” *Cem Concr Compos*, vol. 32, no. 9, pp. 731–739, Oct. 2010, doi: 10.1016/j.cemconcomp.2010.07.001.

[10] K. Soudki and T. Alkhrdaji, “Guide for the Design and Construction of Externally Bonded FRP Systems for Strengthening Concrete Structures (ACI 440.2R-02),” 2005.

[11] Y. Zhang *et al.*, “Flexural behaviors and capacity prediction on damaged reinforcement concrete (RC)bridge deck strengthened by ultra-high performance concrete (UHPC)layer,” *Constr Build Mater*, vol. 215, pp. 347–359, Aug. 2019, doi: 10.1016/j.conbuildmat.2019.04.229.

[12] M. G. Lee, Y. C. Wang, and C. te Chiu, “A preliminary study of reactive powder concrete as a new repair material,” *Constr Build Mater*, vol. 21, no. 1, pp. 182–189, Jan. 2007, doi: 10.1016/j.conbuildmat.2005.06.024.

[13] A. Ramachandra Murthy, B. L. Karihaloo, and D. S. Priya, “Flexural behavior of RC beams retrofitted with ultra-high strength concrete,” *Constr Build Mater*, vol. 175, pp. 815–824, Jun. 2018, doi: 10.1016/j.conbuildmat.2018.04.174.

[14] Z. J. Wu and J. M. Davies, “Mechanical analysis of a cracked beam reinforced with an external FRP plate,” *Compos Struct*, vol. 62, no. 2, pp. 139–143, 2003, doi: 10.1016/S0263-8223(03)00108-9.

[15] Y. Huang, S. Grünewald, E. Schlangen, and M. Luković, “Strengthening of concrete structures with ultra high performance fiber reinforced concrete (UHPFRC): A critical review,” *Constr Build Mater*, vol. 336, no. March, p. 127398, 2022, doi: 10.1016/j.conbuildmat.2022.127398.

[16] C. Aggregates, “Standard Practice for Fabricating and Testing Specimens of Ultra-High,” vol. i, pp. 1–4, doi: 10.1520/C1856.

[17] Z. Fang, W. Liang, H. Fang, H. Jiang, and S. Wang, “Experimental investigation on shear behavior of high-strength friction-grip bolt shear connectors in steel-precast UHPC composite structures subjected to static loading,” *Eng Struct*, vol. 244, Oct. 2021, doi: 10.1016/j.engstruct.2021.112777.

[18] B. A. Graybeal, “Design and Construction of Field-Cast UHPC Connections,” 2014, doi: 10.13140/2.1.2839.0087.

[19] D. Y. Yoo, J. H. Lee, and Y. S. Yoon, “Effect of fiber content on mechanical and fracture properties of ultra high performance fiber reinforced cementitious composites,” *Compos Struct*, vol. 106, pp. 742–753, Dec. 2013, doi: 10.1016/j.compstruct.2013.07.033.

[20] B. A. Graybeal, “Properties and Behavior of UHPC-Class Materials.” [Online]. Available: https://www.researchgate.net/publication/323525846

[21] B. A. Graybeal, “Properties and Behavior of UHPC-Class Materials.” [Online]. Available: https://www.researchgate.net/publication/323525846

[22] W. Nadir, I. K. Harith, and A. Y. Ali, “Optimization of ultra-high-performance concrete properties cured with ponding water,” *International Journal of Sustainable Building Technology and Urban Development*, vol. 13, no. 4, pp. 454–471, 2022, doi: 10.22712/susb.20220033.

[23] Ben Graybeal, “Bond Behavior of Reinforcing Steel in Ultra-High Performance Concrete,” *FHWA-HRT-14-089*, 2014.

[24] K. Zmetra and B. A. Graybeal, “Design and Construction of UHPC-Based Bridge Preservation and Repair Solutions,” 2022, doi: 10.21949/1521867.

[25] N. Bertola, P. Schiltz, E. Denarié, and E. Brühwiler, “A Review of the Use of UHPFRC in Bridge Rehabilitation and New Construction in Switzerland,” *Frontiers in Built Environment*, vol. 7. Frontiers Media S.A., Nov. 16, 2021. doi: 10.3389/fbuil.2021.769686.

[26] M. A. Al-osta, M. N. Isa, M. H. Baluch, and M. K. Rahman, “Flexural behavior of reinforced concrete beams strengthened with ultra-high performance fiber reinforced concrete,” *Constr Build Mater*, vol. 134, pp. 279–296, 2017, doi: 10.1016/j.conbuildmat.2016.12.094.

[27] P. R. Prem and A. R. Murthy, “Acoustic emission and flexural behaviour of RC beams strengthened with UHPC overlay,” *Constr Build Mater*, vol. 123, pp. 481–492, 2016, doi: 10.1016/j.conbuildmat.2016.07.033.

[28] N. Bertola, P. Schiltz, E. Denarié, and E. Brühwiler, “A Review of the Use of UHPFRC in Bridge Rehabilitation and New Construction in Switzerland,” *Front Built Environ*, vol. 7, no. November, pp. 1–18, 2021, doi: 10.3389/fbuil.2021.769686.

[29] M. A. Al-Osta, “Exploitation of Ultrahigh-Performance Fibre-Reinforced Concrete for the Strengthening of Concrete Structural Members,” *Advances in Civil Engineering*, vol. 2018, 2018, doi: 10.1155/2018/8678124.

[30] B. A. Graybeal and F. Baby, “Development of Direct Tension Test Method for Ultra-High-Performance Fiber-Reinforced Concrete.”

[31] T. M. Ahlborn, D. K. Harris, D. L. Misson, and E. J. Peuse, “Characterization of strength and durability of ultra-high-performance concrete under variable curing conditions,” *Transp Res Rec*, no. 2251, pp. 68–75, Dec. 2011, doi: 10.3141/2251-07.

[32] C. T. Liu and J. S. Huang, “Fire performance of highly flowable reactive powder concrete,” *Constr Build Mater*, vol. 23, no. 5, pp. 2072–2079, May 2009, doi: 10.1016/j.conbuildmat.2008.08.022.

[33] T. L. vande Voort, “Design and field testing of tapered H-shaped Ultra High Performance Concrete piles.” [Online]. Available: https://lib.dr.iastate.edu/rtd/15388

[34] Z. B. Haber, K. Zmetra, and B. A. Graybeal, “Design and Construction of UHPC - Based Bridge Preservation and Repair Solutions,” no. May, 2022, doi: 10.21949/1521867.

[35] I. M. I. Qeshta, P. Shafigh, and M. Z. Jumaat, “Research progress on the flexural behaviour of externally bonded RC beams,” *Archives of Civil and Mechanical Engineering*, vol. 16, no. 4. Elsevier B.V., pp. 982–1003, Sep. 01, 2016. doi: 10.1016/j.acme.2016.07.002.

[36] A. H. Al-Saidy, H. Saadatmanesh, S. El-Gamal, K. S. Al-Jabri, and B. M. Waris, “Structural behavior of corroded RC beams with/without stirrups repaired with

CFRP sheets," *Materials and Structures/Materiaux et Constructions*, vol. 49, no. 9, pp. 3733–3747, Sep. 2016, doi: 10.1617/s11527-015-0751-y.

[37] P. R. Prem and A. R. Murthy, "Acoustic emission and flexural behaviour of RC beams strengthened with UHPC overlay," *Constr Build Mater*, vol. 123, pp. 481–492, Oct. 2016, doi: 10.1016/j.conbuildmat.2016.07.033.

[38] A.-H. Zureick, C. A. Erian Armanios, L. F. Kahn, C. T. Russell Gentry, and R. T. Leon, "REPAIR AND STRENGTHENING OF PRE-1970 REINFORCED CONCRETE CORNER BEAM-COLUMN JOINTS USING CFRP COMPOSITES," 2008.

[39] N. Bertola, P. Schiltz, E. Denarié, and E. Brühwiler, "A Review of the Use of UHPFRC in Bridge Rehabilitation and New Construction in Switzerland," *Frontiers in Built Environment*, vol. 7. Frontiers Media S.A., Nov. 16, 2021. doi: 10.3389/fbuil.2021.769686.

[40] L. Hussein and L. Amleh, "Structural behavior of ultra-high performance fiber reinforced concrete-normal strength concrete or high strength concrete composite members," *Constr Build Mater*, vol. 93, pp. 1105–1116, Jul. 2015, doi: 10.1016/j.conbuildmat.2015.05.030.

[41] N. Bertola, P. Schiltz, E. Denarié, and E. Brühwiler, "A Review of the Use of UHPFRC in Bridge Rehabilitation and New Construction in Switzerland," *Frontiers in Built Environment*, vol. 7. Frontiers Media S.A., Nov. 16, 2021. doi: 10.3389/fbuil.2021.769686.

[42] C. Aggregates, "Standard Practice for Fabricating and Testing Specimens of Ultra-High," vol. i, pp. 1–4, doi: 10.1520/C1856.

[43] E. Brühwiler and E. Denarié, "Rehabilitation and strengthening of concrete structures using ultra-high performance fibre reinforced concrete," *Structural Engineering International: Journal of the International Association for Bridge and Structural Engineering (IABSE)*, vol. 23, no. 4, pp. 450–457, 2013, doi: 10.2749/101686613X13627347100437.

[44] F. J. Alaee and B. L. Karihaloo, "Retrofitting of Reinforced Concrete Beams with CARDIFRC," *Journal of Composites for Construction*, vol. 7, no. 3, pp. 174–186, 2003, doi: 10.1061/(asce)1090-0268(2003)7:3(174).

[45] M. G. Lee, Y. C. Wang, and C. Te Chiu, "A preliminary study of reactive powder concrete as a new repair material," *Constr Build Mater*, vol. 21, no. 1, pp. 182–189, 2007, doi: 10.1016/j.conbuildmat.2005.06.024.

[46] G. E. Thermou, D. Ph, S. J. Pantazopoulou, M. Asce, A. S. Elnashai, and F. Asce, "Flexural Behavior of Brittle RC Members Rehabilitated with Concrete Jacketing," no. October, pp. 1373–1384, 2007.

[47] Z. J. Wu and J. M. Davies, “Mechanical analysis of a cracked beam reinforced with an external FRP plate,” vol. 62, pp. 139–143, 2003, doi: 10.1016/S0263-8223(03)00108-9.

[48] E. Prestressing, “Strengthening of Concrete Beams by External Prestressing lli ~ l”.

[49] Dat Duthinh and Monica Starnes, “Strengthening of Reinforced Concrete Beams with Carbon FRP,” *Composites for Construction*, vol. 1, pp. 493–498, 2001.

[50] T. A. Faculty, M. Engindeniz, and I. P. Fulfillment, “REPAIR AND STRENGTHENING OF PRE-1970 REINFORCED CONCRETE CORNER BEAM-COLUMN JOINTS USING CFRP COMPOSITES REPAIR AND STRENGTHENING OF PRE-1970 REINFORCED CONCRETE CORNER BEAM-COLUMN JOINTS USING,” no. August, 2008.

[51] E. S. Júlio, F. Branco, and V. D. Silva, “Structural rehabilitation of columns with reinforced concrete jacketing,” *Progress in Structural Engineering and Materials*, vol. 5, no. 1, pp. 29–37, 2003, doi: 10.1002/pse.140.

[52] H. Toutanji, L. Zhao, and Y. Zhang, “Flexural behavior of reinforced concrete beams externally strengthened with CFRP sheets bonded with an inorganic matrix,” *Eng Struct*, vol. 28, no. 4, pp. 557–566, 2006, doi: 10.1016/j.engstruct.2005.09.011.

[53] M. Genedy, “A New CFRP-UHPC System for Strengthening Reinforced Concrete T-Beams.” [Online]. Available: https://digitalrepository.unm.edu/ce_etdshttps://digitalrepository.unm.edu/ce_etds/93

[54] P. R. Prem, A. R. Murthy, G. Ramesh, B. H. Bharatkumar, and N. R. Iyer, “Flexural Behaviour of Damaged RC Beams Strengthened with Ultra High Performance Concrete”, doi: 10.1007/978-81-322-2187-6.

[55] Duthinh, D. and M. Stranes, “Strengthening of Reinforced Concrete Beams with Carbon FRP,” vol. 1, 2001.

[56] K. Soudki and T. Alkhrdaji, *Guide for the Design and Construction of Externally Bonded FRP Systems for Strengthening Concrete Structures (ACI 440.2R-02)*. 2005. doi: 10.1061/40753(171)159.

[57] R. J. Gravina and S. T. Smith, “Flexural behaviour of indeterminate concrete beams reinforced with FRP bars,” *Eng Struct*, vol. 30, no. 9, pp. 2370–2380, 2008, doi: 10.1016/j.engstruct.2007.12.019.

[58] N. Attari, S. Amziane, and M. Chemrouk, “Flexural strengthening of concrete beams using CFRP, GFRP and hybrid FRP sheets,” *Constr Build Mater*, vol. 37, pp. 746–757, 2012, doi: 10.1016/j.conbuildmat.2012.07.052.

[59] J. J. Kim, H. C. Noh, M. M. Reda Taha, and A. Mosallam, “Design limits for RC slabs strengthened with hybrid FRP-HPC retrofit system,” *Compos B Eng*, vol. 51, pp. 19–27, 2013, doi: 10.1016/j.compositesb.2012.12.012.

[60] H. Toutanji, L. Zhao, and Y. Zhang, “Flexural behavior of reinforced concrete beams externally strengthened with CFRP sheets bonded with an inorganic matrix,” *Eng Struct*, vol. 28, no. 4, pp. 557–566, 2006, doi: 10.1016/j.engstruct.2005.09.011.

[61] A. Mosallam, M. M. Reda Taha, J. J. Kim, and A. Nasr, “Strength and ductility of RC slabs strengthened with hybrid high-performance composite retrofit system,” *Eng Struct*, vol. 36, pp. 70–80, 2012, doi: 10.1016/j.engstruct.2011.11.022.

[62] A. C. I. Committee, *ACI 440.1R-15: Guide for the Design and Construction of Structural Concrete Reinforced with FRP Bars*.

[63] O. Gunes, D. Lau, C. Tuakta, and O. Büyüköztürk, “Ductility of FRP – concrete systems : Investigations at different length scales,” *Constr Build Mater*, vol. 49, pp. 915–925, 2013, doi: 10.1016/j.conbuildmat.2012.10.017.

[64] L. Hussein and L. Amleh, “Structural behavior of ultra-high performance fiber reinforced concrete-normal strength concrete or high strength concrete composite members,” *Constr Build Mater*, vol. 93, pp. 1105–1116, 2015, doi: 10.1016/j.conbuildmat.2015.05.030.

[65] H. Yin, W. Teo, and K. Shirai, “Experimental investigation on the behaviour of reinforced concrete slabs strengthened with ultra-high performance concrete,” *Constr Build Mater*, vol. 155, pp. 463–474, 2017, doi: 10.1016/j.conbuildmat.2017.08.077.

[66] A. Ramachandra Murthy, B. L. Karihaloo, and D. S. Priya, “Flexural behavior of RC beams retrofitted with ultra-high strength concrete,” *Constr Build Mater*, vol. 175, pp. 815–824, 2018, doi: 10.1016/j.conbuildmat.2018.04.174.

[67] H. M. Tanarslan, N. Alver, R. Jahangiri, Yalçınkaya, and H. Yazıcı, “Flexural strengthening of RC beams using UHPFRC laminates: Bonding techniques and rebar addition,” *Constr Build Mater*, vol. 155, pp. 45–55, Nov. 2017, doi: 10.1016/j.conbuildmat.2017.08.056.

[68] S. A. Paschalis, A. P. Lampropoulos, and O. Tsioulou, “Experimental and numerical study of the performance of ultra high performance fiber reinforced concrete for the flexural strengthening of full scale reinforced concrete members,” *Constr Build Mater*, vol. 186, pp. 351–366, 2018, doi: 10.1016/j.conbuildmat.2018.07.123.

[69] Y. Zhang *et al.*, “Flexural behaviors and capacity prediction on damaged reinforcement concrete (RC)bridge deck strengthened by ultra-high performance concrete (UHPC)layer,” *Constr Build Mater*, vol. 215, pp. 347–359, Aug. 2019, doi: 10.1016/j.conbuildmat.2019.04.229.

[70] Y. Zhang, X. Li, Y. Zhu, and X. Shao, “Experimental study on flexural behavior of damaged reinforced concrete (RC) beam strengthened by toughness-improved ultra-high performance concrete (UHPC) layer,” *Compos B Eng*, vol. 186, Apr. 2020, doi: 10.1016/j.compositesb.2020.107834.

[71] M. K. Ismail and A. A. A. Hassan, “Structural performance of large-scale concrete beams reinforced with cementitious composite containing different fibers,” *Structures*, vol. 31, pp. 1207–1215, Jun. 2021, doi: 10.1016/j.istruc.2021.02.028.

[72] C. Wei, Q. Zhang, Z. Yang, M. Li, Z. Cheng, and Y. Bao, “Flexural cracking behavior of reinforced UHPC overlay in composite bridge deck with orthotropic steel deck under static and fatigue loads,” *Eng Struct*, vol. 265, Aug. 2022, doi: 10.1016/j.engstruct.2022.114537.

[73] C. Zanotti and N. Randl, “Are concrete-concrete bond tests comparable?,” *Cem Concr Compos*, vol. 99, no. February, pp. 80–88, 2019, doi: 10.1016/j.cemconcomp.2019.02.012.

[74] A. Momayez, M. R. Ehsani, A. A. Ramezanianpour, and H. Rajaie, “Comparison of methods for evaluating bond strength between concrete substrate and repair materials,” *Cem Concr Res*, vol. 35, no. 4, pp. 748–757, 2005, doi: 10.1016/j.cemconres.2004.05.027.

[75] M. Naderi, “Effects of cyclic loading, freeze-thaw and temperature changes on shear bond strengths of different concrete repair systems,” *Journal of Adhesion*, vol. 84, no. 9, pp. 743–763, 2008, doi: 10.1080/00218460802352934.

[76] M. Lukovi, G. Ye, and K. Van Breugel, “RELIABLE CONCRETE REPAIR-A CRITICAL REVIEW,” 2006.

[77] Y. Zhu, Y. Zhang, H. H. Hussein, and G. Chen, “Flexural strengthening of reinforced concrete beams or slabs using ultra-high performance concrete (UHPC): A state of the art review,” *Engineering Structures*, vol. 205. Elsevier Ltd, Feb. 15, 2020. doi: 10.1016/j.engstruct.2019.110035.

[78] B. Bissonnette and P. Gaudette, “Committee 364 – Rehabilitation,” vol. 546, pp. 2020–2021, 2021.

[79] S. Aaleti, A. M. Asce, S. Sritharan, and M. Asce, “Quantifying Bonding Characteristics between UHPC and Normal-Strength Concrete for Bridge Deck Application,” vol. 24, no. 2010, pp. 1–13, 2019, doi: 10.1061/(ASCE)BE.1943-5592.0001404.

[80] Z. B. Haber, K. Zmetra, and B. A. Graybeal, “Design and Construction of UHPC - Based Bridge Preservation and Repair Solutions,” no. May, 2022, doi: 10.21949/1521867.

[81] Y. Huang, S. Grünewald, E. Schlangen, and M. Luković, “Strengthening of concrete structures with ultra high performance fiber reinforced concrete (UHPFRC): A critical review,” *Constr Build Mater*, vol. 336, no. March, p. 127398, 2022, doi: 10.1016/j.conbuildmat.2022.127398.

[82] M. A. Sakr, A. A. Sleemah, T. M. Khalifa, and W. N. Mansour, “Shear strengthening of reinforced concrete beams using prefabricated ultra-high performance fiber

reinforced concrete plates: Experimental and numerical investigation," *Structural Concrete*, vol. 20, no. 3, pp. 1137–1153, Jun. 2019, doi: 10.1002/suco.201800137.

[83] S. Rabie and J. Mendenhall, "Design, Construction, and Evaluation of UHPC Bridge Deck Overlays for NJDOT," New Jersey.

[84] S. Aaleti, A. M. Asce, S. Sritharan, and M. Asce, "Quantifying Bonding Characteristics between UHPC and Normal-Strength Concrete for Bridge Deck Application," vol. 24, no. 2010, pp. 1–13, 2019, doi: 10.1061/(ASCE)BE.1943-5592.0001404.

[85] A. C. I. Committee, "318-19 Building Code Requirements for Structural Concrete and Commentary," *318-19 Building Code Requirements for Structural Concrete and Commentary*, 2019, doi: 10.14359/51716937.

[86] M. M. Reda, N. G. Shrive, and J. E. Gillott, "Microstructural investigation of innovative UHPC," vol. 29, no. April 1998, pp. 323–329, 1999.

[87] P. Schießl, O. Mazanec, and D. Lowke, "SCC and UHPC – Effect of Mixing Technology on Fresh Concrete Properties".

[88] "Designation: C230/C230M − 14 Standard Specification for Flow Table for Use in Tests of Hydraulic Cement 1", doi: 10.1520/C0230_C0230M-14.

[89] "Standard Test Method for Flow of Hydraulic Cement Mortar 1", doi: 10.1520/C1437.

[90] IQS. (1984), "Iraqi Specifications No. (5)," *1984 for Portland Cement*.

[91] "the Iraqi Standard Specification (IQS)."

[92] Quickmast 108, "https://www.dcp-int.com/qa/ar/products/kwyk-mast-108 ."

[93] "Standard Specification for Steel Fibers for Fiber-Reinforced Concrete 1", doi: 10.1520/A0820_A0820M-11.

[94] "Standard Specification for Steel Fibers for Fiber-Reinforced Concrete 1", doi: 10.1520/A0820_A0820M-11.

[95] ASTM A615/A615M, "Specification for Deformed and Plain Carbon-Steel Bars for Concrete Reinforcement," *ASTM*, 2016, doi: 10.1520/A0615_A0615M-16.

[96] Fosrok, "https://www.fosroc.com.au/product/nitobond-ep," *Nitobond EP*.

[97] M. Imam, L. Vandewalle, and F. Mortelmans, "Are current concerete strength tests suitable for high strength concrete?," *Mater Struct*, vol. 28, no. 7, pp. 384–391, Aug. 1995, doi: 10.1007/BF02473073.

[98] G. Benjamin A., "Material Property Characterization of Ultra-High Performance Concrete," *FHWA*, no. FHWA-HRT-06-103, p. 186, 2006.

[99] B. Graybeal and M. Davis, “Cylinder or Cube: Strength Testing of 80 to 200 MPa (11.6 to 29 ksi) Ultra-High-Performance Fiber-Reinforced Concrete,” *ACI Mater J*, vol. 105, no. 6, pp. 105-M68, 2008.

[100] O. Q. Aziz and G. H. Ahmed, “Mechanical properties of Ultra High Performance Concrete (UHPC),” in *Twelfth International Conference on Recent Advances in Concrete Technology and Sustainability Issues Prague*, 2012. doi: 10.14359/51684273.

[101] Y. Kusumawardaningsih, E. Fehling, and M. Ismail, “UHPC compressive strength test specimens: Cylinder or cube?,” in *Procedia Engineering*, 2015, pp. 1076–1080. doi: 10.1016/j.proeng.2015.11.165.

[102] “Standard Test Method for Compressive Strength of Hydraulic Cement Mortars (Using 2-in. or [50-mm] Cube Specimens) 1”, doi: 10.1520/C0109_C0109M-16A.

[103] ASTM C1856, “Standard Practice for Fabricating and Testing Specimens of Ultra-High Performance Concrete,” *ASTM International*, vol. i, p. 4, 2017, doi: 10.1520/C1856.

[104] ASTM C469, “Standard Test Method for Splitting Tensile Strength of Cylindrical Concrete Specimens,” *ASTM*, vol. i, pp. 1–5, 2011, doi: 10.1520/C0496.

[105] “Standard Test Method for Flexural Strength of Concrete (Using Simple Beam with Third-Point Loading) 1.” [Online]. Available: www.astm.org

[106] P. Qiao, Z. Zhou, and S. Allena, “Developing Connections for Longitudinal Joints between Deck Bulb Tees-Development of UHPC Mixes with Local Materials,” no. October, 2016.

[107] ASTM C109/109M, “Standard test method for compressive strength of hydraulic cement mortars (Using 2-in. or cube specimens),” *ASTM*, vol. i, pp. 1–10, 2016, doi: 10.1520/C0109.

[108] British Standards Institution., *Testing hardened concrete. Part 3, Compressive strength of test specimens.* BSI, 2002.

[109] O. Gunes, D. Lau, C. Tuakta, and O. Büyüköztürk, “Ductility of FRP – concrete systems : Investigations at different length scales,” *Constr Build Mater*, vol. 49, pp. 915–925, 2013, doi: 10.1016/j.conbuildmat.2012.10.017.

[110] D. Yoo and Y. Yoon, “Structural performance of ultra-high-performance concrete beams with different steel fibers,” *Eng Struct*, vol. 102, pp. 409–423, 2015, doi: 10.1016/j.engstruct.2015.08.029.

[111] “STRUCTURAL ASSEMBLAGES FROM LABORATORY TESTING,” vol. 22, no. 3, pp. 155–166, 1989.

[112] B. Li, “Initial Stiffness of Reinforced Concrete Columns and Walls,” in *15th World Conference on Earthquake Engineering*, 2012, p. 10.

[113] K. Shirai, H. Yin, and W. Teo, “Flexural capacity prediction of composite RC members strengthened with UHPC based on existing design models,” *Structures*, vol. 23, pp. 44–55, Feb. 2020, doi: 10.1016/j.istruc.2019.09.017.

[114] M. M. A. Kadhim, A. Jawdhari, W. Nadir, and L. S. Cunningham, “Behaviour of RC beams strengthened in flexure with hybrid CFRP-reinforced UHPC overlays,” *Eng Struct*, vol. 262, Jul. 2022, doi: 10.1016/j.engstruct.2022.114356.

[115] A. P. Lampropoulos, S. A. Paschalis, O. T. Tsioulou, and S. E. Dritsos, “Strengthening of reinforced concrete beams using ultra high performance fibre reinforced concrete (UHPFRC),” *Eng Struct*, vol. 106, pp. 370–384, 2016, doi: 10.1016/j.engstruct.2015.10.042.

[116] H. Yin, W. Teo, and K. Shirai, “Experimental investigation on the behaviour of reinforced concrete slabs strengthened with ultra-high performance concrete,” *Constr Build Mater*, vol. 155, pp. 463–474, Nov. 2017, doi: 10.1016/j.conbuildmat.2017.08.077.

[117] H. M. Tanarslan, “Flexural strengthening of RC beams with prefabricated ultra high performance fibre reinforced concrete laminates,” *Eng Struct*, vol. 151, pp. 337–348, 2017, doi: 10.1016/j.engstruct.2017.08.048.

Appendix A

Design of reference specimen based on ACI 318-19

No.	Calculation and discussion	Code Ref.
1.	**Specimen Dimension** • Assume the section and dimension as shown in Figure 1. 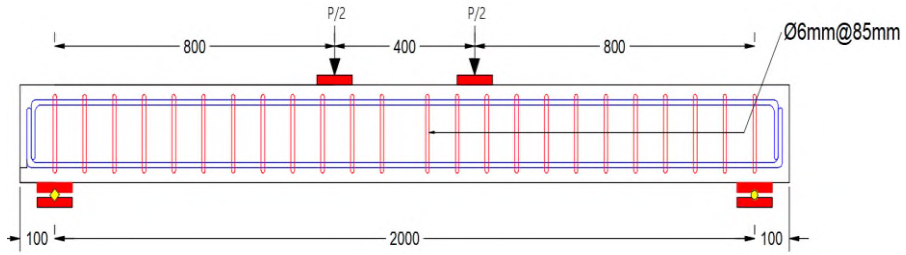 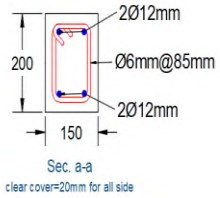	
	a) Beam dimension Use 150mm in width and 200 mm in total depth	
2.	**Design of beam**	
	b) Flexural strength of the specimen	
	$b = 150\ mm, h = 200\ mm,\ \ f_y = 400Mpa\ and\ f_c^{`} = 30\ Mpa$ $d = 200 - 20 - 6 - 6 = 168mm$ $\frac{shearspan(800mm)}{total\ depth\ (200mm)} = 4.0 > 2.0\ (shallow\ beam)$ …. ACI 9.9.1.1 b $A_s = 2\emptyset 12mm\ and\ A_s^{`} = 2\emptyset 12mm$ $\rho = \frac{A_s}{bd} = 0.009, \quad \rightarrow \quad \rho_{min.} < \rho < \rho_{max.}$ $a = \frac{A_s f_y}{0.85 f_c^{`} b} = \frac{2 \times 113.1 \times 400}{0.85 \times 30 \times 150} = 23.65\ mm$ $M_n = A_s f_y (d - a/2) = 14.13\ kN.m$ $\rightarrow P = 35.32\ kN \quad control$	
	C) strength of the specimen Shear	
	$V_c = 0.17\sqrt{f_c^{`}}\ b_w\ d$ $V_c = 0.17 \times \sqrt{30} \times 150 \times 168 \times 10^{-3} = 23.46kN$ $V_s = \frac{A_v \times f_{yt} \times d}{s}$	ACI 318 ACI 318

No.	Calculation and discussion	Code Ref.
	$V_s = \frac{2 \times (\pi/4) \times 6^2 \times 400 \times 168}{85 \times 1000} = 44.7\ \text{kN} < V_{s,max.} = 2/3\ \sqrt{f_c`}\ b_w\ d$ $= 92kN$ $V_s \leq \frac{1}{3}\sqrt{f_c'} b_w d \rightarrow S_{max.}$ $= \text{min. of} \begin{cases} d/2 = 84mm \approx 85mm \\ 600mm \end{cases}$ $ACI9.7.6.2.2$ $V_n = (V_c + V_s)$ $\rightarrow P/2 = (44.7 + 23.46) \rightarrow \text{P} = 136.32\ \text{kN}$ $\rightarrow diff.between\ flexural\ failure\ and\ shear\ failure\ is \frac{136.32 - 35.32}{35.32}$ $= 2.86$ If use Ø8 mm @85 mm then, $V_s = \frac{2 \times (\pi/4) \times 8^2 \times 400 \times 164}{85 \times 1000} = 77.58\ \text{kN} < V_{s,max.} = 2/3\ \sqrt{f_c`}\ b_w\ d$ $= 89.8kN$ $V_s > \frac{1}{3}\sqrt{f_c'} b_w d \rightarrow S_{max.} = \text{min. of} \begin{cases} d/4 = 41mm < 85mm\ \textit{not ok} \\ 300mm \end{cases}$ $V_n = (V_c + V_s)$ $\rightarrow P/2 = (87.93 + 22.9) \rightarrow \text{P} = 221.66\ \text{kN}$ $\rightarrow diff.between\ flexural\ failure\ and\ shear\ failure\ is \frac{221.66 - 34.42}{34.42}$ $= 5.44$	ACI 318
	$\Delta_{center} = \frac{(P/2)a}{24\ E_c I_e}(3l^2 - 4a^2)$ $f_c` = 30MPa, d = 168\ mm, E_c$ $= 25743MPa,\ n$ $= 7.7, I_g$ $= 100 \times 10^6 mm^4$ $f_r = 0.62\sqrt{f_c`} = 3.4kN,\ M_{cr}$ $= \frac{f_r \times I_g}{y_t} = 3.4kN.m$ $y_{cr} = 47.4mm, I_{cr}$ $= 31.8 \times 10^6 mm^4$ $M_a = 0.4P = 14.13kN.m$ $> M_{cr}(3.4kN.m)$ $I_e = I_{cr} + \left(\frac{M_{cr}}{M_a}\right)^3 \times (I_g - I_{cr})$ $= 32.75 \times 10^6 mm^4$ 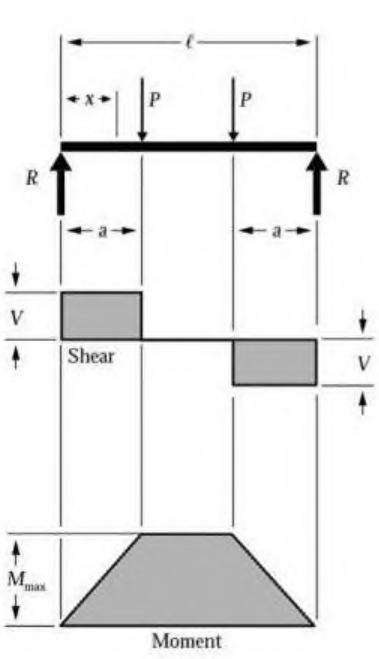 	ACI 318

No.	Calculation and discussion	Code Ref.
	$\Delta_{center}=\frac{(17.66\times10^3)\times800}{24\times25743\times32.75\times10^6}\times(3\times2000^2-4\times800^2)$ $=6.6\,mm$ $<l/180\,(11.11mm)$	
	e)Check crack width	ACI 318
	$w_{max.}=0.0132\times10^{-3}\times f_s\times\sqrt[3]{A\,c_e}$ $f_s=0.6f_y=240MPa,\ \ A=3000mm^2, c_e=52mm$ $w_{max.}=0.124mm<0.33mm$	
	f) Check the development length	ACI 318
	$l_d=\left(\frac{f_y}{1.1\lambda\sqrt{f_c'}}\frac{\psi_e\psi_t\psi_s}{\left(\frac{c_b+k_{tr}}{d_b}\right)}\right)d_b\geq300\,mm$ Where: λ=1.0 for normal weight concrete **1. ψ_t =bar location factor** Ψ_t =1.3 for top bars defined as horizontal reinforcement, placed so that more than 300mm of fresh concrete is below the development length, or splice Ψ_t =1.0 for all other reinforcement **2. ψ_e =coating factor** ψ_e =1.5 for epoxy-coated bars or wires with cover less than 3*db* or clear spacing less than 6*db* ψ_e=1.2 for all other epoxy coated bars or wires ψ_e =1.0 for uncoated and zinc-coated (galvanized) reinforcement (However, the value of the $\psi_t\psi_e$ product should not exceed 1.7.) **3. ψ_s =bar size factor** ψ_s =0.8 for Ø19 or smaller bars and deformed wires ψ_s =1.0 for Ø20 and larger bars $\left(\frac{c_b+k_{tr}}{d_b}\right)\leq2.5\ say=2.5$ $l_d=\left(\frac{400}{1.1\times1\times\sqrt{30}}\frac{1\times1\times0.8}{2.5}\right)\times12=255mm<300\,mm$ $use\ l_d=300mm$ The provide development length = 1.0 m > required (0.3m) ok	

جمهورية العراق
وزارة التعليم العالي والبحث العلمي
جامعة بابل
كلية الهندسة
قسم الهندسة المدنية

دراسة مخبرية عن تصرف الاعتاب الخرسانية المسلحة و المقواة بطبقة من الخرسانة فائقة الأداء

رسالة

مقدمة الى كلية الهندسة - جامعة بابل و هي جزء من متطلبات
نيل درجة الماجستير في الهندسة / الهندسة المدنية / انشاءات

من قبل
ظافر مردان سعود مشهد

اشراف
الأستاذ المساعد عبد الرضا صالح الفتلاوي

2023م **1444هـ**

الخلاصة

إن متانة المباني الخرسانية المسلحة عرضة للعديد من التهديدات والأضرار البيئية الشديدة وغيرها من الاجهادات الخارجية. لزيادة العمر التشغيلي للمباني ، غالبًا ما يتم استخدام طرق التقوية والإصلاح لتحسين قوتها ومتانتها. نظر هذا البحث في تأثير إضافة طبقة UHPC إلى الاعتاب الخرسانية المسلحة ، سواء مع أو بدون مفاصل انشائية في طبقة UHPC. تضمن البرنامج العملي اختبار تسعة عشر عتب من الخرسانة المسلحة و كانت العوامل التي تم دراستها هي استمرارية طبقة UHPC ، ونوع التسليح في طبقة UHPC ، وموقع المفصل الانشائي في طبقة UHPC ، وشكل المفصل الانشائي. وفقًا للنتائج ، فإن إضافة طبقة UHPC إلى جانب الشد للعتب الخرساني المسلح عزز بشكل كبير الصلابة (20-132 ٪) وأخر ظهور التشققات. في الوقت نفسه ، قلل المفصل الانشائي في طبقة UHPC من فاعلية التقوية. يتأثر أداء العتب المقواة بشكل كبير بنسبة التسليح في طبقة UHPC. أظهرت النتائج أنه بالمقارنة مع العينة المرجعية ، فإن طبقة UHPC الذي تم تسليحها بقضبان فولاذية 2 × 10 ملم كان له تحمل اقصى أعلى (17.5-23.1٪) وصلابة (78٪). علاوة على ذلك ، فإن استخدام GFRP كتسليح لطبقة UHPC يحسن من قدرة التحمل ، والصلابة ، ويؤخر ظهور شقوق الانحناء في العينات المقواة. أظهرت النتائج أن طبقة UHPC لها ترابط ممتاز بما يكفي بالخرسانة مما أدى إلى زيادة قدرة تحمل الأحمال بنسبة 40٪ وزيادة الصلابة بنسبة 30٪. يتم تخفيف تأثير المفصل الانشائي عن طريق استخدام الفولاذ أو GFRP كتسليح لطبقة UHPC. نتيجة لذلك ، لم يكن لشكل أو موضع المفصل الانشائي أي تأثير على سلوك العينات المقواة بطبقة UHPC. وبالتالي ، يُنصح باستخدام وصلات عمودية في طبقة UHPC إذا لزم الأمر. قبل أن تعمل الاعتاب المقواة بكامل طاقتها ، فصل الغطاء الخرساني في نهايات طبقة UHPC و ادى إلى فشل الحزم الفولاذية / GFRP المقوى الذي تم تقويته بواسطة UHPC. هذه مشكلة كبيرة ، لذلك يجب توخي الحذر أثناء استخدام هذا الإجراء لتقوية الاعتاب.